# A MORPHOLOGICAL AND FUNCTIONAL INVESTIGATION OF THE ENAMEL ORGAN AND ENAMEL IN THE RAT INCISOR

by

· Marc D. McKee

A thesis submitted to the Faculty of Graduate Studies and Research in partial fulfillment of the requirements for the degree of Doctor of Philosophy

Department of Anatomy

McGill University

Montreal, Quebec, Canada

© M.D. McKee, 1987

Short Title

STRUCTURE AND FUNCTION OF THE ENAMEL ORGAN AND ENAMEL

Marc D. McKee, Ph.D. Department of Anatomy McGill University

\$ 15

l

-

•

` **à**'

## ABSTRACT'

A morphological and functional investigation of the enamel organ and enamel was carried out on the incisor of the rat. Using transmission electron microscopy and other electron optical techniques, the ultrastructure of enamel hydroxyapatite crystallites and the morphology of the cells of the enamel organ related to these crystallites were examined. In the enamel putative cell communication via matched secretion zone, approaches of rough endoplasmic reticulum to the ameloblast cell membrane was not confirmed. Throughout the enamel organ, extracellular permeability was assessed using radiolabeled proteins as tracers. Regional differences were found, especially related to the two types of maturation ameloblasts. Several modified histochemical techniques were successfully applied to the enamel such that the functional contribution of each type of In this way it was demonstrated that ameloblast was ascertained. several functional cell subpopulations exist and that they can be correlated with different calcium and protein distributions In vivo injection of vinblastine, and in within the enamel. vitro treatments with other drugs, all severely modified the enamel maturation staining pattern and 45Ca uptake. In addition. it was found that ruffle-ended maturation zone ameloblasts possess higher levels of specific transferrin receptor sites relative to smooth-ended ameloblasts, a finding that may be directly related to the deposition of iron within the enamel.

Marc D. McKee: Ph.D., Department of Anatomy, McGill University: A morphological and functional investigation of the enamel organ, and enamel in the rat incisor.

## RESUNE

\*Une recherche sur la structure et la fonction de l'organe de l'émail et de l'émail associée a été faite sur les incisives du L'ultrastructure des cristaux d'hydroxyapatite de l'émail et la morphologie des cellules de l'organe de l'émail qui y sont associées, ont été étudié à l'aide du microscope électronique et autres méthodes optiques. Dans la zone de secrétion de l'émail, le rôle des cisternes du réticulum endoplasmique d'améloblastes adjacents dans la communication intercellulaire n'a pu être La perméabilité extracellulaire dans l'organe de l'émail à été évaluée à l'aide de protéines radioactives. différences régionales de cette perméabilité ont été observées en fonction des deux stades de maturation des améloblastes. Plusieurs méthodes histochimiques ont été utilisées avec succés dans l'étude de l'émail, c'est ainsi qu'une variation dans l'activité fonctionelle des divers types d'améloblastes à pu'être Plusieur's sous-populations d'améloblastes ont été distinguées et associées à des régions ou zones de l'émail dont la composition en calcium et en protéines présente charactères distinctifs. L'injection de vinblastine dans l'organe de l'émail in vivo et le traitement de l'émafl diverses substances chimiques in vitro produisent modifications / marquées de la coloration de l'émail et de la captation du 45Ca par l'émail en maturation. Nous avons enfin observé que l'extrémitée striée des améloblastes de la zone de maturation contient plus de récepteurs de la transférine que l'extrémité non-striée des améloblastes également présents dans

cette zone ce qui suggère un rôle plus actif de certains améloblastes dans la déposition du fer dans l'émail.

Marc D. McKee: Ph.D., Department of Anatomy, McGill University: Etude morphologique et fonctionelle de l'organe de l'émail et de l'émail de l'incisive du rat.

To my wife, Darlene

#### **ACKNOWLEDGEMENTS**

I wish to offer my gratitude to the following persons:

- to Dr. Hershey Warshawsky for having accepted me into his laboratory, for his expert and critical supervision of my work, and for his friendship.
- to Drs. D.G. Osmond and Y. Clermont for giving me the opportunity to work in this department.
- to Dr. S.-W. Bai for providing my initial training and helping with many of the experiments.
- to Drs. B. Martineau-Doizé, N.J. Nadler, A. Nanci, C.E. Smith and T. Uchida for participating in some of the work described in Chapters 2 and 9, 1, 5 and 8 and 10, 8, and 6, respectively, and to J. Brown, L. Wedlich, S. Zalzal and C. Zerounian for their help with some of the experiments.
- to Drs. A. Nanci and C.E. Smith for endless hours of enthusiastic, encouraging and motivating discussions.
- to Drs. J.J.M. Bergeron, W. Lai, M.F. Lalli and N.J. Nadler for their help throughout the course of this work.
  - to A. Graham for his assistance with photography.
- to F. Evaristo. P. Hales, K. Hewitt and J. Mui for their technical assistance.
  - to J. Khan for his assistance with animal care.
- to Proctor and Gamble for supplying the bisphosphonate used in Chapter 3.
- to the Medical Research Council of Canada and the Faculty of Graduate Studies and Research of McGill University for their financial support.

# TABLE OF CONTENTS

Page
GENERAL INTRODUCTION
Dynamics of the rat incisor
Presecretion zone enamel organ
Secretion zone enamel organ and enamel
Maturation zone enamel organ and enamel 4
Organic matrix of enamel
Crystallites of enamel
CHAPTER ONE: QUANTITATIVE ANALYSIS OF ROUGH ENDOPLASMIC RETICULUM APPROACHES TO THE CELL MEMBRANE IN THE SECRETORY AMELOBLAST OF THE RAT INCISOR.
SYNOPSIS 11
INTRODUCTION 12
MATERIALS AND METHODS
Animal procedures and tissuc processing 14
Counting of subsurface cisternae
RESULTS 16
Morphological appearance of SSC
Statistical analysis of SSC 16
Determination of random probability of SSC matching 17
DISCUSSION
TABLE 1 20
TABLE 2 21
APPENDIX 22
REFERENCES 23
FIGURE LEGENDS 28

THE STRUCTURE AND DEVELOPMENT OF THE PAPILLARY LAYER AND THE PENETRATION OF VARIOUS MOLECULAR-WEIGHT PROTEINS INTO THE ENAMEL ORGAN AND ENAMEL

CHAPTER TWO:

OF THE RAT INCISOR.	
SYNOPSIS	30
INTRODUCTION	32
MATERIALS AND METHODS	34
Tissue processing for electron microscopy	34
Dipping experiment	35
Systemic injection experiment	36
RESULTS	37
Presecretion zone enamel organ morphology	37
Secretion zone enamel organ morphology	38
Maturation zone enamel organ morphology	39
Calcitonin penetration	42
Insulin penetration	43
Epidermal growth factor penetration	44
Albumin penetration	44
DISCUSSION	, 45
·	n
Enamel organ morphology	
Use of labeled proteins as biological tracers	46
Significance of the dipping experiments	<sup>4</sup> 8
Significance of the systemic injection experiments	49
REFERENCES	53
TECHNO	60

-viii-
CHAPTER THREE: EFFECTS OF VARIOUS AGENTS ON STAINING OF THE MATURATION PATTERN AT THE SURFACE OF RAT INCISOR ENAMEL.
SYNOPSIS
INTRODUCTION
MATERIALS AND METHODS
Experimental procedures prior to staining 76
Enamel staining with GBHA and PAS
Ground sectioning 77
RESULTS 78
Untreated incisors
Treated incisors 79
Guanidine treatment 79
EDTA treatment 80
HEBP treatment
Acid treatment 80
Ground sections 81
DISCUSSION 81
REFERENCES 86
FIGURE LEGENDS 90
CHAPTER FOUR: MODIFICATION OF THE ENAMEL MATURATION PATTERN BY VINBLASTINE AS REVEALED BY GLYOXAL BIS(2-HYDROXYANIL) (GBHA) STAINING AND 45CALCIUM RADIOAUTOGRAPHY.
SYNOPSIS
INTRODUCTION 94
MATERIALS AND METHODS
Animal procedures 95
Fnamel staining with GBHA

Radioautography of enamel after 45Ca injection 96
RESULTS 97
GBHA staining: Normal incisors 97
GBHA staining: Vinblastine-treated incisors 97
Radioautography: Normal incisors
Radioautography: Vinblastine-treated incisors 99
DISCUSSION 99
Microtubules and the ruffled border 99
GBHA staining and the state of calcium binding 100
Radioautography and the state of calcium binding, 101
REFERENCES 103
FIGURE LEGENDS 106
CHAPTER FIVE: USE OF BACKSCATTERED ELECTRON IMAGING ON DEVELOPED RADIOAUTOGRAPHIC EMULSIONS: APPLICATION TO VIEWING THE RAT INCISOR ENAMEL MATURATION PATTERN FOLLOWING 45 CALCIUM INJECTION.
SYNOPSIS 107
INTRODUCTION 109
MATERIALS AND METHODS111
45Calcium radioautography
Backscattered electron imaging (BEI) 112
RESULTS 112
45Calcium radioautography in routine preparations_viewed by light microscopy
BEI of the 45 calcium radioautographs
DISCUSSION 115
BEI of developed radioautographic emulsions 115
The enamel maturation pattern 117

**.** 

, 11

1

•
, ,
<b>-x-</b>
Calcium dynamics
REFERENCES
FIGURE LEGENDS
CHAPTER SIX: A RADIOAUTOGRAPHIC STUDY OF THE EFFECTS OF VINBLASTINE ON THE FATE OF INJECTED <sup>45</sup> CALCIUM AND <sup>125</sup> I-INSULIN IN THE RAT INCISOR.
SYNOPSIS 128
INTRODUCTION 129
MATERIALS AND METHODS
45Calcium experiment
125 <sub>I</sub> -insulin experiment
RESULTS 131
Localization of 45 calcium
Localization of 125I-insulin
DISCUSSION
REFERENCES
FIGURE LEGENDS 138
CHAPTER SEVEN: IN VITRO STAINING OF ENAMEL USING HISTO- CHEMICAL COMPLEXING METHODS FOR CALCIUM.
SYNOPSIS 139
INTRODUCTION 140
MATERIALS AND METHODS
Animal and tissue handling procedures prior to staining. 142
GBHA staining of incisors
Histochemical complexing stains for calcium applied to incisor enamel
RESULTS

DISCUSSION 14	. 5
Calcium dynamics	Ģ
Staining reactions	6
Interpretation of staining patterns 15	0
REFERENCES	5
FIGURE LEGENDS	1
CHAPTER EIGHT: IN VITRO STAINING OF ENAMEL PROTEINS USING SEVERAL COMMON HEAVY METAL AND HISTOLOGICAL STAINS.	G
SYNOPSIS 16	2
INTRODUCTION 16	3
MATERIALS AND METHODS	4
Animal and tissue handling prior to staining 16	4
Staining procedures	5
Backscattered electron imaging of stained incisors 16	6
35S-methionine_injection and radioautography 160	6
RESULTS 16	<b>7</b>
Staining patterns $\uparrow$ 16	
Radioautography after 35S-methionine injection 170	0
DISCUSSION	0
Staining reactions	0
Interpretation of staining patterns	5
REFERENCES	9
FIGURE LEGENDS	5

۷

•	CHAPTER NINE: SPECIFIC BINDING SITES FOR TRANSFERRIN  AMELOBLASTS OF THE ENAMEL MATURATION ZONE  THE RAT INCISOR.	IN
	synopsis 1	187
	INTRODUCTION	88
	MATERIALS AND METHODS	.90
	Charging of transferrin with iron 1	L90
	Iodination of transferrin 1	190
	Animal procedures1	.91 <sup>^</sup>
•	Electron microscopy and X-ray microanalysis 1	L <b>92</b>
	RESULTS	L <b>92</b>
	Light microscope radioautography	192
	Electron microscopy 1	L93
	Energy dispersive X-ray spectroscopy (EDX)1	L94
	DISCUSSION	L94
	TABLE 1	L <b>9</b> 7
	TABLE 2	198
į	REFERENCES 1	L99
	FIGURE LEGENDS	203
	CHAPTER TEN: USE OF ISOLATED ENAMEL CRYSTALLITES IN LATTI IMAGING BY HIGH RESOLUTION TRANSMISSION ELECTRONIC MICROSCOPY.	CE RON
	SYNOPSIS	204
	INTRODUCTION 2	2 <b>ð</b> 5
	MATERIALS AND METHODS	206
	Preparation of isolated enamel crystallites 2	906
	Electron optical analyses 2	207

RESULTS	208
Electron diffraction	208
Lattice fringes on single and isolated crystallites	209
Moiré interference patterns produced by overlapping crystallites	209
DISCUSSION	210
REFERENCES	214
FIGURE LEGENDS	215
	•
GENERAL SUMMARY AND CONCLUSIONS	218
ORIGINAL CONTRIBUTIONS	227

# GENERAL INTRODUCTION\*

## Dynamics of the rat incisor >

The continuously erupting rat incisor is an excellent model system in which to study the complex phenomena comprising In the rat incisor, continuous attrition at the amelogenesis. incisal end of the tooth is balanced by the continuous production of dentin and enamel at the apical end of the tooth. Amelogenesis in teeth of limited eruption is similar to that of the incisor (reviewed by Warshawsky et al., 1981). The rat incisor is particularly advantageous in that all the stages of enamel development appear simultaneously and in sequence along the length of the same tooth. In a well-oriented longitudinal section through the incisor, a continuous layer of ameloblasts can be seen on the labial surface of the tooth. contains the entire sequence of developmental stages related to enamel production and has been morphologically and functionally divided into several different zones of amelogenesis (Warshawsky and Smith, 1974). According to this classification, the enamel organ is divided into the following zones: (1) presecretory zone, (2) secretory zone and, (3) maturation zone. At the end of the maturation zone the ameloblasts become dramatically reduced in height and end their life cycle as desquamating cells around the gingival margin at the beginning of the erupted portion of the The proportion of time spent by the cells in each of tooth. these zones is proportional to the incisor length which they occupy, indicating that the cells' apparent migration rate is

<sup>\*</sup>Literature cited included in References of Chapter One.

about the same at the various stages of their life cycle (Leblond and Warshawsky, 1979).

## Presecretion zone enamel organ

The presecretion zone is devoted mainly to the differentiation of ameloblasts. Within this zone the ameloblasts lengthen, become tall columnar, and undergo a reversal in cell polarity relative to the basement membrane. More incisally, the ameloblasts develop all the morphological features of secretory ameloblasts except for Tomes' processes. Concurrently, the other layers of the enamel organ (i.e. stratum intermedium, stellate reticulum and outer dental epithelium) become more distinct.

Renewal of the cell populations in the presecretion zone has been studied using <sup>3</sup>H-thymidine (Smith and Warshawsky, 1975). Using radioautography it has been established that a cohort of cells from each layer of the enamel organ is carried incisally with the erupting incisor and all of the cells in this cohort reach the gingival margin at the same time relative to their starting positions. Continuous eruption therefore requires a continuous production of cohorts at the apical end of the tooth.

### Secretion zone enamel organ and enamel

In the secretion zone, ameloblasts are responsible for secreting the entire enamel layer. The first enamel to be elaborated is termed initial enamel and is released from the flattened apical ends of the secretory ameloblasts. This enamel contains the organic matrix and numerous thin hydroxyapatite crystallites generally oriented perpendicular to the dentinoenamel junction. Continued secretion and further differentiation

of the ameloblasts results in the formation of a long, apical projection known as Tomes' process that is distal to the distal junctional complex and terminal cell web. Tomes' process can be further subdivided into proximal and distal portions that are responsible for secreting interrod and rod enamel, respectively. The ameloblasts then cooperate as a physiological syncytium in order to elaborate the intricate decussating pattern of rod and interrod enamel characteristic of mammals. Following the secretion of the inner and outer enamel layers, the ameloblasts lose their Tomes' processes and complete enamel synthesis by laying down a final layer of enamel in which the crystallites are again arranged perpendicular to the surface of the tooth.

Ameloblasts in the secretion zone are highly-differentiated polarized cells. The cytoplasm of the ameloblast is subdivided into infranuclear, nuclear, supranuclear and distal portions (Warshawsky, 1968). The infranuclear cytoplasm houses most of the cell's mitochondria (Watson and Avery, 1954), some rough endoplasmic reticulum, and the proximal junctional complex and cell web (Ronnholm, 1962). The supranuclear cytoplasm contains much rough endoplasmic reticulum oriented parallel to the long axis of the cell and an extensive tubular-shaped Golgi apparatus (Kallenbach et al., 1963). Smooth membrane vesicles, coated vesicles, secretion granules, lysosomes, and a few profiles of rough and smooth endoplasmic reticulum are present in the supranuclear cytoplasm (Warshawsky, 1968). Separating the distal cytoplasm from the supramuclear cytoplasm is an extensive cell web (Kallenbach et al., 1965) and distal junctional complex

(Warshawsky, 1978). Tomes' process is relatively devoid of organelles but contains some free ribosomes, microtubules, coated vesicles and a core of secretion granules. In the region of inner enamel secretion, the stratum intermedium consists of a single continuous layer of cuboidal cells with large spherical nuclei. The organization of the discrete layer of stellate reticulum seen in the presecretion zone is lost in the secretion zone. The stratum intermedium, stellate reticulum and the outer dental epithelium are considered to collectively make up the devaloping papillary layer. Further into the secretion zone the papillary layer increases in height and regularity as the thickness of the enamel layer increases.

## Maturation zone enamel organ and enamel

Just prior to the maturation zone in a region termed postsecretory transition, there is a massive programmed death of about 25% of the ameloblast population (Smith and Warshawsky, 1977). This degenerative phase does not appear to include the developing papillary layer; however, the cells of the papillary layer reorganize and the integrity of the stratum intermedium as a layer is lost. As the ameloblasts enter the maturation zone there is a dramatic reorganization of the apical end of the cell such that the ameloblasts assume one of two general morphologies related to the maturing enamel: ruffle-ended or smooth-ended. The two types of maturation ameloblasts are distinct not only in their morphology but in their distribution and type of intercellular junction (Warshawsky and Smith, 1974; Josephsen and Fejerskov, 1977; Boyde and Reith, 1976, 1977). Ruffle-ended

ameloblasts present tight junctional complexes distally while smooth-ended ameloblasts do not show any evidence of these distal junctional complexes. Analysis of cellular renewal and turnover have shown that ameloblast cohorts are produced apically in a cshaped arrangement and these ameloblasts remain as such until they reach the gingival margin (Smith and Warshawsky, 1975, This C-shaped distribution of ameloblasts has been 1977). histologically visualized in the maturation zone of the rat incisor (Takano and Ozawa, 1980; Reith and Boyde, 1981a; Warshawsky, 1985) and furthermore has been correlated with dramatic banding patterns in the enamel visualized by radioautography after injection of 45 calcium and various in vitro staining procedures (Boyde and Reith, 1981, 1982; Reith and Boyde, 1981b; Takano et al., 1982; Reith et al., 1982, 1984). The correlation of the ameloblast distribution pattern with the enamel banding pattern in the maturation zone indicates that the biochemical and physicochemical processes, constituting enamel maturation are under the strict control of the overlying enamel organ.

It was previously suggested that ameloblasts modulate from one morphology to the other as they migrate with the tooth through the enamel maturation zone (Josephsen and Fejerskov, 1977; Smith, 1979; Reith et al., 1982; Takano et al., 1982). Indeed, recently Smith et al. (1987) have confirmed that ruffleended and smooth-ended ameloblasts modulate from one morphology to the other, and in addition have shown that this modulation occurs at a rate far faster than the incisor erupts. This wave of modulation occurs in an incisal direction and the cells

alternate between the two cell types as frequently as three times per day.

Presumably, the alternating changes that occur in the ameloblasts are in some way related to the maturative changes that occur within the enamel at this stage. It is during enamel maturation that most of the organic matrix produced during the secretory stage is removed and the mineral content of the enamel is increased (Deakins, 1942; Weinmann et al., 1942; Reith and Cotty, 1962; Allan, 1967; Robinson et al., 1977). This decrease in protein content has been explained by several theories. Proteins may leave the enamel by simple diffusion, a process possibly aided by the pressure exerted from growing crystallites (Eastoe, 1963). Alternatively, proteolytic enzymes known to be present within the enamel (Suga, 1970; Shimizu et al., 1979; Carter et al., 1984; Crenshaw and Bawden, 1984) may break down enamel proteins into small peptides or amino acids, and these in turn may diffuse out of the enamel or may be intracellularly degraded within ameloblasts of the maturation zone (Nanci et al., 1987).

of the enamel organ is now referred to as the papillary layer since this layer is arranged into a complex network of ridges which run generally perpendicular to the long axis of the tooth. The original three layers of the developing papillary layer (stratum intermedium, stellate reticulum and outer dental epithelium) are no longer distinguishable and numerous capillaries deeply invaginate between ridges of papillary cells.

Presumably, the arrangement of this intricate vascular network is necessary for the bidirectional flow of materials that occurs between the blood supply and the maturing enamel. Although there is little documentation of the development, morphology and function of the papillary layer cells, the presence of numerous cell processes, coated pits and vesicles, mitochondria and gap junctions indicate that these cells may be actively involved in the enamel maturation process.

## Organic matrix of enamel

The organic matrix of enamel consists mainly of protein. These proteins are very heterogeneous in that they differ greatly in amino acid composition, molecular size, charge density and their ability to interact with the mineral phase of enamel (reviewed by Robinson and Kirkham, 1985). Characterized by amino acid composition, enamel proteins can be divided into two broad subfamilies: the amelogenins and the enamelins. Amelogenins are the predominant protein, making up approximately 80% of the developing matrix prior to the maturation process described above. Enamelins are the major protein found in fully mature enamel. Although enamelins are also found in young enamel, it is the selective loss of the amelogenin components that allows them to persist and predominate during enamel maturation.

Amelogenins were first described by Eastoe (1960, 1964) and their properties have become well-documented (reviewed by Fincham and Belcourt, 1985). Amelogenins are characterized by having an amino acid composition relatively high in proline, histidine, glutamine and leucine. They are greatly hydrophobic, poorly

phosphorylated or glycosylated and are soluble in guanidine hydrochloride. Molecular weight determination of amelogenins has demonstrated a wide variety of sizes ranging from 5,000 to 40,000 daltons. Recent studies using mRNA translation products suggest that the size of the primary amelogenin gene product may be approximately 20,000 daltons (Zeichner-David et al., 1984; A complete amino acid sequence for Shimokawa et al., 1984). bovine amelogenin of 170 residues weighing 19,350 daltons has been determined by Takagi et al. (1984). It has been suggested that the 40,000 dalton amelogenin protein present in young enamel may be a proamelogenin molecule and that the amelogenin structure shown immunocytochemically to be within the cell (Nanci et al., 1984) may be a pre-proamelogenin. Regardless of the exact nature of the primary amelogenin, it is generally accepted that degradation of amelogenins occurs in such a way as to produce smaller and smaller peptides with the progression of enamel maturation. Both the exact mechanism of degradation and removal of amelogenin fragments has yet to be determined.

The enamelins (Eastoe, 1960, 1964; Termine et al., 1980) of the organic matrix are acidic proteins, are highly phosphorylated and glycosylated, and are rich in serine, asparagine, glutamine and glycine (reviewed by Robinson and Kirkham, 1985). They range in molecular weight from 8,000 to 72,000 daltons. The fate of enamelins during maturation is not clear. Presumably, they break down and/or are modified since the protein present in fully mature enamel consists of peptide fragments or highly insoluble material. It is believed that these proteins are closely associated with the growing crystallites in enamel since

hydroxyapatite dissolution greatly aids in solubilizing enamelins from enamel. Furthermore, it has been suggested that they may, when arranged in a linear manner, serve to nucleate and delineate the long axes of the crystallites. Further crystallite growth might require the removal of bound enamelins from the crystallite surface. This function of enamelins is consistent with the finding that in vitro incubation of apatite crystals with enamelins almost completely inhibits crystal growth (Doi et al., 1984). Together, amelogenins and enamelins constitute a highly dynamic organic matrix that is necessary to nucleate, promote and control enamel crystallite growth.

## Crystallites of enamel

The structure of the inorganic phase of enamel essentially that of the mineral hydroxyapatite (Ca<sub>10</sub>[PO<sub>4</sub>]<sub>6</sub>[OH]<sub>2</sub>) though some substitutions do occur. In enamel, extremely long hydroxyapatite crystallites are bundled together to form either discrete enamel rods or a continuum of interrod enamel separating the individual rods (Leblond and Warshawsky, 1979; Warshawsky et al., 1981). Individual crystallites, as seen by transmission electron microscopy of isolated crystallites (Menanteau et al., 1984) and in freeze-fracture replicas (Leblond and Warshawsky, 1979; Bai and Warshawsky, 1985; Warshawsky, 1985) are long thin flattened ribbons which gradually spiral along their c-axes. crystallites begin at or near the dentino-enamel junction and end at or near the surface of the enamel. When the final thickness of the enamel layer has been achieved and the crystallites attain -their maximal length, the ongoing process of crystal growth

continues throughout maturation such that the width and thickness dimensions continue to increase. Finally, near the end of enamel maturation, when most of the organic matrix and water have been removed, the intercrystalline spaces diminish such that the individual crystallites grow into each other, leaving their impressions on adjacent crystallites (Warshawsky, 1985). This density of crystallite packing together with the complex intermixing of decussating rods and interrod enamel results in the formation of an enamel layer of great strength and rigidity.

The work presented in this thesis was designed to further investigate fundamental aspects of enamel formation and development. The morphology and certain dynamic principles of amelogenesis in the continuously-erupting rat incisor are well-characterized, and this work represents a logical extension of experiments constructed to examine other morphological and functional aspects of the enamel organ and enamel. It is believed that the ensuing chapters contribute to an understanding of the complex interrelationship between cellular and extracellular components in the tooth, and that some of this knowledge may be further applied to the mineralization process in general as it relates to the other mineralized tissues of the body.

CHAPTER ONE: QUANTITATIVE ANALYSIS OF ROUGH ENDOPLASMIC APPROACHES TO THE CELL MEMBRANE IN THE SECRETORY AMELOBIAST OF THE RAT INCISOR.

# SYNOPŠIS

The distribution of approaches of rough endoplasmic reticulum to the cell membrane within the supranuclear region of the secretory ameloblast of the rat incisor was quantitated using In ameloblasts cut in cross section, most of a Zeiss MOP-3. these approaches appeared as circular profiles representing cross sections of elongated cisternae, which were aligned parallel to the long axis of the cell. Because of their position, orientation, and distribution of ribosomes, these approaches were consistent with the appearance of subsurface cisternae. cross-sectioned ameloblasts, the lengths of apposed plasma membranes either between or within rows of cells were measured from electron micrographs. Along these lengths, matched approaches of rough endoplasmic/reticulum from opposite sides of Thirteen percent of the apposed plasma membranes were counted. approaches were matched between rows of ameloblasts; and 13.5% of the approaches were matched within rows, demonstrating no significant difference between the two sites. Furthermore, mathematical analysis showed that the theoretical probability of two approaches coinciding was 17.0%. The experimental values were not statistically different from the theoretical probability, and it is concluded that the matching of rough endoplasmic reticulum approaches to the plasma membrane, or subsurface cisternae, occurs at random in the secretory ameloblast.

#### INTRODUCTION

Secretory ameloblasts of the rat incisor are arranged in rows parallel to the cross-sectional plane of the tooth. Freezefracture studies (Warshawsky, 1978) have demonstrated different topographical relationships among neighboring secretory ameloblasts between adjacent rows as compared to cells It was shown that tight junctions are better developed between adjacent rows; whereas gap junctions are larger between cells within the rows. However, little is known concerning a possible differential distribution of cellular organelles and how it relates to the organization of ameloblasts into rows. In particular, numerous approaches of rough endoplasmic reticulum (rER) to the cell membrane have been observed in the secretory Approaches of rER to the cell membrane were ameloblast. described in fibroblasts by Ross and Benditt (1964). These were which the cisternal membrane regions in characteristically void of ribosomes. These approaches also resemble the subsurface cisternae (SSC) originally described by Engström (1958).

Since the detailed description of SSC by Rosenbluth (1962), the occurrence of SSC has been documented in a variety of cells. They have been observed in nerve cells of both the central and peripheral nervous system and in sensory cells (reviewed by Takahashi and Wood, 1970; Le Beux, 1972). Subsurface cisternae also occur in the seminiferous tubules of the mouse and cat at the junctional specializations between Sertoli cells in the seminiferous epithelium (Flickinger and Fawcett, 1967). Another

type of SSC has been described in the acinar cells of the rat parotid gland at regions of close apposition of nerves and acinar cells (Hand, 1970, 1972). They have been demonstrated in hepatocytes of mice (Trump et al., 1962,1965; Perissel et al., 1973; Tandler and Hoppel, 1974), in fetal sheep choroid plexus epithelium (Mollgard and Saunders, 1977), and in cultured KB carcinoma cells (Kumegawa et al., 1968). The morphological features of the different types of SSC mentioned above varies considerably, both in terms of the ultrastructure of the individual cisternae themselves as well as their relationship to the plasma membrane.

Subsurface cisternae have also been noted in the enamelproducing ameloblasts of the rat incisor (Kallenbach, 1968; Moe, These were described in the infranuclear region of the 1971). ameloblast as flattened sacs running parallel to the lateral cell membrane at a distance of 10-15 nm. They display ribosomes on the surface facing the cytoplasm but are agranular on the surface facing the cell membrane. Subsurface cisternae begin to appear in ameloblasts related to dentin and are best developed in secretory ameloblasts. In maturation ameloblasts they are still present, but the number of SSC is much fewer in smooth-ended than in ruffle-ended ameloblasts (Josephsen and Fejerskov, 1977). Subsurface cisternae are also present in the supranuclear region. Most often, SSC are not found opposite each other in neighboring cells; however, occasionally they are seen to be matched in apposing ameloblasts. The close proximity between SSC and the plasma membrane may suggest ap attachment between (Smith and Sjostrand, 1961; Rosenbluth, 1962). Rosenbluth (1962)

speculated that SSC might have an effect on cell membrane permeability, possibly in connection with ion transport.

Kallenbach (1968) suggested that SSC may match as a consequence of their having a direct effect on the content of the extracellular space or, conversely, the extracellular contents may exert an effect on SSC that results in their matching.

This work presents a quantitative analysis of approaches of rER to the plasma membrane within the supranuclear region of the secretory ameloblast. The frequency with which these approaches are found opposite each other in neighboring cells within rows or between adjacent rows has been determined and compared to the prediction of random matching of these elements.

## MATERIALS AND METHODS

## Animal procedures and tissue processing

The teeth used in this study were obtained from three male Sherman rats approximately 1 month old weighing 100 ± 5 gm. The animals were anesthetized with an intraperitoneal injection of Nembutal and sacrificed by intracardiac perfusion with 2.5% glutaraldehyde and 2% acrolein. The lower right hemimandibles were decalcified in 4.13% isotonic, neutral disodium EDTA (Warshawsky and Moore, 1967) and were cut into segments which were washed in 0.1 M sodium cacodylate buffer, pH 7.3. The incisor segments were subsequently postfixed in 2% osmium tetroxide, dehydrated through graded acetones and embedded in Epon so that each segment was oriented for sectioning in a plane tangential to the long axis of the incisor. One-micrometer-thick

sections were cut with glass knives on a Reichert OM-U2 ultramicrotome and stained with toluidine blue. An area containing secretory ameloblasts cut in cross section within the supranuclear region was then trimmed, and thin sections were cut with a diamond knife, mounted on copper grids, and stained with uranyl acetate and lead citrate.

## Counting of subsurface cisternae

For each animal, a single section was selected from which 20-30 electron micrographs were taken at a magnification of These were enlarged to a magnification of X22,000. This final magnification was selected as one which would clearly resolve approaches of rER from other vesicular profiles in crosssectioned ameloblasts. Because of the C-shaped curvature of the enamel organ; the plane of section and the area that was trimmed from the Epon block, the series of electron micrographs represented a random sample of pictures from all levels of the supranuclear region of the ameloblast. Care was taken in order not to overlap any of the electron micrographs in order that an approach would not be counted more than once. A Zeiss MOP-3 was used to measure the apposed lengths of plasma membrane between neighboring ameloblasts. All measurements were separated according to whether the apposed membranes were between or within rows of ameloblasts. Along these lengths, approaches of rER from either side of the apposed membranes were counted. was defined as a profile of rER which, at X22,000 magnification, appeared to make contact with the plasma membrane. Maintaining the same criteria for an approach as above, matched approaches

were counted when two approaches from opposite sides of the apposed plasma membranes coincided within a distance of 1 mm.

#### RESULTS

## Morphological appearance of SSC

The tangential plane of section showed ameloblasts cut in cross section. Within the supranuclear region at the level of the Golgi apparatus, the hexagonal or pentagonal shape of the ameloblasts and their arrangement into rows was seen (Fig. 1). Numerous profiles of rER were present and most approaches of rER to the cell membrane appeared as circular profiles (Fig. 2). Longitudinal sections of the supranuclear region of the ameloblasts showed that approaches of rER were cut parallel to their long axis (Figs. 3,4) and resembled the typical SSC (Fig. 5) described by Kallenbach (1968) and Moe (1971). Subsurface cisternae were matched by other SSC or unmatched but always lacked ribosomes on the side apposed to the plasma membrane and were separated from the plasma membrane by a uniform distance.

# Statistical analysis of SSC

Counts for matched and unmatched approaches of rER to the lengths of apposed plasma membrane measured between rows and within rows of ameloblasts are shown in Table 1. Similar lengths were measured among the experimental animals. Table 2 shows that these counts were not significantly different per millimeter of apposed plasma membrane whether found between rows or within rows. Furthermore, the 13.0% of approaches that were matched between rows did not differ significantly from the 13.5% of

approaches that were matched within rows.

# Determination of random probability of SSC matching

The possibility that these percentages occurred simply by random chance was then investigated. Statistical analysis (see Appendix) showed that the probability that two approaches of rER should coincide under the defined criteria is 17.0%. The experimental values were not statistically different from the theoretical probability, and it was concluded that the matching of approaches of rER to the cell membrane in the form of SSC occurred at random.

### DISCUSSION

Intercellular communication may be partly responsible for the coordinated effort of a row of ameloblasts to produce enamel rods that incline differently from those immediately in front of and behind them. In the rat incisor, alternate rows of secretory ameloblasts have different three-dimensional arrangements as well as ultrastructural variations (Warshawsky, 1978). The ameloblast body is curved so that the proximal and distal ends of the cell point in the same direction, either mesially or laterally, and the central part of the cell bulges out in the opposite direction. A row of cells consists of a mesial-lateral aggregation of similarly curved cells. A row of cells that are curved so that their proximal and distal ends are laterally directed will be sandwiched between two rows in which the cells curve in the opposite direction. In addition, tight junctions are larger between cells in a row. This different threedimensional arrangement displays its functional significance by producing alternating inclinations of enamel rods. The present work was undertaken to determine whether a correlation exists between neighboring ameloblasts and the distribution of rough endoplasmic reticulum.

A striking feature of cross-sectioned ameloblasts is the frequent approaches of rER profiles to the cell membrane (Nanci and Warshawsky, 1984). Some approaches of rER are similar to the SSC described in the infranuclear region of the secretory ameloblast by Kallenbach (1968) and Moe (1971), and to SSC in other cell types. Because most ER in ameloblasts is oriented parallel to the long axis of the cell, longitudinal sections are less likely to intersect approaches of rER to the plasma membrane than are cross sections, and thus approaches are quantitatively more numerous in cross sections of ameloblasts. However, in longitudinally cut ameloblasts, only very specific planes of section would show these approaches as typical subsurface cisternae (Figs. 3-5).

This report has presented data pertaining to the distribution of approaches of rER to the cell membrane in the supranuclear cytoplasm of the secretory ameloblast. The results show that despite the frequent matching of these approaches, this is only a random phenomenon as emphasized by the large number of approaches that are unmatched. This does not rule out the possibility that the approaches themselves may occur at a frequency that is greater than random, that is, there may be a differential distribution of rER within the supranuclear cytoplasm. However, these data demonstrate that the percentage

of matched approaches to unmatched approaches does not differ whether between rows or within rows.

The results do not suggest any obvious function mediated by the distribution of SSC, nor do they refute any of the previously proposed functions of SSC (Rosenbluth, 1962; Kallenbach, 1968). It remains entirely possible that SSC are responsible for some form of intercellular communication. However, if such a mode of communication exists, then it does not occur as a direct consequence of the number of matched and unmatched SSC, since these occur equally both between and within rows of secretory ameloblasts.

TABLE 1

Plasma membrane lengths of adjacent ameloblasts and the corresponding counts of matched and unmatched approaches of rER from ameloblasts cut in cross section

, • -	Exp. Animal	_ Between Rows	Within Rows
Apposed lengths of	1	20,411	21,860
plasma membrane (mm) <sup>1</sup>	2	19,102	20,248
<b>.</b>	3	20,040	20,703
Approaches of rER from either	1	1,224	1,476
side of the apposed plasma mem-	2	1,368	1,560
branes (unmatched approaches).	3 °	1,630	1,869
Approaches of rER on opposite	1	170	204
sides of the apposed plasma mem-	2	202	236
branes that coincided within 1 mm (matched approaches).	a 3	184	202

las measured in the electron micrographs.

TABLE 2

The number of matched and unmatched approaches of rER to the approach plasma membranes and the frequency of matched approaches

٠	Exp.	Between	Within
	Animal	Rows	Rows
Unmatched approaches of rER	. 1	. 060	.068
per millimeter of apposed plasma membranes.	, <b>2</b> - 3	.071	.077
Matched approaches of rER per, millimeter of apposed plasma membranes.	1	.008 <sup>7</sup>	.009
	2	.010	.012
	3	.009	.010
Percentage matched to unmatched	1	13.9	13.8
	2	14.1	15.6
	3	11.1	11.0
Average	•	13.0%	13.5%

#### APPENDIX

Method to determine whether or not the occurrence of matched approaches of rER to the cell membrane is a random phenomenon

Consider electron micrographs magnified 22,200 times, in which the distance between two approaches to the same membrane is b mm (see Fig. 1). If an approach from the apposing cell is located at random, then the probability that it will strike within a certain distance (a) to either side of either of the first two approaches is a. The mean probability for N observations will be:

$$\sum_{n=1}^{n=N} \frac{\underline{a}}{b_n} \quad \text{where n is the observation number 1,2,...N}$$

Measuring b in 216 observations, the value of  $\sum_{n=1}^{n=216} \frac{1}{b_n}$  was 18.7

mm. Using a = 2 mm (1 mm to either side of an approach) and the value obtained above (18.7 mm), the theoretical probability was calculated to be 17.0% according to the expression for mean probability over N observations. Experimentally, the incidence where the second approach struck within 2 mm of the first approach was 13.0% between rows and 13.5% within rows. These values are not statistically different from the theoretical ratio of 17.0% ( $p \le 0.05$ ). Therefore, it is concluded that the matching of approaches of rER to the cell membrane occurs at random.

#### REFERENCES

Allan JH 1967 Maturation of enamel. In: Structural and Chemical Organization of Teeth. Ed. Miles AEW. Academic Press, New York. pp. 467-492.

Bai P and Warshawsky H 1985 Morphological studies on the distribution of enamel matrix proteins using routine electron microscopy and freeze-fracture replicas in the rat incisor. Anat Rec, 212:1-16.

Boyde A and Reith EJ 1976— Scanning electron microscopy of the lateral cell surfaces of rat incisor ameloblasts. J Anat, 122:603-610.

Boyde A and Reith EJ 1977 Scanning electron microscopy of rat maturation ameloblasts. Cell Tiss Res, 178:221-228.

Boyde A and Reith EJ 1981 Display of maturation cycles in ratincisor enamel with tetracycline labelling. Histochem, 72:551-561.

Boyde A and Reith EJ 1982 In vitro histological and tetracycline staining properties of surface layer rat incisor enamel also reflect the cyclical nature of the maturation process. Histochem, 75: 341-351.

Carter J, Smillie AC and Shepherd MG 1984 Proteolytic enzyme in developing porcine enamel. In: Tooth Enamel IV. Eds. Fearnhead RW and Suga S. Elsevier Science Publishers, Amsterdam. pp. 229-233.

Crenshaw MA and Bawden JW 1984 Proteolytic activity in embryonic bovine secretory enamel. In: Tooth Enamel IV. Eds. Fearnhead RW and Suga S. Elsevier Science Publishers, Amsterdam. 109-113.

Deakins M 1942 Changes in the ash, water and organic content of pig enamel during calcification. J Dent Res, 21:429-435.

Eastoe JE 1960 Organic matrix of tooth enamel. Nature 187:411.

Eastoe JE 1963 The amino acid composition of proteins from the oral tissues. II. The matrix proteins in dentine and enamel from developing human deciduous teeth. Archs Oral Biol, 8:633-652.

Eastoe JE 1964 The chemical composition of bone and teeth. Adv Fluorine Res Dent Caries Prevent, 3:5-16.

Engström H 1958 On the double innervation of the sensory epithelia of the inner ear. Acta Otolaryng, 49:109-118.

Fincham AG and Belcourt AB 1985 Amelogenin biochemistry: Current concepts. In: The Chemistry and Biology of Mineralized Tissues. Ed. Butler WT. Ebsco Media, Birmingham. pp. 240-247.

Flickinger C and Fawcett DW 1967 The junctional specializations of Sertoli cells in the seminiferous epithelium. Anat Rec, 158:207-222.

Hand AR 1970 Nerve-acinar relationships in the rat parotid gland. J Cell Biol, 47:540-543.

Hand AR 1972 Adrenergic and cholinergic nerve terminals in the rat parotid gland. Electron microscopic observations on permanganate-fixed glands. Anat Rec, 173:131-140.

Josephsen K and Fejerskov 0 1977 Ameloblast modulation in the maturation zone of the rat incisor enamel organ. A light and electron microscopic study. J Anat, 124:45-70.

-Kallenbach E 1968 Fine structure of rat incisor ameloblasts during enamel maturation. J Ultrastruct Res, 22:90-119.

Kallenbach E, Sandborn E and Warshawsky H 1963 The Golgi apparatus of the ameloblast of the rat at the stage of enamel matrix formation. J Cell Biol, 16:629-632.

Kallenbach E, Clermont Y and Leblond CP 1965 The cell web in the ameloblast of the rat incisor. Anat Rec, 153:55-70.

Kumegawa M, Cattoni M and Rose GG 1968 Electron microscopy of oral cells in vitro. II. Subsurface and intrácytoplasmic confronting cisternae in strain KB cells. J Cell Biol, 36:443-452.

Le Beux YJ 1972 Subsurface cisterns and lamellar bodies: Particular forms of the endoplasmic reticulum in the neurons. Z Zellforsch, 133:327-352.

Leblond CP and Warshawsky H 1979 Dynamics of enamel formation in the rat incisor tooth. J Dent Res, 58(B):950-975.

Menanteau J, Mitre D and Daculsi G 1984 Aqueous density fractionation of mineralizing tissues: An efficient method applied to the preparation of enamel fractions suitable for crystal and protein studies. Calcif Tiss Int, 36:677-681.

Moe H 1971 Morphological changes in the infranuclear portion of the enamel-producing cells during their life cycle. J Anat, 108:43-62.

Mollgard K and Saunders NR 1977 A possible transepithelial pathway via endoplasmic reticulum in foetal sheep choroid plexus. Proc Roy Soc Lond, 199:321-326.

Nanci A, Bendayan M, Bringas P and Slavkin HC 1984 High resolution immunocytochemical localization of enamel proteins in situ and in cultured mouse ameloblasts. In: Tooth Morphogenesis and Differentiation. Eds. Belcourt AB and Ruch J-V. Inserm

Publications, Paris. pp. 333-340.

Nanci A and Warshawsky H 1984 Characterization of putative secretory sites on ameloblasts of the rat incisor. Am J Anat, 171:163-189.

Nanci A, Slavkin HC and Smith CE Immunocytochemical and radioautographic evidence for secretion and intracellular degradation of enamel proteins by ameloblasts during the maturation stage of amelogenesis in the rat incisor. Anat Rec, 217:107-123.

Perissel B, Malet P and Geneix A 1973 Associations jonctionsorganites cellulaires dans le foie neo-natal de souris. Z Zellforsch, 140:77-89.

Reith EJ and Cotty VF 1962 Autoradiographic studies on calcification of enamel. Archs Oral Biol, 7:365-372.

Reith EJ and Boyde A 1981a The arrangement of ameloblasts on the surface of maturing enamel of the rat incisor tooth. J Anat, 133:381-388.

Reith EJ and Boyde A 1981b The cyclical entry of calcium into maturing enamel of the rat incisor tooth. Archs Oral Biol, 26:983-988.

Reith EJ, Boydé A and Schmid MI 1982 Correlation of rat incisor ameloblasts with maturation cycles as displayed on the enamel surface with EDTA. J Dent Res, 61:1563-1573.

Reith EJ, Schmid MI and Boyde A 1984 Rapid uptake of calcium in maturing enamel of the rate incisor. Histochem, 80:409-410.

Robinson C, Lowe NR and Weatherell JA 1977 Changes in amino acid composition of developing rat incisor enamel. Calcif Tiss Res, 23:19-31.

Robinson C and Kirkham J 1985 Dynamics of amelogenesis as revealed by protein compositional studies. In: The Chemistry and Biology of Mineralized Tissues. Ed. Butler WT. Ebsco Media, Birmingham. 2487263.

Ronnholm E 1962 An electron microscope study of amelogenesis in human teeth. I. The fine structure of ameloblasts. J Ultrastruct Res, 6:229-248.

Rosenbluth J 1962 Subsurface cisterns and their relationship to the neuronal plasma membrane. J Cell Biol, 13:405-421.

Ross 'R and Benditt EP 1964 Wound healing and collagen formation. IV. Distortion of ribosomal patterns of fibroblasts in scurvy. J Cell Biol, 22:365-390.

Shimizu M, Tanabe T and Fukae M 1979 Proteolytic enzyme in porcine immature enamel. J Dent Res, 58(B):782-788,

Shimokawa H, Wassmer P, Sobel ME and Termine JD 1984 Characterization of cell-free translation products of mRNA from bovine ameloblasts by monoclonal and polyclonal antibodies. In: Tooth Enamel IV. Eds. Fearnhead RW and Suga S. Elsevier Science Publishers, Amsterdam. pp. 161-166.

Smith CA and Sjostrand FS 1961 A synaptic structure in the hair cells of the guinea pig cochlea. J Ultrastruct Res, 5:184-192.

Smith CE 1979 Ameloblasts: Secretory and resorptive functions. J Dent Res, 58(B):695-706.

Smith CE and Warshawsky H 1975 Cellular renewal in the enamel organ and the odontoblast layer of the rat incisor as followed by radioautography using  $^3\text{H-thymidine}$ . Anat Rec, 183:523-562.

Smith CE and Warshawsky H 1977 Quantitative analysis of cell turnover in the enamel organ of the rat incisor. Evidence for cell death immediately after enamel matrix secretion. Anat Rec, 187:63-98.

Smith CE, McKee MD and Nanci A 1987 Cyclic induction and rapid movement of sequential waves of new smooth-ended ameloblast modulation bands in rat incisors as vizualized by polychrome fluorescent labelling and GBHA-staining of maturing enamel. J Dent Res, In Press.

Suga S 1970 Histochemical observation of proteolytic enzyme activity in the developing dental hard tissues of the rat. Archs Oral Biol, 15:555-558.

Takagi T, Susuki M and Baba T 1984 Complete amino acid sequence of amelogenin in developing bovine enamel. Biochem Biophys Comm, 121:592-597.

Takahashi K and Wood RL 1970 Subsurface cisterns in the Purkinje cells of the cerebellum of Syrian hamster. Z Zellforsch, 133:327-352.

Takano Y and Ozawa H 1980 Ultrastructural and cytochemical observations on the alternating morphological changes of the ameloblasts at the stage of enamel maturation. Archs Hist Jap, 43:385-399.

Takano Y, Crenshaw MA, Bawden JW, Hammarström L and Lindskog S 1982 The visualization of the pattern of ameloblast modulation by the glyoxal bis(2-hydroxyanil) staining method. J Dent Res, 61:1580-1586.

Tandler B and Hoppel CL 1974 Subsurface cisterns in mouse hepatocytes. Anat Rec, 179:273-284.

Termine JD, Belcourt AB, Christner PJ, Conn KM and Nylen MU 1980 Properties of dissociatively extracted fetal tooth enamel proteins. I. Principal molecular species in developing bovine enamel. J Biol Chem, 255:9760-9768.

Trump BF, Goldblatt PJ and Stowell RE 1962 An electron microscopic study of early cytoplasmic alterations in hepatic parenchymal cells of mouse liver during necrosis in vitro (autolysis). Lab Invest, 11:986-1015.

Trump BF, Goldblatt PJ and Stowell RE 1965 Studies on necrosis in vitro of mouse hepatic parenchymal cells. Ultrastructural alterations in endoplasmic reticulum, Golgi apparatus, plasma membrane, and lipid droplets. Lab Invest, 14:2000-2028.

Warshawsky H 1968 The fine structure of secretory ameloblasts in the rat incisor. Anat Rec, 161:211-230.

Warshawsky H · 1978 A freeze-fracture study of the topographic relationship between inner enamel-secretory ameloblasts in the rat incisor. Am J Anat, 152:153-208.

Warshawsky H 1985 Ultrastructural studies on amelogenesis. In: The Chemistry and Biology of Mineralized Tissues. Ed. Butler WT. Ebsco Media, Birmingham. pp. 33-45.

Warshawsky H and Moore G 1967 A technique for the fixation and decalcification of rat incisors for electron microscopy. J Histochem Cytochem, 15:542-549.

Warshawsky H and Smith CE 1974 Morphological classification of rat incisor ameloblasts. Anat Rec, 179:423-446.

Warshawsky H, Josephsen K, Thylstrup A and Fejerskov O 1981 The development of enamel structure in rat incisors as compared to the teeth of monkey and man. Anat Rec, 200:371-399.

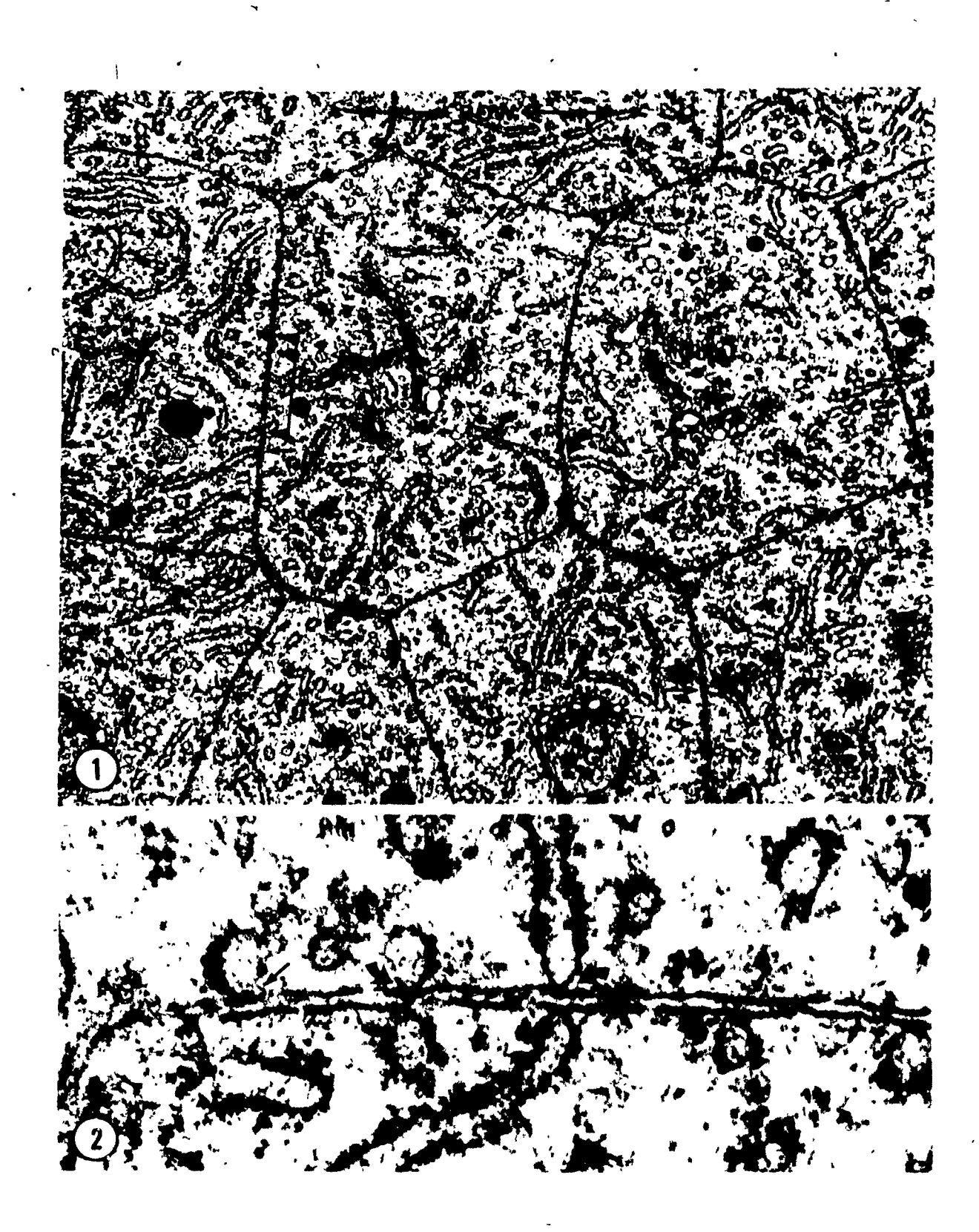
Watson ML and Avery JK 1954 The development of the hamster lower incisors as observed by electron microscopy. Am J Anat, 95:109-161.

Weinmann J, Wessinger GD and Reed G 1942 Correlation of chemical and histological investigations on developing enamel. J Dent Res, 21:171-182.

Zeichner-David M, Snead M and Slavkin HC 1984 Genetic differences in enamel gene products amongst mammalian species. In: Tooth Morphogenesis and Differentiation. Eds. Belcourt AB and Ruch J-V. Inserm Publications, Paris. pp. 355-362.

Figure 1. Tangential plane of section shows ameloblasts cut in cross section within the supranuclear region at the level of the Golgi apparatus (G). Ameloblasts are hexagonal or pentagonal in shape and are arranged into rows. Matched profiles of rER (curved arrows) and unmatched profiles (straight arrows) are numerous. Thin wedgelike projections of cytoplasm (asterisks) insinuate between two adjacent cells. Occasional coated vesicles (cv) may be seen. Arrowheads indicate distance b (see Appendix). X20,000.

Figure 2. Higher magnification shows detail of matched (curved arrows) and unmatched (straight arrows) approaches of rER between rows of ameloblasts at the apposed plasma membranes. Note the absence of ribosomes on the side of the approach facing the plasma membrane. X84,000.



Figures 3-5. Longitudinal sections of secretory ameloblasts showing matched (Fig. 3, X63,000) and unmatched (Fig. 4, X88,000) SSC cut parallel to their long axis. Figures 3 and 4 are at the supranuclear level, whereas Figure 5 (X63,000) shows similarly matched SSC in the infranuclear region. In all cases, SSC lack ribosomes on the surface apposed to the plasma membrane and are separated from it by a uniform distance. Curved arrows, matched SSC; straight arrows, unmatched SSC and rER approaches; m, mitochondrion.



CHAPTER TWO: THE STRUCTURE AND DEVELOPMENT OF THE PAPILLARY
LAYER AND THE PENETRATION OF VARIOUS MOLECULARWEIGHT PROTEINS INTO THE ENAMEL ORGAN AND ENAMEL
OF THE RAT INCISOR.

### SYNOPSIS

During enamel maturation, most of the organic matrix is removed as the mineral content increases; it is postulated that proteolytic enzymes within enamel break down large proteins into more mobile fragments. To predict how such fragments might leave the enamel, the morphology of the enamel organ and the entry and penetration of various proteins into it was examined. Rats (100 gm) were injected via the external jugular vein with 1251iodinated calcitonin (mol. wt. 3,600), insulin (mol. wt. 5,700), epidermal growth factor (EGF; mol. wt. 6,100) and albumin (mol. wt. 68,000). The animals were sacrificed after 10 min and radioautographs were made to visualize these molecules in the incisor enamel organ and enamel. In addition, dissected incisors were wiped free of their enamel organs, dipped in the iodinated protein solutions for 10 min, and processed for radioautography. In all dipped teeth, except those exposed to albumin, there was a gradient of silver grain density over the entire thickness of enamel in both the secretion and maturation zones. injected animals, enamel labeling in the secretion zone was only s!ightly above background. In the maturation zone of animals injected with calcitonin and insulin, many grains were over enamel adjacent to smooth-ended ameloblasts but not ruffle-ended ameloblasts. Animals injected with EGF and albumin had no labeled enamel in the maturation zone. Thus dipped rat incisor

enamel was permeable to proteins with molecular weights as high as 6,100 daltons. Localization of injected proteins indicates that the enamel organ restricts their passage to the enamel, but proteins with molecular weights as high as 5,700 daltons may pass into enamel through or between smooth-ended ameloblasts. As exogenous proteins readily diffused into the enamel, it seems likely that enamel proteins of similar size can leave enamel by a similar route.

#### INTRODUCTION

Enamel formation requires a high degree of cellular interaction in the enamel organ (Warshawsky and Smith, 1974). In the secretion zone, the primary function of the enamel organ is to elaborate the organic matrix of enamel (reviewed by Weinstock and Leblond, 1971; Slavkin et al., 1976; Warshawsky, 1979; Karim and Warshawsky, 1979). In the maturation zone, most of the organic matrix is removed whereas the mineral content, in the form of hydroxyapatite, is increased (Deakins, 1942; Weinmann et al., 1942; Allan, 1967; Reith and Cotty, 1962; Robinson et al., 1977). The mechanism whereby organic matrix is removed and the mineral content increased is still not clear. Immediately adjacent to the maturing enamel are two distinct forms of maturation ameloblast (Suga, 1959), each with a different distribution and type of intercellular junction (Warshawsky and Smith, 1974; Josephsen and Fejerskov, 1977; Boyde and Reith, Several studies have demonstrated the band-like 1976, 1977). arrangement of smooth-ended and ruffle-ended ameloblasts across the rat incisor (Takano and Ozawa, 1980; Reith and Boyde, 1981a; Warshawsky, 1985; Nanci et al., 1987). Other studies have correlated various banding patterns in rat bincisor enamel with the distribution of the two types of maturation ameloblast (Boyde and Reith, 1981, 1982; Reith and Boyde, 1981b; Reith et al., 1982, 1984; Takano et al., 1982; Josephsen, 1983; Smith et al., These correlations indicate that the maturation pattern of rat incisor enamel is under the strict control of the overlying enamel organ.

Regulation of the local environment at various body surfaces is an important homeostatic function of epithelial tissues. tight junction is the structure that limits epithelial, permeability through the intercellular spaces. The tightness and leakiness of such junctions has been assessed by examining the extracellular penetration of such tracers as lanthanum (Garant, 1972; Takano and Crenshaw, 1980; Shaklai and Tavassoli, 1982) and horseradish peroxidase (Skobe and Garant, 1974; Takano and Ozawa, 1980; Kallenbach, 1980a,b). However, some controversy exists as to the dimensions, ionic charges and effects of these molecules. Revel and Karnovsky (1967) assumed that, in their technique, / lanthanum is in colloidal form and therefore acts as a passive tracer of extracellular space. However, Schatzki and Newsome (1975) showed that at physiological pH, at least 70% of lanthanum is in the ionic form, and that deposits observed by electron microscopy may be due to it having either colloidal or noncolloidal dimensions. In addition, due to its cationic nature, lanthanum may bind to cell glycoproteins, cell membrane phospholipids and calcium-binding sites (reviewed by Shaklai and Tavassoli, 1982). Horseradish peroxidase (HRP) exhibits anomalous behaviour relative to its molecular size (Mazariegos et al., 1984; Mazariegos and Hand, 1985); it may damage cell membranes and junctions through its peroxidative activity and glycoproteinaceous nature. Furthermore, certain rat strains suffer a histamine reaction with increased vascular permeability after injection of HRP (Simionescu et al., 1975).

To avoid the pitfalls of using certain exogenous tracers, we have employed various normally-occurring proteins to trace access

to the enamel layer. Proteins of different molecular weight were labeled with \$125\$I and radioautography was used to localize these molecules within the enamel organ and enamel of the rat incisor. In addition, the structure and development of the papillary layer was investigated so as to morphologically identify possible access routes for proteins as they pass to the enamel. The main purpose of this work was to study the behavior of enamel proteins during secretion and maturation. Newly-synthesized enamel proteins randomize through enamel soon after secretion (reviewed by Leblond and Warshawsky, 1979). Proteolytic enzymes within maturing enamel may break down large proteins into more mobile fragments that can diffuse freely out of the enamel and through the ameloblast layer (Suga, 1970). This investigation might serve to predict how enamel proteins enter and leave the enamel.

## MATERIALS AND METHODS

### Tissue processing for electron microscopy

Sherman and Sprague-Dawley rats were anesthetized with an intraperitoneal injection of Nembutal and sacrificed by perfusion through the left ventricle. The vasculature was prerinsed with lactated Ringer's solution (Abbott Laboratories) for 30 sec followed by perfusion for 15 min with 5% glutaraldehyde in 0.05 M sodium cacodylate buffer, pH 7.3. The mandibles were dissected and immersed in the above fixative for 4 h at 4°C followed by washing in 0.1 M sodium cacodylate buffer containing CaCl<sub>2</sub>, pH 7.3. The mandibles were decalcified in 4.13% isotonic neutral disodium EDTA (Warshawsky and Moore, 1967) and were cut into

segments that were washed extensively in the above 0.1 M sodium cacodylate buffer. The incisor segments subsequently were postfixed in reduced osmium for 2 h at 4°C, dehydrated through a graded acetone series and embedded in Epon 812. Each segment was oriented for sectioning in a plane perpendicular to the long axis of the incisor. One-micrometer-thick sections were cut with glass knives on a Reichert OM-U2 ultramicrotome and stained with toluidine blue. Areas for thin sectioning were trimmed and cut with a diamond knife, mounted on copper grids and stained with uranyl acetate and lead citrate. Sections were examined with a JEOL 2000FX at 80 kV.

### Dipping experiment

•

Under pentobarbital anesthesia, mandibular incisors from 100 gm male Sherman and Sprague-Dawley rats were dissected quickly from the surrounding alveolar bone. The enamel organs were wiped from the teeth with gauze moistened in normal saline. Each incisor was then immersed for 10 min in a 3 ml saline solution at 4°C containing 0.5 ml (approximately 500 x 106 cpm) of one of the following freshly-prepared iodinated proteins in phosphate buffer: 125I-salmon calcitonin (mol. wt. 3,600), 125<sub>I-porcine</sub> insulin (mol. wt. 5,700), 125I-murine epidermal growth factor (EGF; mol. wt. 6,100) or  $^{125}I$ -bovine serum albumin (mol. wt. The iodinations were performed by the Chloramine T method (Hunter and Greenwood, 1962; Posner et al., 1978); the iodinated proteins were purified on Sephadex columns and had specific activities of 650, 142, 163 and 13 µCi/µg, respectively. After removal from the radioactive solutions, incisors were

rinsed for 5 sec in saline and immersion-fixed for 4 h at 4 °C in 2.5% glutaraldehyde in 0.05 M sodium cacodylate buffer. They were then demineralized in 4.13% EDTA and cut into segments which were washed and postfixed in 2% osmium tetroxide. The segments were dehydrated through graded acetones and embedded in Epon. One-micrometer-thick sections were cut, stained with iron hematoxylin and processed for radioautography according to Kopriwa and Leblond (1962).

# Systemic injection experiment

Under pentobarbital anesthesia, male Sherman and Sprague-Dawley rats, approximately 3 wks old and weighing 60  $\pm$  10 gm, were injected via the external jugular vein with approximately 0.2 ml (160-300 x  $10^6$  cpm) of one of the iodinated proteins in 0.05 M phosphate buffer, pH 7.4. The animals were sacrificed 10 'min after injection by intracardiac perfusion with lactated " Ringer's solution for 30 sec followed by perfusion for 10 min with 2.5% glutaraldehyde in 0.05 M sodium cacodylate buffer, pH The mandibles were dissected and immersed in the fixative for 4 h at 4°C followed by demineralization, postfixation, dehydration and embedding as above. Sections were processed for light microscope radioautography. The extent of the background labeling in the radioautographs was assessed for each of the four molecules used; an area of 68,890 um<sup>2</sup> was chosen in unlabeled dentin and the number of silver grains was counted within that The background level of labeling for each experiment varied between 5 and 7 grains/500 um2. Representative counts over similar areas of enamel were compared to the background counts.

#### RESULTS

# Presecretion zone enamel organ morphology

In the zone of presecretion, just prior to the synthesis of the organic matrix of enamel, tall columnar ameloblasts formed a compact epithelial layer apposed to the dentin (Fig. 1). Their apical surfaces marked the site of the future dentino-enamel junction where numerous cell processes from the ameloblasts interdigitated with collagen fibers of the dentin matrix. Occasional odontoblast processes traversed the dentin and appeared to make contact with the ameloblasts. Small accumulations of an enamel-like substance were present at this stage. The remaining layers of the enamel organ, referred to as the developing papillary layer in the presecretion zone, were situated immediately between the ameloblasts and the capillary bed related to the labial side of the tooth.

The developing papillary layer traditionally has been subdivided into three cellular regions: (1) the stratum intermedium (closest to the ameloblasts), (2) the stellate reticulum and, (3) the outer dental epithelium (closest to the blood supply).

of 2 to 3 irregular layers of closely-packed cuboidal cells that were immediately adjacent to the basal sulges of the ameloblasts (Fig. 2). The cells were packed such that the stratum intermedium maintained a uniform thickness across the developing papillary layer. The cells tightly interdigitated with each other via their irregular outlines and numerous cell processes.

Desmosomes commonly were present between stratum intermedium cells, and between cells of the stratum intermedium and the stellate reticulum and the ameloblasts. The cytoplasm of cells of the stratum intermedium had a range of staining densities such that dark and light cells could be identified.

Interposed between the stratum intermedium and the outer dental epithelium was the stellate reticulum, a layer consisting of loosely-arranged, stellate-shaped cells (Fig. 3). Processes branched from the cells towards each other and often were connected by desmosomes. Within the stellate reticulum the extracellular space was extensive.

The outer dental epithelium, the outermost layer of the enamel organ, was separated from the capillaries and the periodontal connective tissue by a basement membrane which derived from the original embryological invagination of the oral epithelium (Fig. 3). Immediately adjacent to the basement membrane was the capillary endothelium and periodontal connective tissue. The outer dental epithelium consisted of a single layer of cuboidal cells tightly interlocked by numerous cell processes and sometimes connected by desmosomes. Occasional lipid droplets and glycogen deposits were present within these cells, along with a moderate amount of cellular organelles.

## Secretion zone enamel organ morphology

In the secretion zone, ameloblasts were actively engaged in synthesizing and secreting the organic matrix of enamel. The tall columnar ameloblasts developed the interdigitating portions of Tomes' processes that interdigitated with interrod enamel

(Fig. 4). Tomes' processes showed both rod and interrod growth sites and numerous secretory granules in the interdigitating portion of Tomes' process. Occasional branching of Tomes' process was observed (Fig. 4).

The stratum intermedium of the developing papillary layer was adjacent to the secretory ameloblasts and consisted of a single layer of cuboidal cells with large spherical nuclei (Fig. 5). The cells all stained uniformly, had moderate amounts of cellular organelles, and were connected by desmosomes. Apposing cell membranes had numerous interdigitating cell processes with more extracellular space between them than in the presecretion zone. The thickness of the stratum intermedium was fairly constant throughout the secretion zone.

The stellate reticulum and outer dental epithelium of the developing papillary layer were no longer visible as distinct layers (Fig. 6). The deeper invagination of capillaries caused the developing papillary ridges to be more pronounced. The cells of the papillae were loosely-arranged and extracellular space was extensive. The cells had numerous cell processes and mitochondria appeared to be more frequent. Separating the papillae from the flattened fibroblasts and collagen of the periodontal connective tissue was a basement membrane which invested the entire enamel organ.

## Maturation zone enamel organ morphology

In the maturation zone of amelogenesis, ameloblasts could generally be considered as being either ruffle-ended or smoothended with regard to their distal cell surface. Ruffle-ended

ameloblasts (Fig. 7) occupied the majority of the maturation zone and were identified by their highly-invaginated distal cell membrane which formed a distinctive ruffled border related to the maturing enamel. The exact nature of the ruffling varied depending on the region of the maturation zone, but in general, adjacent ruffled borders between cells were sealed by tight junctions (Fig. 8). Mitochondria accumulated just proximal to the ruffled borders and occasionally would slip in between individual membrane invaginations. Numerous vesicular profiles were found in close proximity to the ruffled border. Hemidesmosomes were observed on ruffle-ended ameloblasts where a basement membrane-like material was present between the cells and the enamel.

Smooth-ended ameloblasts were found less frequently than ruffle-ended ameloblasts but were easily identified by their lack of a distal ruffled border (Fig. 9). The cells had numerous mitochondria homogeneously dispersed throughout the cytoplasm. Tonofilaments and a moderate amount of other cellular organelles were present. Most obvious was the extensive extracellular space containing what appeared to be membrane remnants. The distal portions of smooth-ended ameloblasts were not sealed by tight junctions and frequently the extracellular space between ameloblasts was continuous up to the basement, membrane-like In the most distal material adjacent to the enamel (Fig. 9). cytoplasm of the ameloblasts, numerous vesicles were present among randomly-distributed mitochondria (Fig. 10). The vesicles often appeared as one ring of membrane enclosed by another. Hemidesmosomes were numerous where the slightly-undulated distal

cell membrane made contact with the basement membrane-like material.

In the maturation zone, the three distinct layers of developing papillary layer were indistinguishable and collectively they formed the papillary layer (Fig. The papillary ridges were very prominent as defined by the deeplyinvaginated capillaries. The papillary layer cells were so closely packed and had such extensive interdigitating regions of cell membrane that individual cell profiles were difficult to discern. The nuclei of these cells were generally spherical and numerous mitochondria, junctional complexes, annular junctions and vesicles were present in these cells. Figure 12 shows, at higher magnification, a region of the papillary layer adjacent to an invaginated capillary. Most of the capillaries throughout the enamel organ in all the zones of amelogenesis were highly fenestrated. The cells of the papillary layer in the maturation zone were closely apposed to the capillaries and the junctions between cells formed channels of cell processes that appeared to radiate away from the capillaries (open arrows, Fig. Frequently observed in regions of papillary layer cells closest to the capillaries were areas of cytoplasm that contained numerous vesicular and tubular structures (Figs. 12, brackets; 13,14). These "foot pads" were separated from the endothelium of the capillaries by the investing basement membrane of the enamel organ, some loose connective tissue, and the basement membrane of the capillaries. The membranous profiles in the "foot pads" Were either coated, smooth, cup-shaped and/or elongated tubules (Figs.

13,14). Occasionally, coated pits, gap junctions and apparent fusions of membranous profiles were observed (Fig. 14).

A common feature of all enamel organ capillaries was their highly-fenestrated endothelium. Figure 15 shows such a capillary in the maturation zone which is deeply invaginated between two papillae of the papillary layer. Higher magnification of a similar capillary (Fig. 16) shows that these fenestrations are closed by diaphragms, often with a small electron dense knob in their center. Another feature of enamel organ capillaries was the occasional presence of multiple layers of basement membrane between the capillary endothelium and the papillary layer cells (Fig. 17).

## Calcitonin penetration

In the freshly-dissected incisor wiped free of its enamel organ, an intact enamel layer covered the surface of the tooth (Figs. 18a,b). In the secretion zone, the enamel had surface pits due to the removal of ameloblasts and the interdigitating portions of Tomes' processes (Fig. 18a). Maturation zone enamel had no pits and its outer surface was smooth and continuous (Fig. 18b). Radioautography revealed the distribution of 125I-calcitonin in the dipped tooth. In the secretion zone, most of the silver grains were over the outermost enamel with a decreasing gradient of intensity toward the dentino-enamel junction. The enamel closest to the dentin and the dentin itself showed only background labeling (Fig. 18a). In the maturation zone (Fig. 18b), the distribution of grains was similar to that in the secretion zone. This labeling pattern was continuous

along the length of the 'tooth.

After systemic injection, secretory ameloblasts (Fig. 18c), ruffle-ended ameloblasts of the maturation zone (Fig. 18d) and adjacent enamel had a background level of labeling. Smooth-ended ameloblasts also had background labeling, but there were many grains over the adjacent enamel (Fig. 18e; 19 grains/500 µm² of enamel). This reaction was present in the enamel of all regions covered by smooth-ended ameloblasts in the maturation zone.

## Insulin penetration

Radioautography of the wiped incisor, dipped for 10 min in \$125 I-insulin, revealed silver grains over the enamel in the secretion (Fig. 19a) and maturation (Fig. 19b) zones of the tooth. Most grains were toward the surface of the enamel, with a decreasing gradient toward the dentin, which had background labeling only. Cellular remnants of the enamel organ also were heavily labeled (Fig. 19b).

In the secretion zone after injection of \$125\$I-insulin, the enamel organ and enamel had labeling similar to background (Fig. 19c). In the maturation zone, many grains were found over ruffle-ended ameloblasts and the adjacent papillary layer cells, specific binding of insulin was localized to the endothelial cells of the invaginated capillaries (Martineau-Doizé et al., 1986). No labeling of the enamel was observed (Fig. 19d). In the regions of smooth-ended ameloblasts there were some grains over the enamel organ but most striking was the reaction over the adjacent enamel (Fig. 19e; 41 grains/500 µm² of enamel). This reaction was present over all regions covered by smooth-ended

ameloblasts, but not over enamel adjacent to ruffle-ended ameloblasts.

### EGF penetration

Radioautography of the wiped incisor, dipped for 10 min in  $^{125}\text{I-EGF}$ , revealed silver grains over the enamel in the secretion (Fig. 20a) and maturation (Fig. 20b) zones of the tooth. The distribution of grains as a gradient was similar to that of  $^{125}\text{I-}$  calcitonin and  $^{125}\text{I-}$  insulin.

After injection of <sup>125</sup>I-EGF, a heavy reaction was observed over the developing papillary layer of the secretion zone (Fig. 20c) and the papillary layer of the maturation zone (Figs. 20d,e). The ameloblasts and enamel of both zones had background labeling only (Figs. 20c-e).

### Albumin penetration

Dipped incisors had a different labeling pattern from that of the other iodinated proteins. In the secretion zone, grains were observed only at the surface of the enamel, presumably in the pits exposed by the removal of Tomes' processes (Fig. 21a). In the maturation zone, some labeling was present at the surface, but there was only background labeling over the enamel itself (Fig. 21b).

Systemically-injected <sup>125</sup>I-albumin led to only weak labeling in the enamel secretion zone (Fig. 21c). In the maturation zone, ruffle-ended ameloblasts were heavily labeled (Fig. 21d) while smooth-ended ameloblasts and the papillary layer were only weakly labeled (Figs. 21d,e), and few grains were over the enamel of the maturation zone (Figs. 21d,e).

## Enamel organ morphology

Papillary layer cells are located between the ameloblast layer and the extensive capillary bed on the labial side of the enamel organ. The term "papillary layer" (Williams, 1896; Elwood and Bernstein, 1968) is commonly used to indicate the papillated nature of the enamel organ. Reith (1959) described the papillae as a series of parallel ridge's running across the enamel organ at right angles to the long axis of the incisor, and numerous investigators have identified the network of capillaries that separates the papillary ridges from each other (Kindlova and Matena, 1959; Adams, 1962; Kallenbach!, 1966, 1967; Garant and Nalbandian, 1968; Garant and Gillespie, 1969; Iwaku and Ozawa, Because of this intricate association 1979; Skobe, 1980). between cellular papillae and the blood supply, it has been hypothesized that the developing and mature papillary layer may in some way be involved in the movement and/or transport of nutrients, proteins, ions and minerals to and from the enamel (Addison and Appleton, 1922; Williams, 1923; Marsland, 1952; Bernick, 1960; Adams, 1962; Reith and Cotty, 1962; Bawden et al., 1982; Crenshaw and Takano, 1982).

The presence of numerous and highly-fenestrated capillaries in the enamel organ supports the concept of a flow of materials, through the papillary layer, to and from the enamel (Garant and Gillespie, 1969). Fenestrated capillaries are common in organs known to be involved in rapid exchange of fluid and solutes (Majno, 1965) such as the glomerular capillaries in the kidney

(Pappenheimer et al., 1951). The papillary layer cells possess elaborate interdigitating channels of cell processes which project into the extracellular space, and numerous mitochondria and vesicles, all of which are structural characteristics also found in the salt glands of various marine birds (Komnick, 1965). In these birds, such features are related to the active transport of electrolytes. Substances passing through the enamel organ to enter of leave the enamel must traverse the extracellular space of the papillary layer or enter the papillary layer cells themselves. The presence of numerous coated pits and vesicles in the papillary layer cells is indicative of uptake of material by endocytosis. Alternatively, and/or concomitantly, tight junctions are scarce among these cells, suggesting that substantial material may pass through the papillary layer by an extracellular route. In any case, the papillary layer should be considered as an important component of the enamel organ, actively participating in and allowing movement of precursors or products involved in enamel formation and maturation. investigation of enamel organ permeability must consider the functional role of the papillary layer and its relationship to ameloblasts and developing enamel.

## Use of labeled proteins as biological tracers

The proteins used in this study were chosen because they are physiological molecules of various molecular weights without the adverse properties that affect the behavior of lanthanum and horseradish peroxidase as tracers. Calcitonin, insulin and EGF are biologically-active polypeptide hormones (reviewed by

Blundell and Wood, 1982). Their iodination by the Chloramine T method is a mono-iodination of a single tyrosine residue, with retention of their globular confirmation and hormonal activity (reviewed by Teitelbaum, 1983). Albumin is a long, single-chain polypeptide with four connected globular segments and 17 disulphide bridges that stabilize the conformation (reviewed by Peters, 1970). Iodination retains this conformation and hence the electrophoretic mobility of the native protein (Mancini, 1963; Kinoshita, 1979; Ogura and Kinoshita, 1983). The iodinated proteins used here were purified on Sephadex gels to remove any contaminating peptide fragments, aggregates and/or free iodide.

The time interval of 10 min was too short to allow any significant reutilization of the iodinated tyrosine residues, which would involve catabolism of the protein and incorporation of the labeled tyrosine into newly-synthesized proteins. Hence, all radioautographic reactions probably represented the location and binding of the intact protein molecule. Presence of the molecule could be due either to physiological binding, as with hormone to specific receptor, or to nonspecific binding with other biological substances. Absence of labeled protein could be attributed to washing out of unbound protein, to inaccessibility of that compartment because of molecular weight or size, or to exclusion by cellular mechanisms such as junctional complexes.

Radioautography using <sup>3</sup>H-proline as a precursor to the organic matrix of enamel shows that newly-synthesized enamel proteins are released from Tomes' processes and immediately begin to spread throughout the enamel in a process termed randomization (reviewed by Leblond and Warshawsky, 1979). A time interval of

10 min between intravenous injection of the tracer and the death of the animal, and 10 min for dipping, was chosen so as to reflect as closely as possible the early events in the randomization of newly-secreted enamel proteins.

# Significance of the dipping experiments

These experiments revealed that \$125\$I-calcitonin, \$125\$I-insulin and \$125\$I-EGF were all capable of penetrating deeply into the enamel throughout the length of the tooth, but iodinated albumin did not penetrate within 10 min. Thus, rat incisor enamel, at the stage of secretion and maturation is permeable to molecules the size of mouse EGF (approximately 6,100 daltons), but may restrict molecules the size of bovine serum albumin (approximately 68,000 daltons).

In the secretion zone, the pattern of labeling resembled the characteristic diffusion pattern of newly-secreted proteins 30 min to 4 h after injection of labeled amino acids as precursors (Greulich and Leblond, 1953; Young and Greulich, 1963; Tiber, 1971; Leblond and Warshawsky, 1979; Warshawsky, 1979). Similar diffusion patterns follow administration of <sup>14</sup>C-bicarbonate (Greulich and Leblond, 1953), <sup>35</sup>S-sulphate (Belanger, 1955; Blumen and Merzel, 1976) and tritiated sugars (Kumamoto and Leblond, 1958). The diffusion pattern is the preliminary stage of the randomization process which distributes newly-secreted protein molecules among older, previously-secreted proteins. As this pattern can be obtained by dipping teeth into radioactive protein solutions, in the absence of the enamel organ, it may be that proteins elaborated by the secretory ameloblasts are

released at the enamel surface and move into the enamel where they randomize by a process which is not mediated by cells.

A possible explanation of the apparent migration of labeled proteins is that proteins could be distributed along continuous Tomes' processes (Warshawsky, 1971, 1978). Support for this concept was obtained by the differential labeling of structural and secretory proteins (Warshawsky and Vugman, 1977). The dipping experiment presented here demonstrates that the movement of tracers can occur through the enamel matrix itself and does not require an intact ameloblast and Tomes' process.

The same diffusion of protein, occurring in the maturation zone, demonstrates the porosity of enamel during maturation without the influence of cells. The maturing enamel has sufficient space between its crystallites to accomodate large molecular-weight proteins such as calcitonin, insulin and EGF. Larger proteins or protein aggregates may be present in enamel and their relationship with the crystals may prevent the diffusion of molecules as large as albumin. Smaller proteins move freely into the enamel, and this raises the possibility that they can just as readily move out passively without cellular control (Warshawsky, 1985).

# Significance of the systemic injection experiments

The enamel organ separates the developing enamel from its blood supply, and presumably controls the passage of molecules between the two (Bawden and Wennberg, 1977; Crenshaw and Takano, 1982). The final barrier to molecules moving extracellularly towards the enamel is likely to be the distal junctional complex

of the ameloblast (Kallenbach et al., 1965; Warshawsky, 1968, . 1978; Hasty, 1983). In the secretion zone, this complex is welldeveloped and has tight junctions arranged in circumscribed Lanthanum (Takano and Crenshaw, plaques (Warshawsky, 1978). 1980) and HRP (Kallenbach, 1980a) studies have shown that in secretory ameloblasts the junctional complex forms a barrier to In this study, the enamel organ and enamel in these molecules. the secretion zone were not labeled after systemic injection of any of the molecules except 125I-EGF which had a reaction over the enamel organ, but not over the enamel. Kinoshita (1979) and Ogura and Kinoshita (1983), using iodinated and fluorochromelabeled albumin, also suggested that a barrier exists in the secretion zone between the extracellular fluid and the enamel matrix.

In the maturation zone, the functional extracellular barrier between the enamel and the extracellular space may also reside in the distal junctional complex of the ruffle- and smooth-ended ameloblasts (Kallenbach et al., 1965; Kallenbach, 1968, 1973). Ruffle-ended ameloblasts have well-developed junctional complexes at both ends, whereas smooth-ended ameloblasts have only proximal ones (Josephsen and Fejerskov, 1977). The distal junctional complex of ruffle-ended ameloblasts is tight to the penetration of various molecules (Skobe and Garant, 1974; Kallenbach, 1980b; Takano and Crenshaw, 1980; Takano and Ozawa, 1980). The degree of tightness of the proximal junctional complex of smooth-ended ameloblasts is still controversial (Josephsen and Fejerskov, 1977; Kallenbach, 1980b; Takano and Ozawa, 1980). The results of

this study found differences in penetration of protein molecules between ruffle- and smooth-ended ameloblasts of the maturation zone. The ability of <sup>125</sup>I-calcitonin and <sup>125</sup>I-insulin to enter the enamel matrix adjacent to smooth-ended ameloblasts as early as 10 min after injection shows that their intercellular junctions are permeable to proteins with molecular weights as great as approximately 5,700 daltons.

Although the proximal junctional complexes of ruffle-ended ameloblasts were generally permeable to certain proteins, the distal junctional complexes prevented all proteins from reaching the enamel. The heavy radioautographic reaction over the enamel organ following injection of <sup>125</sup>I-EGF represents specific binding sites for this hormone (Martineau-Doizé et al., 1987). The results following injection of iodinated proteins show that ruffle-ended ameloblasts of the maturation zone can prevent molecules as large as <sup>125</sup>I-calcitonin (approximately 3,600 daltons) from reaching the enamel.

The findings presented here confirm much of the work done with classical tracers on junctional complexes of the maturation zone. This study shows that the distal junctional complex of ruffle-ended ameloblasts is impermeable to proteins, whereas the junctional complexes of smooth-ended ameloblasts are permeable to rather large protein molecules. Kallenbach (1980a, 1980b) found a similar tracer distribution 10 min after injection of HRP; in the secretion zone, the enamel organ was a barrier between the blood supply and the enamel, whereas in the maturation zone, smooth-ended ameloblasts allowed passage of HRP to the surface of the enamel. However, over longer time periods, some HRP entered

the enamel in the secretion zone and in postsecretory transition (Kallenbach, 1980a). The reason for the changes in permeability characteristics to HRP with increasing time is not clear. Perhaps the toxic (Mazariegos et al., 1984; Mazariegos and Hand, 1985) or the physiological effects (Simionescu et al., 1975) of HRP may have resulted in artifactual tracer distribution.

The results presented here are consistent with the hypothesis that proteolytic enzymes within maturing enamel break down large proteins into more mobile fragments that can freely diffuse out of the enamel and through the ameloblast layer, but only where there are bands of smooth-ended ameloblasts. Furthermore, during secretion and maturation, the enamel stripped of its enamel organ, is permeable to molecules as large as EGF, but not to albumin within a 10 min time period. The distribution of these injected proteins resembles the diffusion pattern seen when newly-secreted proteins mix with older unlabeled proteins.

#### REFERENCES

Adams D 1962 The blood supply to the enamel organ of the rodent incisor. Archs Oral Biol, 7:279-286.

Addison WHF and Appleton JL 1922 The vascularity of the enamel organ in the developing molar of the albino rat. Am J Anat, 31:161-189.

Allan JH 1967 Maturation of enamel. In: Structural and Chemical Organization of Teeth. Ed. Miles AEW. Academic Press, New York. pp. 467-492.

Bawden J and Wennberg A 1977 In vitro study of cellula influence on 45Ca uptake in developing rat enamel. J Dent Res, 56:313-319.

Bawden JW, Crenshaw MA, Takano Y and Hammarström L 1982 Ion transport through the enamel organ - An update. J Dent Res, 61(Sp Iss):1552-1554.

Belanger LF 1955 Autoradiographic detection of radiosulfate incorporation by the growing enamel of rats and hamsters. J Dent Res, 34:20-27.

Bernick S 1960 Vascular supply to the developing teeth of rats. Anat Rec, 137:414-451.

Blumen G and Merzel J 1976 Autoradiographic study with <sup>35</sup>S-sodium sulfate of loss of sulfated glycosaminoglycans during amelogenesis in the guinea-pig. Archs Oral Biol, 21:513-521.

Blundell T and Wood S, 1982 The conformation, flexibility, and dynamics of polypeptide hormones. Ann Rev Biochem, 51:123-154.

Boyde A and Reith EJ 1976 Scanning electron microscopy of the lateral cell surfaces of rat incisor ameloblasts. J Anat, 122:603-610.

Boyde A and Reith EJ 1977 Scanning electron microscopy of rat maturation ameloblasts. Cell Tiss Res, 178:221-228.

Boyde A and Reith EJ 1981 Display of maturation cycles in ratincisor enamel with tetracycline labeling. Histochem, 72:551-561.

Boyde A and Reith EJ 1982 In vitro histological and tetracycline staining properties of surface layer rat incisor enamel also reflect the cyclical nature of the maturation process. Histochem, 75:341-351.

Crenshaw MA and Takano Y 1982 Mechanisms by which the enamel organ controls calcium entry into developing enamel. J Dent Res, 61:1574-1579.

Deakins M 1942 Changes in the ash, water and organic content of pig enamel during calcification. J.Dent Res, 21:429-435.

Eisenmann DR, Ashrafi S and Nieman A 1979 Calcium transport and the secretory ameloblast. Anat Rec, 193:403-422.

Elwood WK and Bernstein MH 1968 The ultrastructure of the enamel organ related to enamel formation. Am J Anat, 122:73-94.

Garant PR 1972 The demonstration of complex gap junctions between the cells of the enamel organ with lanthanum nitrate. J Ultrastr Res, 40:333-348.

Garant PR and Gillespie R 1969 The presence of fenestrated capillaries in the papillary layer of the enamel organ. Anat Rec, 163:71-80.

Greulich RC and Leblond CP 1953 Radioautographic visualization of radiocarbon in the organs and tissues of newborn rats following administration of <sup>14</sup>C-labeled bicarbonate. Anat Rec, 115:559-586.

Hasty DL 1983 Freeze-fracture studies of neonatal mouse incisors. Anat Rec, 205:405-420.

Hunter WM and Greenwood FC 1962 Preparation of iodine-131 labeled human growth hormone of high specific activity. Nature, 194:495-496.

Iwaku F and Ozawa H 1979 Blood supply of the rat periodontal space during amelogenesis as studied by the injection replica SEM method. Arch Histol Jap, 42:81-88.

Josephsen K 1983 Indirect visualization of ameloblast modulation in the rat incisor using calcium-binding compounds. Scand J Dent Res, 91:76-78.

Josephsen K and Fejerskov O 1977 Ameloblast modulation in the maturation zone of the rat incisor enamel organ. A light and electron microscopic study. J Anat, 124:45-70.

Kallenbach E 1966 Electron microscopy of the papillary layer of rat incisor enamel organ during enamel maturation. J Ultrastr Res, 14:518-533.

Kallenbach E 1967 Cell architecture in the papillary layer of rat incisor enamel organ at the stage of enamel maturation. Anat Rec, 157:683-698.

Kallenbach E 1968 Fine structure of rat incisor ameloblasts during enamel maturation. J Ultrastr Res, 22:90-119.

Kallenbach E 1973 The fine structure of Tomes' process of rat incisor ameloblasts and its relationship to the elaboration of enamel. Tiss Cell, 5:501-524.

Kallenbach E 1980a Fate of horseradish peroxidase in the secretion zone of the rat incisor enamel organ. Tiss Cell, 12:491-501.

Kallenbach E 1980b Access of horseradish peroxidase (HRP) to the extracellular spaces of the maturation zone of the rat enamel organ. Tiss Cell, 12:165-174.

Kallenbach E, Clermont Y and Leblond CP 1965 The cell web in the ameloblasts of the rat incisor. Anat Rec, 153:55-70.

ł

Karim A and Warshawsky H 1979 'The effect of colcemid on the structure and secretory activity of ameloblasts in the rat incisor as shown by radioautography after injection of <sup>3</sup>H-proline. Anat Rec, 195:587-609.

Kindlova M and Matena V 1959 Blood circulation in the rodent teeth of the rat. Acta Anat, 37:165-192.

Kinoshita Y 1979 Incorporation of serum albumin into the developing dentin and enamel matrix in the rabbit incisor. Calcif Tiss Int, 29:41-46.

Kopriwa BM and Lebkond CP 1962 Improvement in the coating technique of radioautography. J Histochem Cytochem, 10:269-284.

Kumamoto Y and Leblond CP 1958 Visualization of  $^{14}$ C in the tooth matrix after administration of labeled hexoses. J Dent Res, 37:147-161.

Leblond CP and Warshawsky H 1979 Dynamics of enamel formation in the rat incisor tooth. J Dent Res, 58B:950-975.

Majno G 1965 Ultrastructure of the vascular membrane. În: Handbook of Physiology. Am Physiol Soc, Washington DC. pp. 2293-2375.

Mancini RE 1963 Connective tissue and serum proteins. Int Rev Cytol, 14:193-221.

Marsland EA 1952 Histological investigation of amelogenesis in rats. II. Maturation. Brit Dent J, 92:109-119.

Martineau-Doizé B, McKee MD, Warshawsky H and Bergeron JJM 1986 In vivo demonstration by radioautography of binding sites for insulin in liver, kidney and calcified tissues of the rat. Anat Rec, 214:130-140.

Martineau-Doizé B, Lai WH, Warshawsky H and Bergeron JJM 1987 Specific binding sites for epidermal growth factor in bone and incisor enamel organ of the rat. In: Development and Diseases of Cartilage and Bone Matrix. UCLA Symposium. AR Liss Inc., pp. 389-399.

Mazariegos MR and Hand AR 1985 Horseradish peroxidase: Factors affecting its distribution after retrograde infusion into the rat parotid gland. J Histochem Cytochem, 33:942-950.

Mazariegos MR, Tice LW and Hand AR 1984 Alteration of tight junctional permeability in the rat parotid gland after isoproterenol stimulation. J Cell Biol, 98:1865-1877.

Nanci A, Slavkin HC and Smith CE 1987 Immunocytochemical and radioautographic evidence for secretion and intracellular degradation of enamel proteins by ameloblasts during the maturation stage of amelogenesis in rat incisors. Anat Rec, 217:107-123.

Ogura H and Kinoshita Y 1983 The difference in the distribution pattern of administered serum albumin between developing dentine and enamel matrix in the rabbit incisor. In: Mechanisms of Tooth Enamel Formation. Ed. Suga S. Quintessence, New York. pp. 143-154.

Pappenheimer JR, Renkin EM and Borrero LM 1951 Filtration, diffusion and molecular seiving through peripheral capillary membranes. A contribution to the pore theory of capillary permeability. Am J Physiol, 167:13-46.

Peters T Jr 1970 Serum albumin. Adv Clin Chem, 13:37-111.

Posner BI, Josefsberg Z and Bergeron JJM 1978 Intracellular polypeptide hormone receptors: Characterization of insulin binding sites in Golgi fractions from the liver of female rats. J Biol Chem, 253:4067-4073.

Reith EJ 1959 The enamel organ of the rat's incisor, its histology and pigment. Anat Rec, 133:75-90.

Reith EJ and Cotty VF 1962 Autoradiographic studies on calcification of enamel. Archs Oral Biol, 7:365-372.

Reith EJ and Boyde A 1981a The arrangement of ameloblasts on the surface of maturing enamel of the rat incisor tooth. J Anat, 133:381-388.

Reith EJ and Boyde A 1981b The cyclical entry of calcium into maturing enamel of the rat incisor tooth. Archs Oral Biol, 26:983-988.

Reith EJ, Boyde A and Schmid MI 1982 Correlation of rat incisor ameloblasts with cycles as displayed on enamel surface with EDTA. J Dent Res, 61:1563-1573.

Reith EJ, Schmid MI and Boyde A 1984 Rapid uptake of calcium in maturing enamel of the rat incisor. Histochem, 80:409-410.

Revel JP and Karnovsky MJ 1967 Hexagonal array of subunits in intercellular junctions of the mouse heart and liver. J Cell

Biol, 33:C7-C12.

Robinson C, Lowe NR and Weatherell JA 1977 Changes in amino acid composition of developing rat incisor enamel. Calcif Tiss Res, 23:19-31.

Schatzki PF and Newsome A 1975 Neutralized lanthanum solution: a largely noncolloidal ultrastructural tracer. Stain Tech, 50:171-178.

Shaklai M and Tavassoli M 1982 Lanthanum as an electron microscopic stain. J Histochem Cytochem, 30:1325-1330.

Simionescu N, Simionescu M and Palade G 1975 Permeability of muscle capillaries to small hemipeptides. J Cell Biol, 64:586-607.

Skobe Z 1980 Scanning electron microscopy of the mouse incisor enamel organ in transition between secretory and maturation stages of amelogenesis. Archs Oral Biol, 25:395-189.

Skobe Z and Garant PR 1974 Electron microscopy of horseradish peroxidase uptake by papillary cells of the mouse incisor enamel organ. Archs Oral Biol, 19:387-391.

Slavkin HC, Mino W and Bringas P Jr 1976 The biosynthesis and secretion of precursor enamel protein by ameloblasts as visualized by autoradiography after tryptophan administration. Anat Rec, 185:289-312.

Smith CE, McKee MD and Nanci A 1987 Cyclic induction and rapid movement of sequential waves of new smooth-ended ameloblast modulation bands in rat incisors as visualized by polychrome fluorescent labelling and GBHA-staining of maturing enamel. J Dent Res, In Press.

Suga S 1959 Amelogenesis. Some histological and histochemical observations. Int Dent J, 9:394-420.

Suga S 1970 Histochemical observation of proteolytic enzyme activity in the developing dental hard tissues of the rat. Archs Oral Biol, 15:555-558.

Takano Y and Crenshaw MA 1980 The penetration of intravascularly perfused lanthanum into the ameloblast layer of developing rat molar teeth. Archs Oral Biol, 25:505-511.

Takano Y and Ozawa H 1980 Ultrastructural and cytochemical observations on the alternating morphological changes of ameloblasts at the stage of enamel maturation. Archs Hist Jap, 43:385-399.

Takano Y, Crenshaw MA, Bawden JW, Hammarström L and Lindskog S 1982 The visualization of the patterns of ameloblast modulation by the glyoxal bis(2-hydroxyanil) staining method. J Dent Res,

61:1580-1586.

Teitelbaum AP 1983 Preparing the tracer: Iodination techniques. In: Assay of Calcium-Binding Hormones. Ed. Bikel DD. Springer-Verlag, Berlin.

Tiber A 1971 The patterns of incorporation of <sup>3</sup>H-leucine by the enamel and dentine matrices of the rhesus monkey. An autoradiographic study. Archs Oral Biol, 16:1231-1236.

Warshawsky H 1968 The fine structure of secretory ameloblasts in rat incisors. Anat Rec, 161:211-229.

Warshawsky H 1971 A light and electron microscopic study of the nearly mature enamel of rat incisors. Anat Rec, 169:559-584.

Warshawsky H 1978 A freeze-fracture study of the topographic relationship between inner enamel-secretory ameloblasts in the rat incisor. Am J Anat, 152:153-208.

Warshawsky H 1979 Radioautographic studies on amelogenesis. J Biol Buccale, 7:105-126.

Warshawsky H 1985 Ultrastructural studies on amelogenesis. In: The Chemistry and Biology of Mineralized Tissues. Ed. Butler WT. Ebsco Media, Birmingham. pp. 33-45.

Warshawsky H and Moore G 1967 A technique for the fixation and decalcification of rat incisors for electron microscopy. J Histochem Cytochem, 15:542-549.

Warshawsky H and Smith CE 1974 Morphological classification of rat incisor ameloblasts. Anat Rec, 179:423-446.

Warshawsky H and Vugman I 1977 A comparison of the protein synthetic activity of presecretory and secretory ameloblasts in rat incisors. Anat Rec, 188:143-172.

Weinmann J, Wessinger GD and Reed G 1942 Correlation of chemical and histological investigations on developing enamel. J Dent Res, 21:171-182.

Weinstock A and Leblond CP 1971 Elaboration of the matrix glycoprotein of enamel by secretory ameloblasts of the raincisor as revealed by radioautography after <sup>3</sup>H-galactose injection. J Cell Biol, 51:26-51.

Williams JL 1896 On the formation and structure of dental enamel. Dent Cosmos, 38:101-127.

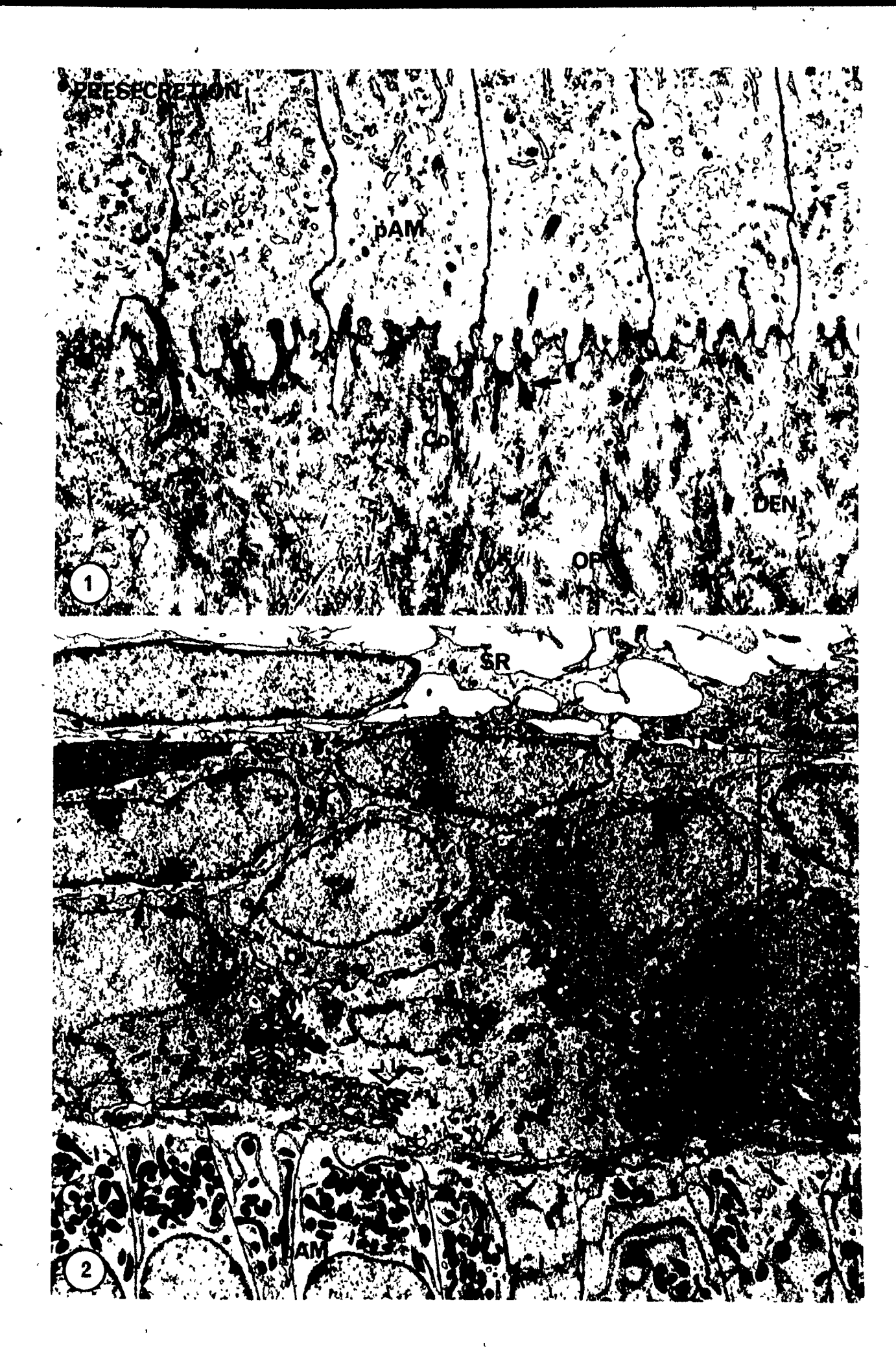
Williams JL 1923 Disputed points and unsolved problems in the normal and pathological histology of enamel. J Dent Res, 5:27-107.

Young RW and Greulich RC 1963 Distinctive autoradiographic patterns of glycine incorporation in rat enamel and dentine matrices. Archs Oral Biol, 8:509-521.

#### FIGURE LEGENDS: CHAPTER TWO

Figure 1. Electron micrograph of the site of the future dentinoenamel junction in the presecretion zone where the distal ends of tall columnar presecretory ameloblasts (pAM) abut against the dentin (DEN). Cell processes from the ameloblasts interdigitate with collagen fibers (Coll) of the dentin and occasionally appear to make contact (stars) with odontoblast processes (OP). Small accumulations of an enamel-like substance (arrows) can be observed near the distal ends of the ameloblasts. X11,500.

Figure 2. The stratum intermedium (SI) of the developing papillary layer in the presecretion zone is found immediately adjacent to the proximal ends of the presecretory ameloblasts (pAM) and the stellate reticulum (SR). It consists of two to three irregular layers of closely-packed cuboidal cells, tightly interlocked with each other via their irregular outlines and numerous cell processes (open arrows). Desmosomes are frequently present among cells within the stratum intermedium and between cells of the stratum intermedium and the stellate reticulum and the ameloblasts (small arrows). Within the stratum intermedium, light-staining (LC) and dark-staining (DC) cells can be identified. The thickness of the stratum intermedium is constant across the developing-papillary layer. X7,000.



Electron micrograph showing the three layers of the Figure 3. developing papillary layer. Interposed between the stratum intermedium (SI) and the outer dental epithelium (ODE) is the stellate reticulum (SR). The stellate reticulum consists of loosely-arranged, stellate-shaped cells often connected by desmosomes (small arrows) and delineated by a large amount of extracellular space (ES). The outer dental epithelium is adjacent to capillaries (CAP) and consists of a single layer of cuboidal cells having numerous cell processes (open arrow) and often containing some lipid droplets and small glycogen deposits. Separating the outer dental epithelium from the capillaries and periodontal connective tissue is a basement membrane which derives from the original embryological invagination of the oral epithelium. X7,000.

Figure 4. Electron micrograph showing ameloblasts and enamel in the secretion zone. Secretory ameloblasts (AM) having Tomes' processes (TP) interdigitate with interrod enamel prongs (EN). Numerous secretory granules (SG) are present in the ameloblasts. Occasional branching of Tomes' process can be observed. X11,500.

Figure 5. The stratum intermedium (SI) of the developing papillary layer in the secretion zone is found immediately adjacent to the basal bulges (BB) of the ameloblasts (AM) as defined by the proximal cell web (PCW). At this stage, the stratum intermedium consists of a single layer of cuboidal cells with large spherical nuclei. The cells stain uniformly, have moderate amounts of cellular organelles, and are connected by desmosomes (small arrows). The cells of the stratum intermedium interdigitate with each other via numerous cell processes (open arrows) surrounded by a narrow extracellular space. Immediately overlying the stratum intermedium is the stellate reticulum (SR).

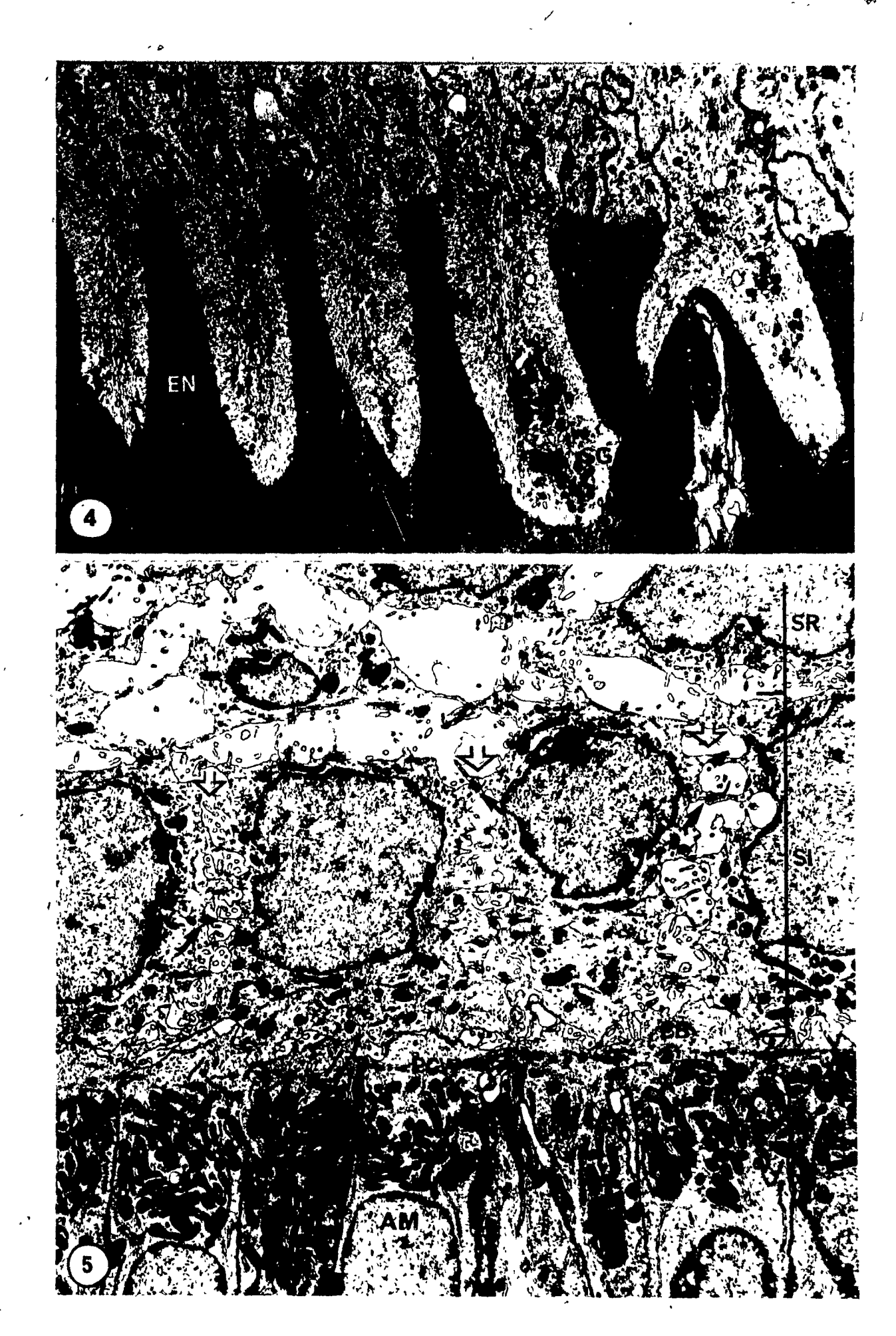


Figure 6. Electron micrograph of the developing papillary layer in the secretion zone. The outer dental epithelium (ODE) and stellate reticulum (SR) are no longer visible as distinct layers. The enamel organ has formed small papillae as capillaries, fibroblasts and collagen (Coll) of the periodontal connective tissue invaginate into it (open arrows). The developing papillary layer is invested by a basement membrane (small arrows). The cells of the papillae are loosely arranged and the extracellular space (ES) between them is extensive. The cells have numerous mitochondria (M) and cell processes. X7,000.



Figure 7. Electron micrograph of ruffle-ended ameloblasts in the enamel maturation zone. These cells are characterized by their highly-invaginated distal cell membrane which forms a ruffled border (RB). The ameloblasts form a compact epithelial layer adjacent to the enamel (EN) but are separated from it by a basement membrane-like structure (arrows). Mitochondria (M) accumulate just proximal to the ruffled border. X7,000.

Figure 8. Higher magnification of Figure 7 showing the ruffled border (RB) of a ruffle-ended ameloblast. Note the deep invaginations of the cell membrane and the presence of vesicular profiles (stars) related to them. Mitochondria (M) accumulate just proximal to the ruffled border and occasionally approach the enamel (EN). Tight junctions (TJ) seal the cells laterally and hemidesmosomes (curved arrows) adhere the ameloblasts to the basement membrane-like structure (straight arrows) distally, X23,000.

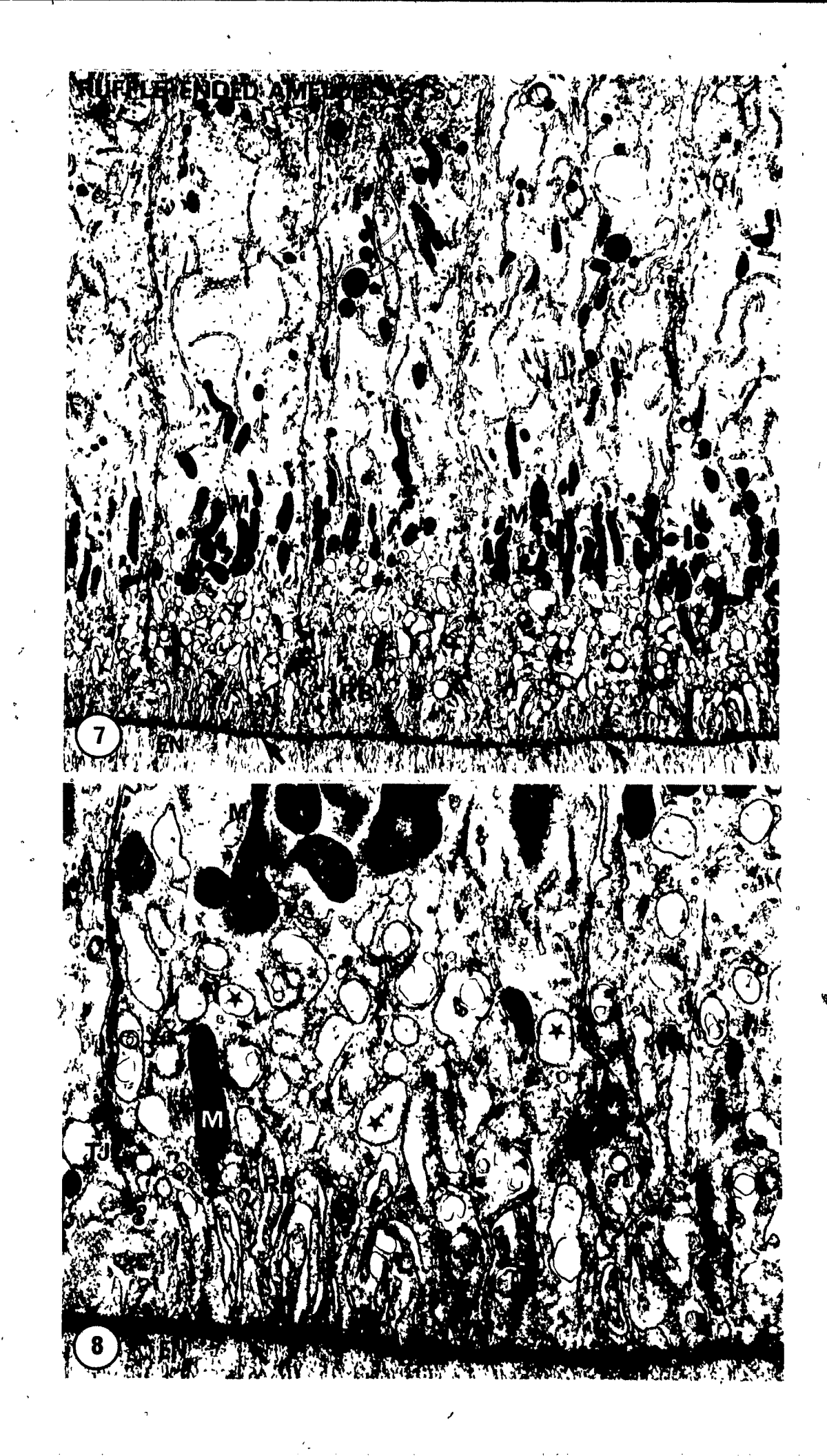


Figure 9. Electron micrograph of smooth-ended ameloblasts in the maturation zone. These cells do not possess a ruffled border related to the enamel space (EnS). The ameloblasts have randomly-dispersed mitochondria (M) and a moderate amount of cellular organelles including tonofilaments (TF). The extracellular space (ES) between the cells is large and contains membrane remnants. The ameloblasts are not sealed at their distal ends by tight junctions and frequently the extracellular space between ameloblasts is open (open arrows) to the basement membrane-like structure (small arrows). X11,000.

Figure 10. Higher magnification of Figure 9 showing the distal cytoplasm of a smooth-ended ameloblast. Intermixed with mitochondria (M) are numerous vesicles (VES), some of which appear as one ring of membrane enclosed by another (arrowheads). Hemidesmosomes (curved arrows) are numerous where the slightly-undulated distal cell membrane makes contact with the basement membrane-like structure (straight arrows). ES, extracellular space. X27,000.



Figure 11. Electron micrograph of the papillary layer in the maturation zone. No distinct layers are visible and the papillary layer cells (PLC) all appear similar. Capillaries (CAP) are deeply invaginated into the enamel organ, forming the characteristic papillary ridges found at this stage of amelogenesis. At the junctions between papillary layer cells, numerous tightly-packed cell processes form channels that appear to radiate away from the capillaries (open arrows). These cells possess many mitochondria, desmosomes, gap junctions, annular gap junctions (solid arrows) and vesicles. X7,000.

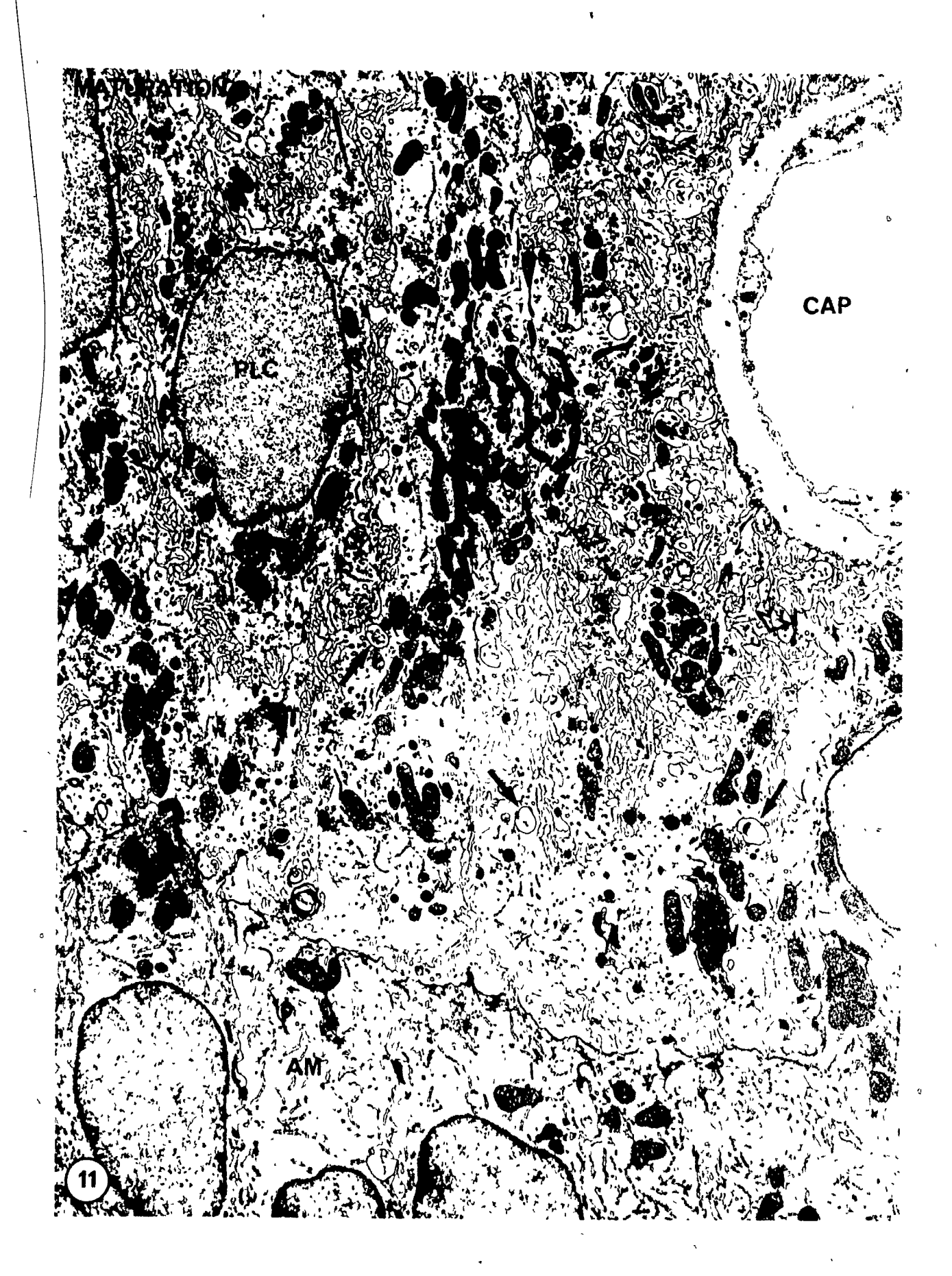
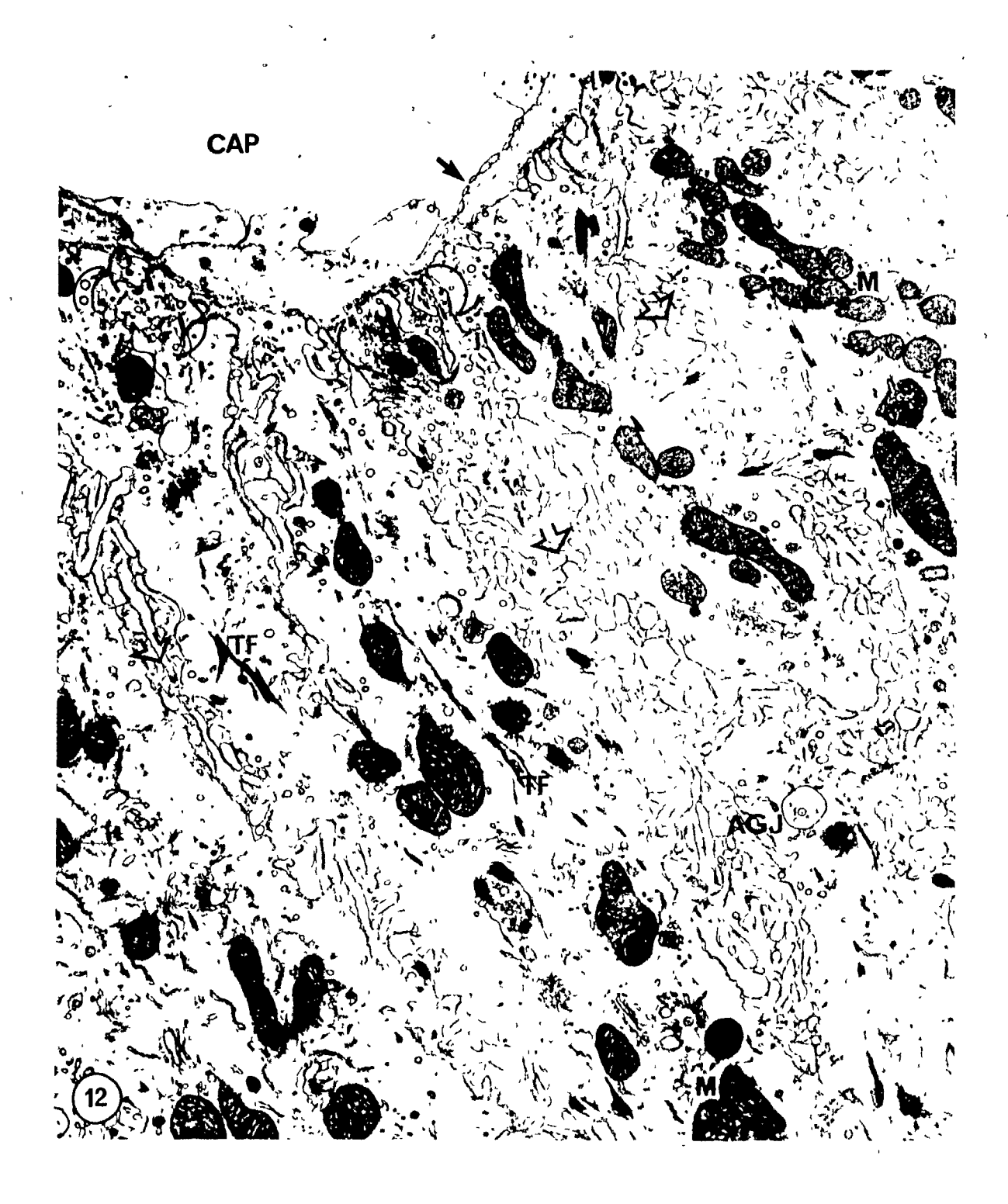


Figure 12. Higher magnification of a region of the papillary layer adjacent to an invaginated capillary. The capillary (CAP) is highly fenestrated (small arrow) and is found deep within the papillary layer. The papillary layer cells have numerous mitochondria (M), tonofilaments (TF), annular gap junctions (AGJ) and vesicles. Cell processes of papillary layer cells interdigitate to form changels that appear to radiate away from the capillary (open arrows). Frequently, "foot pads" of papillary layer cell cytoplasm, containing numerous vesicular structures, are found in close proximity to the capillaries (brackets). These are shown in greater detail in Figures 13 and 14. X11,000.



Figures 13 and 14. Electron micrographs showing a typical "foot pad" of a papillary layer cell closely apposed to a capillary of the enamel organ (Fig. 13). An endothelial cell junction (curved arrow) is present and the capillary is separated from the papillary layer cells by the corresponding basement membranes and connective tissue in the extracellular space (ES). The "foot pads" contain numerous vesicular profiles (VES) that appear coated (CV), smooth (SV), cup-shaped (arrows) and/or as elongated The smooth vesicles (SV) often have a slightly tubules (t). dense material associated with the inner leaflet of the membrane. Coated pits (CP) are continuous with the cell membrane which frequently shows gap junctions (GJ). Occasionally, apparent fusion of membranous profiles is observed; Figure 14 shows a coated vesicle joined with a tubular structure (star). 13, X68,000; Figure 14, X110,000.



Figure 15. Electron micrograph of an entire capillary deeply invaginated into the papillary layer of the maturation zone. The invagination of capillaries causes the enamel organ to form-papillae (P, large arrows). These papillae extend as ridges across the enamel organ. The capillaries (CAP) are associated with some periodontal connective tissue (PCT), are highly fenestrated, (small arrows) and show endothelial cell junctions (stars). X8,000.

Figure 16. Higher magnification of the fenestrations present in endothelial cells of enamel organ capillaries. The fenestrations (straight arrows) are closed by diaphragms, often containing a small, electron dense knob in their center. The basement membrane of the capillary and the papillary layer are clearly visible (curved arrows). LUM, lumen of capillary; PLC, papillary layer cell. X56,000.

Figure 17. Occasionally associated with the fenestrated capillaries (arrow) is a basement membrane complex between the endothelium of the capillary and the papillary layer cells (PLC). Excluding the basement membrane associated with the endothelium and that associated with the enamel organ, up to five other basement membrane layers have been observed. LUM, lumen of capillary. X19,000.

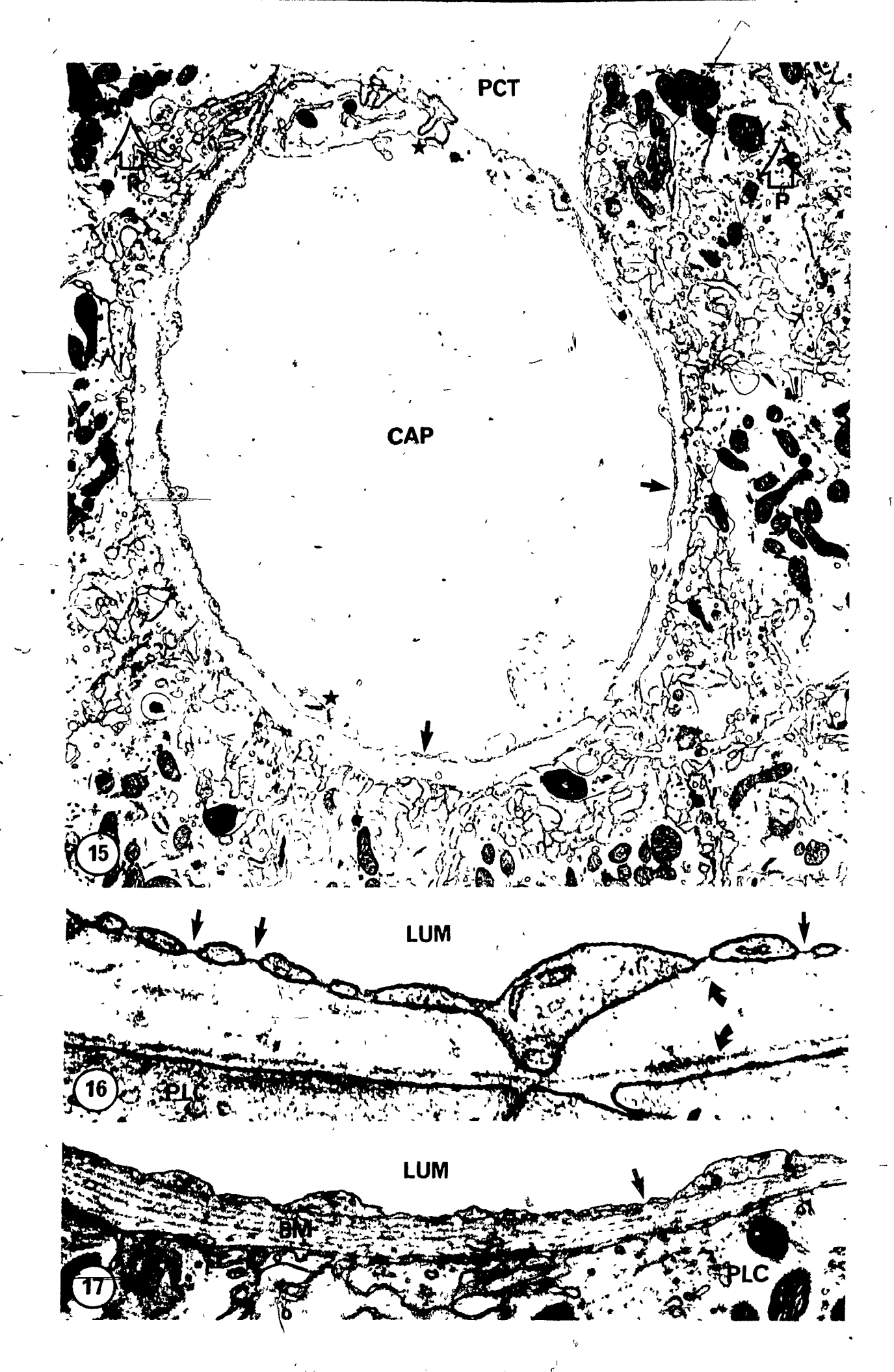


Figure 18. Light microscope radioautographs of dipped (a,b) and systemically-injected (c-e) rat incisors 10 min after administration of  $^{125}$ I-calcitonin. A heavy reaction is seen over enamel in the secretion (a) and maturation zones (b) of incisors that were wiped free of their enamel organs and dipped in 125Icalcitonin. Most of the grains are over the outermost enamel. In the secretion zone of animals systemically-injected with 125Icalcitonin (c), the enamel organ and enamel show only a weak In the maturation zone, the enamel organ and enamel, in regions of ruffle-ended ameloblasts (d) show only background labeling. In regions of smooth-ended ameloblasts (e), the enamel organ shows only background/labeling but many grains are over the en, enamel; den, dentin; pl, papillary layer adjacent enamel. AM, ameloblasts; rAM, ruffle-ended ameloblasts; sAM, smooth-ended ameloblasts. X600.

# Calcitonin - 3,600D

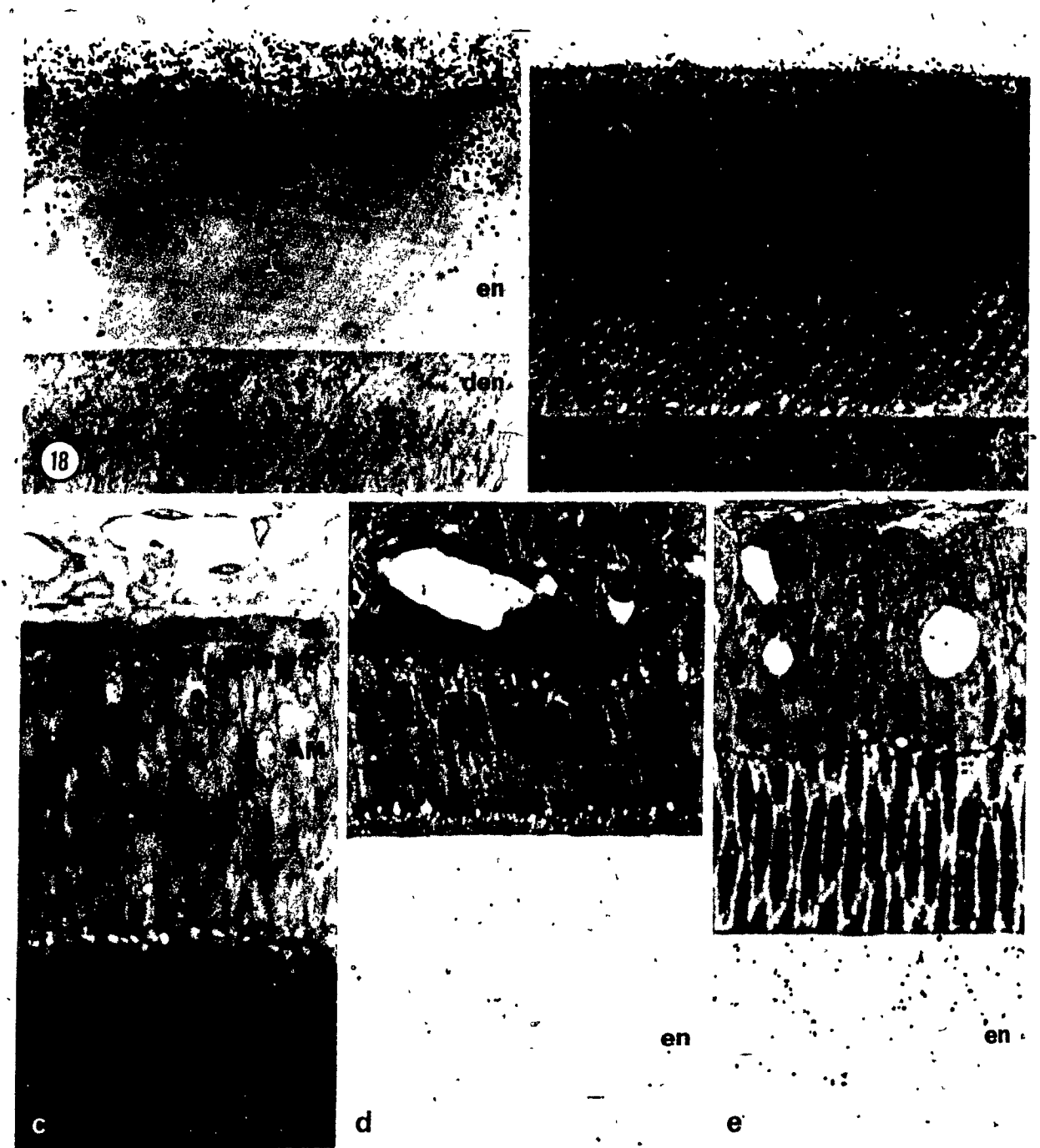


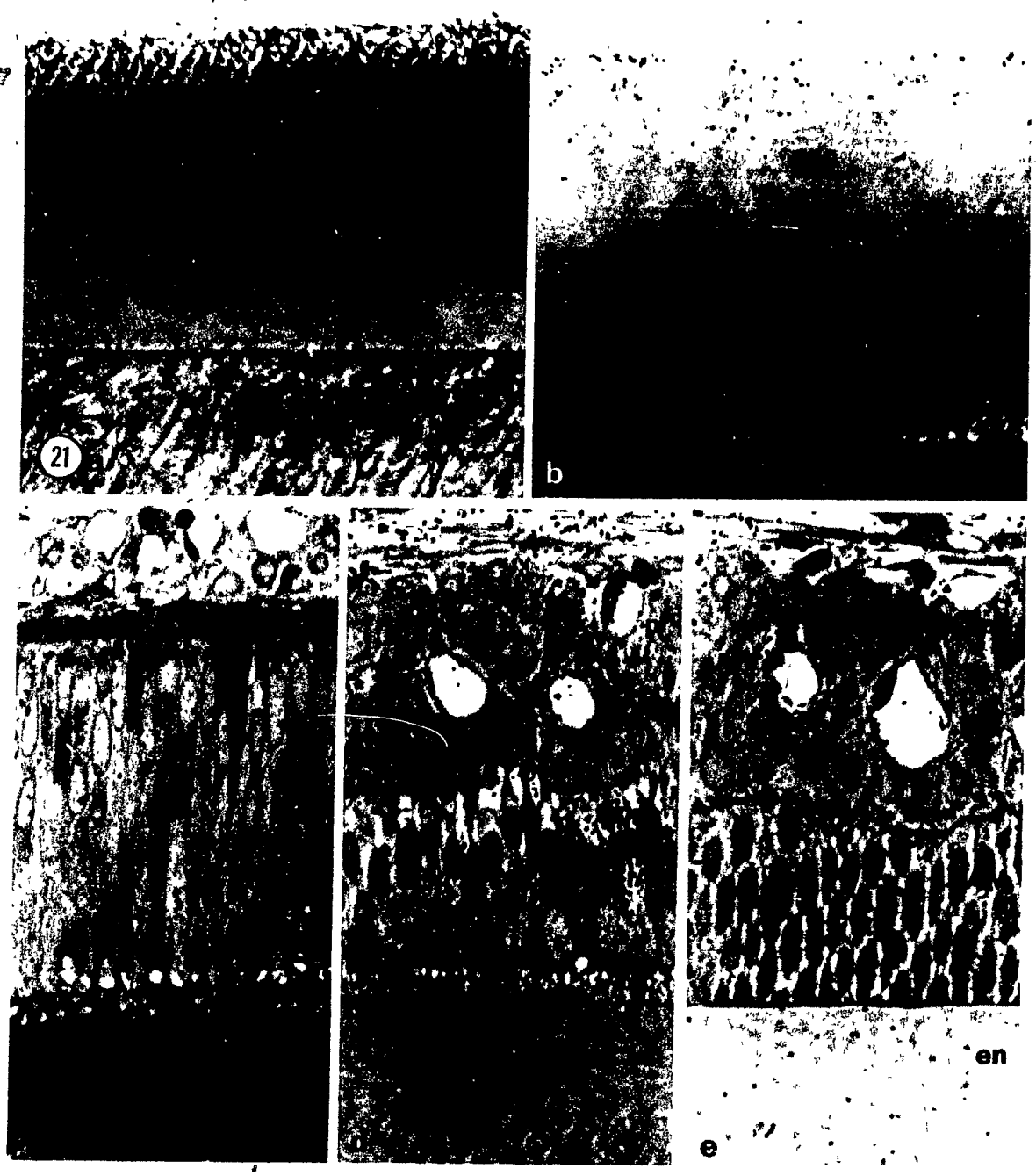
Figure 19. Light microscope radioautographs of dipped (a,b) and systemically-injected (c-e) rat incisors 10 min administration of 125I-insulin. Incisors that were wiped free of their enamel organs and dipped in 125I-insulin show a heavy reaction over enamel in the secretion (a) and maturation zones (d) The grains extend throughout the entire thickness of the Cellular remnants of the enamel organ are heavilylabeled (arrow, b). In the secretion fone of animals systemically-injected with  $^{125}I$ -insulin (c), the enamel organ and enamel show only a weak reaction. In the maturation zone, the enamel organ in regions of ruffle-ended ameloblasts (d) shows heavy labeling, but the adjacent enamel is not labeled. regions of smooth-ended ameloblasts (e), the enamel organ shows a weaker reaction, but many grains are over the adjacent enamel. en, enamel; den, dentin; pl, papillary layer; AM, ameloblasts; ruffle-ended ameloblasts; sAM, smooth-ended ameloblasts. X600.



Figure 20. Light microscope radioautographs of dipped (a,b) and systemically-injected (c-e) rat incisors 10 min after administration of \$^{125}I-EGF. A heavy reaction is seen over enamel in the secretion (a) and maturation zones (b) of incisors that were wiped free of their enamel organs and dipped in \$^{125}I-EGF. At 10 min after injection of \$^{125}I-EGF, reactions are mainly over the developing papillary layer of the secretion zone (c) and the papillary layer of the maturation zone (d,e). The enamel of both zones shows only background labeling (c-e). en, enamel; den, dentin; pl, papillary layer; AM, ameloblasts; rAM, ruffle-ended ameloblasts; sAM, smooth-ended ameloblasts. X600.

Figure 21. Light microscope radioautographs of dipped (a,b) and systemically-injected (c-e) rat incisors 10 administration of 125I-albumin. Incisors that were wiped free of their enamel organs and dipped in 1251-albumin show little or no labeling of the enamel in both the secretion (a) and maturation zones (b). The reaction at the surface of the enamel in (a) is presumably due to albumin in the pits exposed by the removal of Tomes' processes. In the secretion zone of animals systemicallyinjected with 125I-albumin (c), the enamel organ and enamel show only a weak reaction. In the maturation zone at regions of ruffle-ended ameloblasts (d), the papillary layer shows a weak reaction, whereas many grains are over ameloblasts. At regions of smooth-ended ameloblasts, the enamel organ shows weak labeling The enamel throughout the maturation zone shows only background labeling (d,e). en, enamel; den, dentin; pl, papillary layer; AM, ameloblasts; rAM, ruffle-ended ameloblasts; sAM, smooth-ended ameloblasts. X600.

# **Alb**umin - 68,000 D



CHAPTER THREE: EFFECTS OF VARIOUS AGENTS ON STAINING OF THE MATURATION PATTERN AT THE SURFACE OF RAT INCISOR ENAMEL.

#### SYNOPSIS

In the maturation zone, two types of ameloblasts are \_ arranged as bands across the rat incisor; these corresponded with 'a staining pattern at the surface which reflected the alternating pattern of ruffle-ended and smooth-ended ameloblasts. periodic acid-Schiff (PAS) stain showed bands and stripes similar to those following glyoxal bis(2-hydroxyanil)(GBHA) staining; these stains visualize the organic (PAS) and inorganic (GBHA) components of the maturation pattern. To further elucidate the nature of these bands, dissected rat incisors were treated with various agents prior to staining with GBHA or PAS. extraction for 2 h at room temperature showed no maturation pattern when stained with GBHA, as did teeth treated with EDTA and a bisphosphonate (HEBP). Hydrochloric acid and nitric acid removed the layer of outer enamel and incisors did not stain with suggesting that the staining is a surface-related As staining was abolished by either the removal of phenomenon. (EDTA) or protein (quanidine), the concurrent mineral localization of non-crystal-bound calcium by GBHA staining, and glycoprotein by PAS staining, indicates that calcium associated with glycoprotein at the surface of the enamel.

#### INTRODUCTION >

Amelogenesis can be divided into two stages, secretion (reviewed by Weinstock and Leblond, 1971; Slavkin et al., 1976; Warshawsky, 1979; Karim and Warshawsky, 1979) and maturation (Deakins, 1942; Weinmann et al., 1942; Reith and Cotty, 1962; ·Allan, 1967; Robinson et al., 1977; Warshawsky, 1985). During maturation, the organic matrix produced during the secretory stage is removed and the mineral content of the enamel is increased, but the mechanism by which this occurs is not clear. Immediately adjacent to the maturing enamel are two distinctively different types of cells; ruffle-ended and smooth-ended ameloblasts (Suga, 1959; Smith and Warshawsky, 1974; Josephsen and Tejerskov, 1977) arranged as bands across the rat incisor (Takano and Ozawa, 1980; Reith and Boyde, 1981a; Warshawsky, The various banding patterns of rat enamel correlate with the distribution of these ameloblasts (Boyde and Reith, 1981, 1982; Reith and Boyde, 1981b; Takano et al., 1982; Reith et al., 1982, 1984). In particular, the glyoxal bis(2-hydroxyanil)(GBHA) staining method (Kashiwa and Sigman, 1966) has shown dramatic banding patterns (Takano et al., 1982). Takano et al. (1982) and Smith et al. (1987) have shown that the GBHA-stained bands directly correspond to the distribution of smooth-ended ameloblasts on the surface of rat incisor enamel.

GBHA stains inorganic material, presumably non-crystal-bound calcium (Kashiwa and Sigman, 1966). The organic matrix of enamel also has regional staining differences, as revealed by a number of different stains (Boyde and Reith, 1982), which consistently

reflect the alternating pattern of ruffle-ended and smooth-ended ameloblasts. Thus, the maturation pattern of enamel seems to be under the strict control of the overlying enamel organ.

The GBHA stain and the periodic acid-Schiff (PAS) reaction were used to visualize the maturation pattern of rat incisor enamel. A suitable concentration for each stain was determined so as to reveal the narrower stripes as well as the broader bands.

### MATERIALS AND METHODS

## Experimental procedures prior to staining

Sherman and Sprague-Dawley rats weighing 100  $\pm$  20 gm were decapitated under ether anesthesia and the lower incisors were dissected out of the surrounding alveolar bone. The enamel organs were removed from the teeth with gauze moistened in Some incisor teeth were air-dried immediately with no other treatment prior to staining. The remainder were immersed in one of the following solutions for various times immediately after the removal of the enamel organ: (1) physiological saline, (2) 4.0 M quanidine-HCl in 0.05 M Tris-HCl buffer, pH 7.2, (3) 4.13% EDTA, pH 7.4, (4) 1.2% 1-hydroxyethyl-idene-1,1bisphosphonate (HEBP) in saline, (5) 1.3% hydrochloric acid (HCl) and (6) 1.3% nitric acid (HNO3). All treatments were performed at 4°C except for one tooth which was immersed in the guanidine solution at room temperature. The incisors from each animal were kept together as pairs; one was treated with the experimental, agent, whereas the other was treated with saline for the same length of time to serve as a control. The teeth were then airdried.

#### Enamel staining with GBHA and PAS

Following the various experimental treatments described above, the teeth were stained with GBHA except for a normal pair and a guanidine-extracted pair which were stained by the PAS reaction. The incisors were immersed for 30 sec at room temperature in 100 ml of a 75% ethanol solution containing 0.875 gm of GBHA (Sigma) and 0.35 gm of NaOH. In order to correlate staining intensity, all teeth were mounted in a single piece of plasticene and immersed together into the continuously agitated GBHA solution. After staining, the incisors were rinsed briefly in absolute ethanol and allowed to air-dry at room temperature.

Two pairs of incisors, normal and guanidine-extracted, were prepared as above and stained by the PAS technique (McManus, 1946). Briefly, oxidation was performed with 0.5% periodic acid for 10 min at room temperature. The teeth were washed and aldehydes were visualized using 0.5% basic fuchsifi for 10 min at room temperature. The incisors were then reduced for 2 min in 0.5% sodium metabisulphite, rinsed in water and air-dried. All teeth were mounted in plasticene and photographed.

## Ground sectioning

After photography of the staining patterns, the GBHA-stained teeth were rehydrated and then dehydrated through a graded acetone series. The teeth were embedded in Epon and sections were cut with a Gillings-Hamco thin sectioning machine at the mid-point of the maturation zone in a plane perpendicular to the

long axis of the incisor. The sections were then mounted and cover-slipped in Epon.

### RESULTS

### Untreated incisors

Lower incisors that were air-dried immediately after dissection and stained with GBHA or the PAS reaction had a banding pattern on the enamel surface. The location of this pattern sometimes varied slightly on incisors from different animals but, with the contralateral incisor from the same animal, the patterns were usually symmetrical. In GBHA-stained teeth, the pattern consisted of 2 to 5 red bands running across the enamel (Fig. 1, left). Often the most apical band ran transversely across the tooth. The other bands were oblique and their staining intensity decreased incisally so that no bands were observed in the pigmented enamel. The interband regions contained a lightly stained, pink area in which other thinner \_stripes could be observed, and an incisal unstained area. staining intensity of the thin stripes was generally greatest in the second and third interband regions and ran across the second and third darkly-stained bands. The orientation of these stripes did not necessarily follow the curvature of the bands. The enamel apical to the first band, presumably in the secretion zone of the tooth, was lightly-stained. The arrangement and symmetry of these staining characteristics was generally similar between contralateral incisors.

In the PAS-stained teeth, the staining pattern was similar to that observed after staining with GBHA. Two to four magenta

bands ran across the enamel (Fig. 3). The staining intensity of the oblique bands decreased incisally and none were observed in the pigmentation zone. The entire interband regions were lightly stained and also showed the narrower stripes running across the tooth. However, no incisal, unstained area was observed in the interband region. The enamel in the secretion zone was lightly stained.

### Treated incisors

Treatment before staining either modified or removed the stained banding patterns. Immersion of an untreated tooth in physiological saline at 4°C for 2°h prior to GBHA staining caused a reduction in staining intensity (Fig. 1, right) compared to the untreated, immediately-stained, contralateral tooth (Fig. 1, left). Both the lightly-stained enamel in the secretion zone and the bands and stripes in the maturation zone showed this reduction of staining.

## Guanidine treatment

Immersion in a 4.0 M guanidine solution for 2 h at 4°C before GBHA staining removed all the bands except the first oblique one, which was stained less intensely (Fig. 2a, left) compared to the contralateral control that had been immersed in saline for 2 h at 4°C (Fig. 2a, right). The stripes remained slightly visible in the treated tooth, but the transverse band and the enamel in the secretion zone did not stain. Immersion in this guanidine solution for 2 h at room temperature produced no bands or stripes whatsoever when stained with GBHA (Fig. 2b).

Figure 4 shows an incisor immersed for 2 h in the guanidine solution at 4°C (left) and the contralateral incisor immersed in saline for 2 h at 4°C (right), both of which then were stained with the PAS reaction. In the guanidine-immersed tooth, there was no apical transverse band and a reduction of stain uptake in both the oblique bands and the stripes.

### EDTA treatment

Figure 5 shows an incisor pair, one of which was immersed in EDTA for 5 min at 4°C (left), and the other in saline for 5 min at 4°C (right). The control tooth had typical GBHA staining, whereas the EDTA-treated incisor was unstained.

## HEBP treatment

Figure 6 shows an incisor immersed for 2 h at 4°C in HEBP (left) and the contralateral tooth immersed in saline for 2 h at 4°C (right). The HEBP-treated tooth was unstained with GBHA, whereas the control tooth had a typical staining pattern.

# Acid treatment

Incisors treated with hydrochloric and nitric acid also showed removal of the GBHA staining pattern. Figure 7 shows an unstained incisor that was immersed in HCl for 30 sec at 4°C (left) before GBHA staining; the control tooth had typical GBHA staining after 30 sec in saline (Fig. 7, right). Nitric acid for 30 sec at 4°C (Fig. 8, left) removed the GBHA-stained banding pattern which appeared in the control (right).

### Ground sections

These sections revealed a continuous layer of enamel that covered the labial surface of the tooth (Figs. 9-14). In the normal tooth (Fig. 9), the maturing enamel exhibited rod and interrod patterns that allowed the junction between inner and outer enamel to be determined (arrows). After guanidine (Fig. 10), EDTA (Fig. 11) and HEBP (Fig. 12), all teeth showed an intact layer of inner and outer enamel, although a possible slight cracking of the outer enamel was present in the EDTA-treated tooth. The dentin in the guanidine-treated tooth (Fig. 10) was particularly opaque to transmitted light. The HCl- (Fig. 13) and HNO<sub>3</sub>- (Fig. 14) exposure removed the outer enamel and possibly some of the inner enamel, revealing the inner enamel rod pattern at the surface of the tooth (Fig. 13, arrow).

# **DISCUSSION**

These findings show that the maturation pattern of rat incisor enamel as revealed by GBHA staining is similarly shown by the PAS reaction and that this pattern can be affected by various agents when applied prior to staining. The PAS surface staining is similar to GBHA staining, and not only confirms the presence of an enamel maturation pattern consisting of bands, stripes and unstained areas (Boyde and Reith, 1981, 1982; Takano et al., 1982), but also indicates the chemical nature of some of its constituents. The PAS reaction is generally used to localize glycoproteins or any mucous substance containing neutral sugars. The organic matrix of enamel contains carbohydrate residues as demonstrated by radioautography (Weinstock and Leblond, 1971) and

by PAS staining of SDS-polyacrylamide gels used to separate enamel proteins (Termine et al., 1980). It has been shown here that these glycoproteins are concentrated in the bands and stripes.

Binding of calcium by GBHA is dependent on the presence of non-crystal-bound calcium (Kashiwa and Sigman, 1966). not bind to calcium already incorporated hydroxyapatite (Kashiwa and House, 1964), presumably the GBHA staining of enamel indicates the binding of calcium that has not yet contributed to growth of enamel crystallites. This calcium discrete regions of appears to be localized in corresponding to the bands and stripes observed after GBHA Those regions that do not stain with GBHA may be where all the calcium is in the form of hydroxyapatite. The concurrent localization of non-crystal-bound calcium and glycoprotein suggests that the two may be associated. The correlation of these staining patterns with different cell types (Takano et al., 1982; Smith et al., 1987) emphasizes the functional differences between smooth-ended and ruffle-ended ameloblasts and implicates them in glycoprotein and calcium regulation at the surface of the enamel.

The dissociative guanidine extraction technique of Termine et al. (1980) was used to further investigate the possibility that enamel proteins are in some way responsible for some aspect of enamel maturation. This procedure completely dissolves and extracts amelogenin proteins without dissolving the hydroxyapatite crystals. Guanidine extraction for 2 h greatly

diminished (at 4°C) or completely prevented (at room temperature) staining with GBHA. As GBHA presumably stains only the noncrystal-bound calcium present in the bands and stripes and quanidine extraction of the amelogenin proteins completely prevents their staining, then there must be an association between calcium and enamel protein. This is in agreement with Drinkard et al. (1981), who demonstrated calcium binding by the organic matrix of bovine enamel. Thus, enamel proteins may retain calcium in the enamel for further crystal growth. Acidic conditions have been used to extract (Fukae and Shimizu, 1974; Shimokawa and Sasaki, 1978; Fukae et al., 1979) or dissolve (Fincham, 1979) enamel proteins and mineral. Ground sections through incisors treated with HCl or HNO3 revealed that at least the outer enamel had been removed from the surface of the tooth. The failure to stain acid-treated incisors with GBHA indicates that such staining in rat incisor enamel is a surface-related phenomenon.

Treatment of incisors with EDTA prevented all GBHA staining; EDTA is used routinely to chelate calcium, thereby demineralizing hard tissues (Warshawsky and Moore, 1967). If GBHA does stain a calcium-protein complex, as suggested by the outcome of the guanidine extraction experiment, then the non-crystal-bound calcium of this complex may have been chelated and removed by the EDTA and therefore was not available for GBHA binding. A ground section through an EDTA-treated tooth showed that a continuous layer of enamel remained so that loss of GBHA staining could not be attributed to a loss of enamel integrity.

Bisphosphonates, such as HEBP, are analogues pyrophosphate which resist enzymatic hydrolysis and inhibit biological mineralization (Fleisch, 1983). They are similar in their actions to pyrophosphate in that they (a) precipitation of calcium phosphate from clear solutions (Fleisch et al., 1970), (b) block the transformation of amorphous calcium phosphate into hydroxyapatite (Francis, 1969; Francis et al., 1969; Meyer and Nancollas, 1973; Boskey et al., 1979), (c) delay the aggregation of apatite crystals into larger clusters (Hansen et al., 1976), (d) disaggregate apatite crystal clusters (Bisaz et al., 1976) and, (e) slow down crystal dissolution (Fleisch et al., 1969; Russell et al., 1970; Evans et al., 1980). effects seem to be related to their marked affinity for hydroxyapatite (Jung et al., 1973) and amorphous calcium phosphate (Francis et al., 1980). Little is known about the specific effects of bisphosphonates on enamel. In this study it was found that a 2 h application of HEBP to the rat enamel surface caused a loss of GBHA staining, but a complete layer of enamel remained on the tooth. Again, as GBHA staining presumably requires the presence of non-crystal-bound calcium, HEBP treatment must have either removed or prevented GBHA staining of this calcium.

Synthetic calcium-phosphate solutions with concentrations of these ions similar to those of serum contain, in addition to free calcium and phosphate ions, a variety of Ca-P and Ca-P-x complexes (where x = a variety of organic or inorganic ligands; Glimcher, 1976). It may be that enamel proteins in solution act as Ca or Ca-P ligands, so the high affinity of HEBP for these

complexes might prevent the observed binding of GBHA to this calcium. Furthermore, the slowing of crystal dissolution by HEBP would only stabilize that mineral already bound to hydroxyapatite.

The results presented here are consistent with the hypothesis that by controlling the aggregation of mineral ions, the organic matrix may serve as a biological catalyst for initiating mineralization of hard tissues (Neuman and Neuman, 1958; Drinkard et al., 1981). The binding of calcium by anionic sites of the enamel organic matrix may not only provide a mechanism for heterogenous nucleation of crystal formation, but may also form a template for the shape of the crystals, and for propagation and regulation of further crystal growth as the degree of mineralization of enamel increases throughout maturation.

### REFERENCES

Allan JH 1967 Maturation of enamel. In: Structural and Chemical Organization of Teeth. Ed. Miles AEW. Academic Press, New York. pp. 467-492.

Bisaz S, Felix R, Hansen NM and Fleisch H 1976 Disaggregation of hydroxyapatite crystals. Biochim Biophys Acta, 451:560-566.

Boskey AL, Goldberg MR and Posner AS 1979 Effect of diphosphonates on hydroxyapatite formation induced by calcium-phospholipid-phosphate complexes. Calcif Tiss Int, 27:83-88.

Boyde A and Reith EJ 1981 Display of maturation cycles in ratincisor enamel with tetracycline labelling. Histochem, 72,551-561.

Boyde A and Reith EJ 1982 In vitro histological and tetracycline staining properties of surface layer enamel also reflect the cyclical nature of the maturation process. Histochem, 75:341-351.

Deakins M 1942 Changes in the ash, water and organic content of pig enamel during calcification. J Dent Res, 21:429-435.

Drinkard C, Gibson L, Crenshaw MA and Bawden JW 1981 Calcium binding by the organic matrix of developing bovine enamel. Archs Oral Biol, 26:483-485.

Evans JR, Robertson WG, Morgan DB and Fleisch H 1980 Effects of pyrophosphate and diphosphonates on the dissolution of hydroxyapatites using a flow system. Calcif Tiss Int, 31:153-159.

Fincham AG 1979 The amelogenin problem: A comparison of purified enamel matrix proteins. Calcif Tiss Int, 27:65-73.

Fleisch H 1983' Bisphosphonates: Mechanisms of action and clinical applications. In: Bone and Mineral Research. Ed. Peck WA. Elsevier Science Publishers, New York. pp. 319-357.

Fleisch H, Russell RGG and Francis MD 1969 Diphosphonates inhibit hydroxyapatite dissolution in vitro and bone resorption in tissue culture and in vivo. Science, 165:1262-1264.

Fleisch H, Russell RGG, Bisaz S, Muhlbauer RC and Williams DA 1970 The inhibitory effect of phosphonates on the formation of calcium phosphate crystals in vitro and on acrtic and kidney calcification in vivo. Eur J Clin Invest, 1:12-18.

Francis MD 1969 The inhibition of calcium hydroxyapatite crystal growth by polyphosphates. Calcif Tiss Res, 3:151-162.

Francis MD, Russell RGG and Fleisch H 1969 Diphosphonates inhibit formation of calcium phosphate crystals in vitro and

pathological calcification in vivo. Science, 165:1264-1266.

Francis MD, Ferguson, DL, Tofe AJ, Bevan JA and Michaels SE-1980 Comparative evaluation of three diphosphonates: In vitro adsorption (C-14 labeled) and in vivo osteogenic uptake (Tc-99m complexed). J Nucl Med, 21:1185-1189.

Fukae M and Shimizu M 1974 Studies on the proteins of developing bovine enamel. Archs Oral Biol, 19:381-386.

Fukae M, Ijiri H, Tanabe T and Shimizu M 1979 Partial amino acid sequences of two proteins in developing porcine enamel. J Dent Res, 58(B):1000-1001.

Glimcher MJ 1976 Composition, structure, and organization of bone and other mineralized tissues and the mechanisms of calcification. In: Handbook of Physiology-Endocrinology. Williams and Wilkins, Baltimore. pp. 25-116.

Hansen NM Jr, Felix R, Bisaz S and Fleisch H 1976 Aggregation of hydroxyapatite crystals. Biochim Biophys Acta, 451:549-559.

Josephsen K and Fejerskov O 1977 Ameloblast modulation in the maturation zone of the rat incisor enamel organ. A light and electron microscopic study. J Anat, 124:45-70.

Jung A, Bisaz S and Fleisch H 1973 The binding of pyrophosphate and two diphosphonates on hydroxyapatite crystals. Calcif Tiss Res, 11:269-280.

Karim A and Warshawsky H 1979 The effect of colcemid on the structure and secretory activity of ameloblasts in the rat incisor as shown by radioautography after injection of <sup>3</sup>H-proline. Anat Rec, 195:587-609.

Kashiwa HK and House CM Jr 1964 The glyoxal bis(2-hydroxyanil) method modified for localizing insoluble calcium salts. Stain Tech, 39:359-367.

Kashiwa HK and Sigman MD Jr 1966 Calcium localized in odontogenic cells of rat mandibular teeth by the glyoxal bis(2-hýdroxyanil) method. J Dent Res, 45:1796-1799.

McManus JFA 1946 Histological demonstration of mucin after periodic acid. Nature, 158:202.

Meyer JL and Nancollas GH 1973 The influence of multidentate organic phosphonates on the crystal growth of hydroxyapatite. Calcif Tiss Res, 13:295-303.

Neuman WF and Neuman MW 1958 Chemical Dynamis of Bone Mineral. University of Chicago Press, Chicago. pp. 169-187.

Reith EJ and Cotty VF 1962 Autoradiographic studies on calcification of enamel. Archs Oral Biol, 7:365-372.

Reith EJ and Boyde A 1981a The arrangement of ameloblasts on the surface of maturing enamel of the rat incisor tooth. J Anat, 133:381-388.

Reith EJ and Boyde A 1981b The cyclical entry of calcium into maturing enamel of the rat incisor tooth. Archs Oral Biol, 26:983-988.

Reith EJ, Boyde A and Schmid MI 1982 Correlation of rat incisor ameloblasts with maturation cycles as displayed on the enamel surface with EDTA. J Dent Res, 61:1563-1573.

Reith EJ, Schmid MI and Boyde A Rapid uptake of calcium in maturing enamel of the rat incisor. Histochem, 80:409-410.

Robinson C, Lowe NR and Weatherell JA 1977 Changes in amino acid composition of developing rat incisor enamel. Calcif Tiss Res, 23: 19-31.

Russell RGG, Muhlbauer RC, Bisaz S, Williams DA and Fleisch H 1970 The influence of pyrophosphate, condensed phosphates, phosphonates and other phosphate compounds on the dissolution of hydroxyapatite in vitro and on bone resorption induced by parathyroid hormone in tissue culture and in thyroparathyroidectomized rats. Calcif Tiss Res, 6:183-196.

Shimokawa H and Sasaki S 1978 Study on the biosynthesis of bovine enamel protein in vitro. J Dent Res, 57:133-138.

Slavkin HC, Mino W and Bringas P 1976 The biosynthesis and secretion of precursor enamel protein by ameloblasts as visualized by autoradioagraphy after tryptophan administration. Anat Rec, 185:289-312.

Smith CE and Warshawsky H 1974 Morphological classification of rat incisor ameloblasts. Anat Rec, 179:423-446.

Smith CE, McKee MD and Nanci A 1987 Cyclic induction and rapid movement of sequential waves of new smooth-ended ameloblast modulation bands in rat incisors as visualized by polychrome fluorescent labelling and GBHA-staining of maturing enamel. J Dent Res, In Press.

Suga S 1959 'Amelogenesis. Some histological and histochemical observations. Int Dent J, 9:394-420.

Takano Y and Ozawa H 1980 Ultrastructural and cytochemical observations on the alternating morphologic changes of the ameloblasts at the stage of enamel maturation. Archs Hist Jap, 43:385-399.

Takano Y, Crenshaw MA, Bawden JW, Hammarström L and Lindskog S 1982 The visualization of the patterns of ameloblast modulation by the glyoxal bis(2-hydroxyanil) staining method. J Dent Res,

61:1580-1586.

Termine JD, Belcourt AB, Christner PJ, Conn KM and Nylen MU 1980 Prpoerties of dissociatively-extracted fetal tooth matrix proteins. I. Principal molecular species in developing bovine enamel. J Biol Chem, 20:9760-9768.

Warshawsky H 1979 Radioautographic studies on amelogenesis. J Biol Buccale, 7:105-126.

Warshawsky H 1985 Ultrastructural studies on amelogenesis. In: The Chemistry and Biology of Mineralized Tissues. Ed. Butler WT. Ebsco Media, Birmingham. pp. 33-45.

Warshawsky H and Moore G 1967 A technique for the fixation and decalcification of rat incisors for electron microscopy. J Histochem Cytochem, 15:542-549.

Weinmann J, Wessinger GD and Reed G 1942 Correlation of chemical and histological investigations on developing enamel. J Dent Res, 21:171-182.

Weinstock A and Leblond CP 1971 Elaboration of the matrix glycoprotein of enamel by secretory ameloblasts of the incisor as revealed by radioautography after <sup>3</sup>H-galactose injection. J Cell Biol, 51:26-51.

## FIGURE LEGENDS: CHAPTER THREE

Figure 1. A pair of lower incisors stained with GBHA. The apical ends are below. The incisor on the left was not treated prior to staining. The staining pattern consists of an apical band running transversely and several oblique bands across the enamel. The interband regions contain a lightly-stained area within which narrow stripes can be seen, and an incisal, unstained area. The incisor on the right, immersed in saline for 2 h at 4°C prior to GBHA staining, shows a similar pattern but with less staining intensity. X6.5.

Figure 2. Lower incisors stained with GBHA. The incisor on the left of Fig. 2a and the incisor in Fig. 2b were immersed for 2 h in a guanidine solution at 4°C and room temperature, respectively, prior to staining. The incisor on the right in Fig. 2a was immersed in saline for 2 h as a control. Note the reduction (Fig. 2a, at left) and complete lack of (Fig. 2b) the GBHA staining patterns in the guanidine-treated teeth. X6.5.

Figure 3. Incisors stained by the PAS reaction. Neither was treated prior to staining; they show a transverse and several oblique bands across the enamel. The interband regions are lightly-stained, show narrow stripes and do not contain an unstained region. X6.5.

Figure 4. Lower incisors stained by the PAS reaction. That on the left was immersed for 2 h in a guanidine solution at 4°C prior to staining; it shows a lack of the transverse band and reduction in staining intensity of the remaining bands compared to the control incisor on the right, which was immersed for 2 h in saline before staining. X6.5.

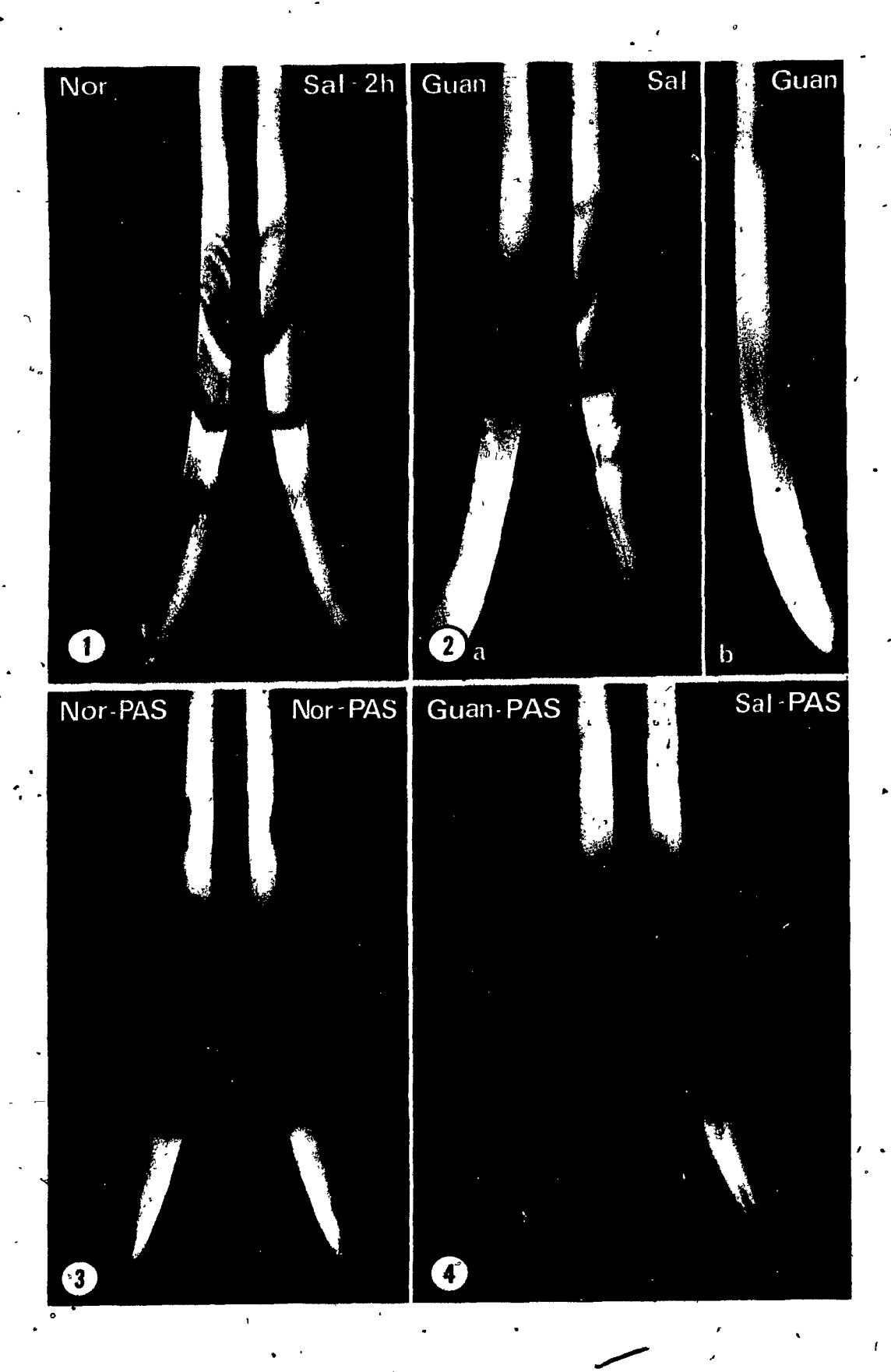


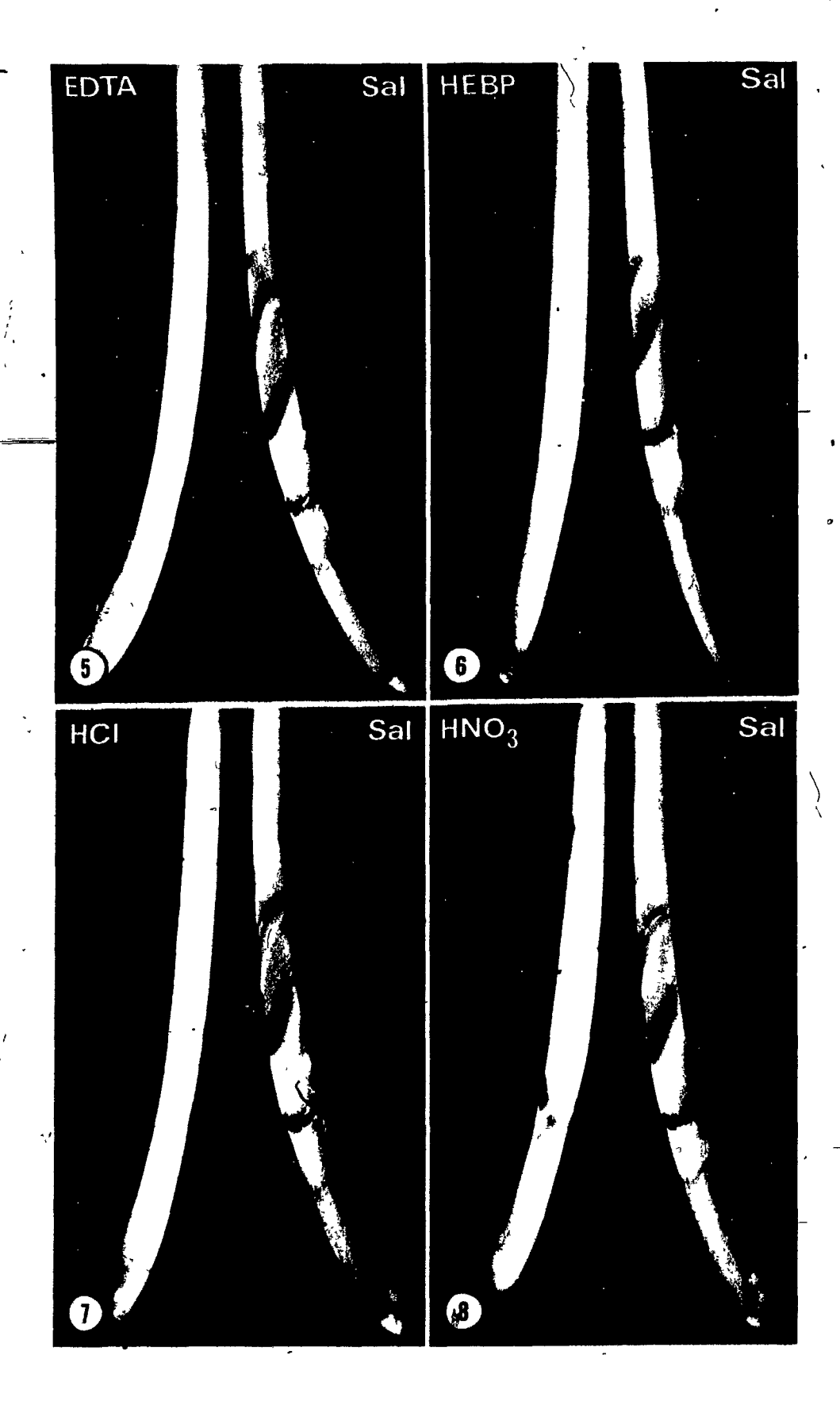
Fig.

Figure 5. Contralateral lower incisors stained with GBHA. Apical ends are below; that on the left was immersed in EDTA for 5 min at 4°C, and the control (right) was immersed in saline for the same time and at the same temperature. The control shows typical GBHA staining; the EDTA-treated incisor shows no staining. X6.5.

Figure 6. A pair of lower incisors stained with GBHA. That on the left was immersed in HEBP for 2 h at 4°C. The control shows the expected staining pattern after 2 h in saline, whereas the HEBP-treated incisor shows no staining. X6.5.

\*Figure 7. A pair of lower incisors stained with GBHA. That on the left was immersed in HCl for 30 sec at 4°C, and the control (right) was immersed in saline for 30 sec at 4°C. The control shows typical GBHA staining; the HCl-treated tooth shows no staining. X6.5.

Figure 8. A pair of lower incisors stained with GBHA. That on the left was immersed in HNO3 for 30 sec at 4°C; the control (right) was immersed in saline for 30 sec. at 4°C. The control shows typical GBHA staining; the HNO3-treated tooth shows no staining. X6.5.

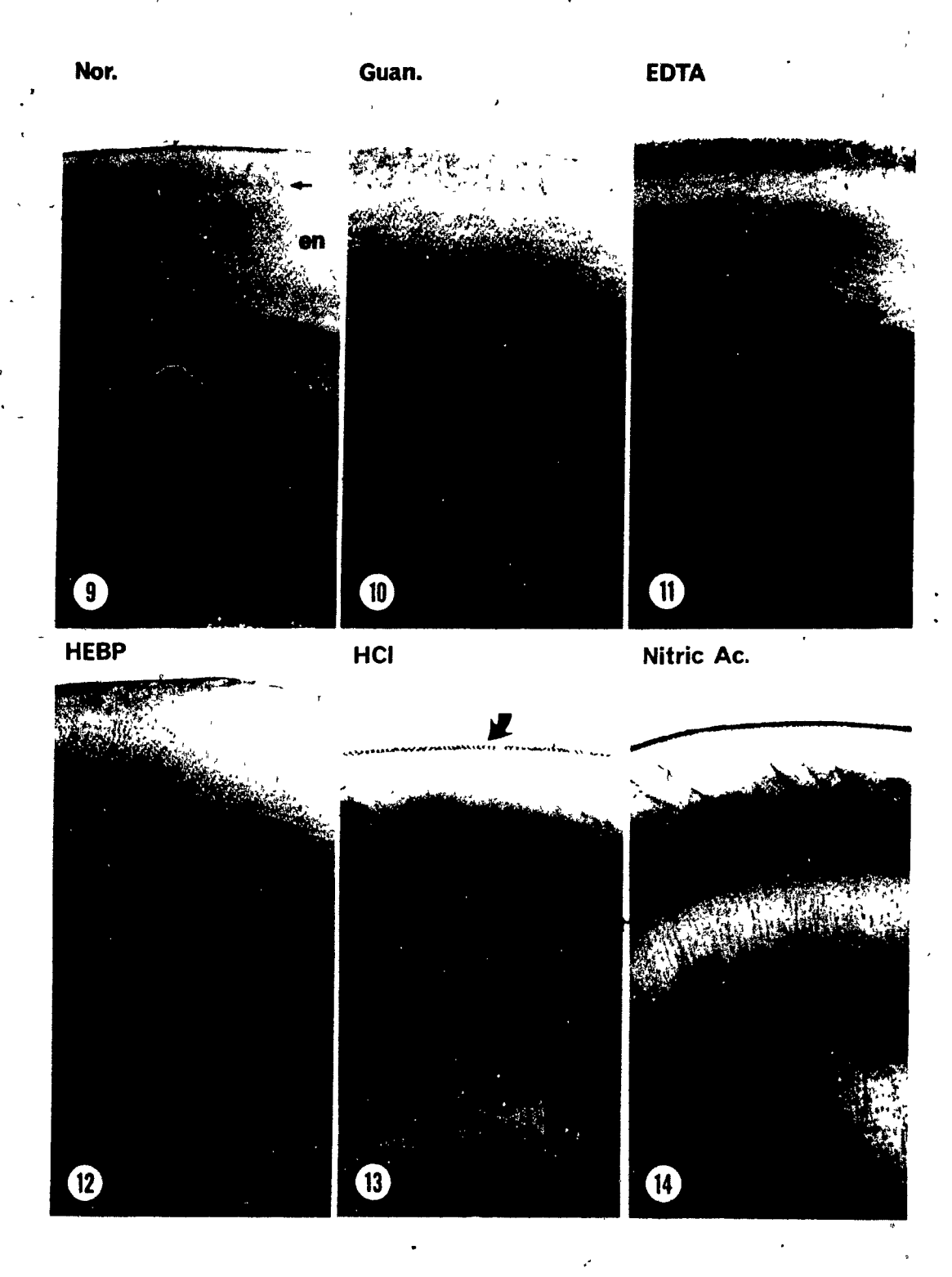


Figures 9-14. Ground sections through normal and treated incisors at the midpoint of the maturation zone in a plane perpendicular to the long axes of the teeth. All teeth were stained with GBHA prior to the ground sectioning.

Figure 9. Light micrograph of a normal, untreated incisor showing a completely intact layer of enamel (en) covering the dentin (den). The arrows indicate the junction between inner and outer enamel. X400.

Figures 10-12. Light micrographs of incisors treated with guanidine (Fig. 10), EDTA (Fig. 11) and HEBP (Fig. 12). An intact layer of inner and outer enamel covers the dentin. X400.

Figures 13, 14 Light micrographs of incisors treated with HCl (Fig. 13) and HNO<sub>3</sub> (Fig. 14). The outer enamel and probably some inner enamel have been removed leaving the inner enamel rod pattern at the surface (arrow, Fig. 13). X400,



CHAPTER FOUR: MODIFICATION OF THE ENAMEL MATURATION PATTERN BY VINBLASTINE AS REVEALED BY GLYOXAL BIS(2->)
HYDROXYANIL) (GBHA) STAINING AND 45 CALCIUM RADIOAUTOGRAPHY.

### SYNOPSIS

Patterns characteristic of enamel maturation can be visualized at the surface of the rat incisor by staining with glyoxal bis(2-hydroxyanil)(GBHA) and radioautography following <sup>45</sup>Ca injection. In this study, the effects of vinblastine on enamel maturation were monitored by these two methods. At 4 h after injection of vinblastine, the darkly-stained GBHA bands had widened incisally into the interband regions when compared to Radioautography at 5 min after calcium normal, control teeth. injection in vinblastine-treated animals (4 h) showed a modified maturation pattern of weaker labeling and less distinct banding. At 8 h after vinblastine injection, most of the enamel stained uniformly with GBHA, and bands and interband regions could not be Radioautography at 5 min after calcium injection resolved. showed that the 8 h vinblastine treatment removed the banding pattern, leaving only a weakly-labeled area. Vinblastine is known to destroy and prevent the formation and turnover of microtubules, and hence the formation of ruffled borders of ruffle-ended ameloblasts (Akita et al. 1983). The concomitant decrease in calcium incorporation implies that events taking place in relation to the ruffled border may affect calcium exchange or accretion within the enamel.

### INTRODUCTION

During enamel maturation, the organic matrix produced during the secretory stage is removed and the mineral content of the enamel is increased. Although the mechanism for such an interchange is not clear, the cyclical nature of this maturation process has been demonstrated within the enamel itself by several different in vitro techniques, such as: glyoxal bis(2hydroxyanil) (GBHA) staining (Takano et al., 1982), tetracycline staining (Boyde and Reith, 1982), radioautography after dipping in <sup>45</sup>Ca (Warshawsky, 1985), and by various histological stains (Boyde and Reith, 1982). In vivo techniques also have demonstrated that the cyclical nature of enamel maturation can be seen at the level of the enamel organ. Such techniques include injection of calcein (Josephsen, 1983), systemic injection of calcium and radioautography (Reith and Boyde, 1981; Reith et al., 1984), tetracycline injection (Boyde and Reith, 1981) and EDTA etching (Reith et al., 1982). Furthermore, the repetitive banding, characteristic of the enamel maturation pattern, has been correlated to the cyclic distribution of ruffle-ended (RA) and smooth-ended (SA) ameloblasts of the enamel organ (Boyde and Reith, 1981, 1982; Reith and Boyde, 1981; Takano et al., 1982; Reith et al., 1982, 1984; Josephsen, 1983). Recently, DenBesten et al. (1985) have shown that fluoride disrupts the cyclic patterns of the maturation stage. Fluorosed enamel showed fewer calcein-stained stripes and fewer cycles of 45Ca uptake.

Microtubules are cellular organelles that have been implicated in various cellular activities including secretion,

resorption, organization and maintenance of cell Vinblastine is a drug which binds to tubulin, the microtubule subunit, destroying existing microtubules and preventing the formation of new ones. Consequently, there is an interruption in cellular organization and function. Vinblastine (Moe and Mikkelsen, 1977; Takuma et al., 1982), colchicine (Kudo 1975) and colcemid (Karim and Warshawsky, 1979) all have been used to alter the secretory activity of ameloblasts during enamel formation. More recently, Akita et al. (1983) showed that vinblastine and colchicine caused a loss of both microtubules and the ruffled border of RAs in the maturation zone of the rat incisor. ruffling of the cell surface frequently is found in cells involved in absorption, resorption, ionic pumping or exchange, this morphological feature of maturation ameloblasts has been assumed to indicate similar functions in enamel maturation. The possibility of resorption has been further strengthened by the finding of enamel proteins in lysosomes of RAs (Nanci et al., Therefore, this study investigated the functional consequences of vinblastine's ability to remove the ruffled border by monitoring changes in the enamel as revealed by GBHA staining and radioautography after injection of 45 calcium.

# MATERIALS AND METHODS

## Animal procedures

Sherman rats weighing  $100 \pm 10$  gm were used in this study. Vinblastine sulphate (Sigma Chemicals) was administered intravenously to four animals via the external jugular vein at a concentration of 0.5 mg in 0.1 ml physiological saline. The

animals were sacrificed by decapitation at 4 h and 8 h after injection. The lower incisors were dissected from the surrounding alveolar bone and the enamel organs were wiped from the teeth with gauze moistened in saline. All incisors were airdried at room temperature. On the incisors of two, untreated control animals, the position of the white opaque boundary (Robinson et al., 1974) was notched in the enamel with a scalpel.

## Enamel staining with GBHA

Following air drying of the vinblastine-treated incisors, they were stained with GBHA to reveal the maturation pattern at the surface of the teeth. The incisors were immersed for 30 sec at room temperature in 100 ml of a 75% ethanol solution containing 0.875 gm of GBHA (Sigma Chemicals) and 0.35 gm NaOH. In order to correlate and compare staining intensity, all teeth were immersed together into the GBHA staining solution. After staining, the incisors were rinsed briefly in absolute ethanol and allowed to air dry at room temperature. The characteristic GBHA staining pattern of normal, untreated teeth served as a control.

# Radioautography of enamel after 45 ca injection

At 4 h and 8 h after intravenous injection of vinblastine, 100 µCi of  $^{45}\text{CaCl}_2$  (New England Nuclear) were injected into the contralateral jugular vein. The animals were sacrificed 5 min later by decapitation and the lower incisors were dissected and dried as described above. Following air drying, all teeth were dipped in a 0.5% gelatin solution containing 0.05 gm chrome alum

for 20 sec at 40°C. The teeth then were dipped in photographic emulsion (Kodak), exposed for 5 d, and developed according to the method of Kopriwa and Leblond (1962). The characteristic <sup>45</sup>Ca radioautographic pattern at 5 min after injection in normal, untreated teeth served as a control. All teeth were fixed to a platform with plasticene and photographed.

### RESULTS

### GBHA staining: Normal incisors

Lower incisors from control normal, untreated animals showed a banding pattern on the surface of the enamel after GBHA staining (Fig. 1). The location of the individual bands of this pattern varied slightly on incisors from different animals, but were generally symmetrical in incisors from the same animal. The staining pattern consisted of up to six red bands running across the enamel, separated by interband regions. The staining intensity of the bands decreased incisally. No bands were observed in the pigmented enamel. Often the most incisal bands showed a thin, darkly-stained line associated with the apical side of the band. The interband regions contained a lightly-stained, pink area apically, and an incisal, unstained area. The enamel apical to the first band was presumably in the secretion zone of the tooth and stained lightly.

# GBHA staining: Vinblastine-treated incisors

Lower incisors from vinblastine-treated animals showed a modification of the GBHA-stained banding pattern. At 4 h after vinblastine injection (Fig. 2), the widening of the intensely-

stained red bands was most striking. These bands widened in an incisal direction, thereby diminishing the width of the lightly-stained, pink interband regions. The unstained areas in the interband region were similar or slightly wider than those in the control. The thin, darkly-stained lines normally close to the incisal dark bands, were separated from these bands and appeared within the unstained regions. The overall staining intensity was slightly greater in the experimental than in the control animals.

At 8 h after vinblastine injection (Fig. 3), the GBHA staining pattern was altered completely. The sharp, darkly-stained red bands were not discernible and the staining pattern could not be divided into band and interband regions. Most of the enamel stained uniformly with GBHA except for a few patches incisally and it was possible to see regions which perhaps corresponded to the unstained bands of the control. The thin, darkly-stained lines observed in the control and the 4 h vinblastine-treated teeth were not present.

## Radioautography: Normal incisors

Five minutes after intravenous injection of <sup>45</sup>Ca into a control animal, radioautography revealed a blackened banded pattern on the tooth surface (Fig. 4), presumably showing incorporation of calcium into the enamel. The pattern consisted of 5 or 6 broad black bands separated by narrow white bands of unlabeled enamel. The intensity of the radioautographic reaction in the heavily-exposed bands decreased incisally. Often the most incisal unlabeled areas had a barely visible, thin black line running through their centers. The enamel in the secretion zone

showed little or no incorporation of calcium. The overall pattern of alternating light and dark bands resembled a negative image of that produced by GBHA staining (compare Figs. 1 and 4), but the unstained bands with GBHA were completely unlabeled in the radioautographs.

# Radioautography: Vinblastine-treated incisors

Lower incisors from vinblastine-treated animals showed a modification of the pattern of calcium incorporation into enamel. At 4 h after vinblastine injection (Fig. 5), the radioautographic reaction was slightly less intense than that of the control and the unlabeled bands were not as obvious and less sharp.

At 8 h after vinblastine injection (Fig. 6), very little radioautographic reaction was present. The alternating pattern of dark and light bands was no longer visible and only a mottled area of calcium incorporation persisted in early maturation. The intensity of this reaction was much weaker than corresponding areas in the control teeth.

### DISCUSSION'

## Microtubules and the ruffled border

The ameloblasts of the maturation zone in the rat incisor show alternating morphologies, especially with regard to their distal cell membranes, and consequently are characterized as being either ruffle-ended or smooth-ended (Suga, 1959; Warshawsky and Smith, 1974; Boyde and Reith, 1976; Josephsen and Fejerskov, 1977). This region is also referred to as the region of ameloblast modulation (Josephsen and Fejerskov, 1977) because

maturation ameloblasts were shown to modulate between the two cell types (Josephsen, 1983; Ishige et al., 1987; Smith et al., 1987). Akita et al. (1983) found that by 8 h after vinblastine injection, no RAs are found in the rat incisor, indicating that the ruffled border had been lost presumably as a result of the anti-microtubular effect of the drug. Thus, vinblastine destroys and interrupts the formation, distribution, and turnover of microtubules, and this in turn prevents the development or maintenance of the extensive cell membrane infoldings of the RAs. This implies that the modulation from ruffled to smooth, and smooth to ruffled, reflects a cyclical redistribution and assembly of new microtubules within the ameloblast as it modulates.

# GBHA staining and the state of calcium binding '

GBHA is a chelometric calcium-binding compound which stains loosely-bound calcium that has not been incorporated into hydroxyapatite (Kashiwa and House, 1964; Kashiwa and Sigman, 1966). The banded maturation pattern of enamel following GBHA staining demonstrates regional differences regarding the presence and concentration of non-crystal-bound calcium within the enamel. Those regions that stain with GBHA contain non-crystal-bound calcium whereas those that do not stain with GBHA probably contain calcium in a crystalline form. It appears that radioautography after <sup>45</sup>Ca injection visualizes both the regions of crystalline and non-crystal-bound calcium. From the radioautographs it appears that only the unstained bands contain enamel which is stable and incapable of exchange or accretion of

radioactive calcium. Since calcium is always present in the enamel either in the form of hydroxyapatite or as transient ionic or loosely-bound calcium, then the regional staining and incorporation differences must indicate differential processing of the available calcium within particular regions. Presumably, the GBHA-stained, non-crystal-bound calcium, is noncrystalline and is associated with the organic matrix of the enamel. Indeed, Drinkard et al. (1981) have demonstrated that calcium binds to the organic matrix of bovine enamel. Guanidine extraction of enamel proteins from intact enamel abolishes the GBHA-stained banding pattern (McKee and Warshawsky, 1986; Chapter Three) thus confirming that the organic matrix binds calcium.

Takano et al. (1982) and Smith et al. (1987) have shown that SAs overlie areas of enamel that stain as intense red bands with the calcium stain GBHA. In the present study, this correlation has been confirmed by demonstrating that vinblastine treatment, which converts RAs to SAs (Akita et al., 1983), results in wider bands of intense GBHA staining at 4 h and continuous non-banded areas at 8 h after injection of vinblastine. Presumably, vinblastine treatment prevents the modulation of SAs into RAs and inhibits the replacement of preexisting microtubules related to the ruffled borders. The ruffled border appears necessary to establish the functional state which leads to regional differences in calcium availability that must be related to normal enamel maturation.

## Radioautography and the state of calcium binding

The banded nature of the enamel maturation pattern as

visualized by radioautography following 45Ca injection was first described by Reith and Boyde (1981), and the regions showing the most calcium incorporation were shown to be those everlain by RAs (Reith and Boyde, 1981; Takano et al., 1982). This study has confirmed this incorporation pattern at 5 min after systemic injection and in addition, has shown that this pattern is Vinblastine treatment dependent on the presence of RAs. dramatically altered the GBHA staining pattern and greatly diminished calcium incorporation. Vinblastine prevents the formation and turnoyer of microtubules, and these in turn prevent the formation of ruffled borders. Since there is a concomitant decrease in 'calcium incorporation, it would imply that events which take place in relation to the ruffled border may affect calcium exchange or accretion within the enamel.

### REFERENCES

Akita H, Kagayama M and Sato R 1983 Light and electron microscopy of the effects of colchicine and vinblastine on maturing rat ameloblasts in vivo. Archs Oral Biol, 28:263-271.

Boyde A and Reith EJ 1976 Scanning electron microscopy of the lateral cell surfaces of rat incisor ameloblasts. J Anat, 122:603-610.

Boyde A and Reith EJ 1981 Display of maturation cycles in ratincisor enamel with tetracycline labelling. Histochem, 72:551-561.

Boyde A and Reith EJ 1982 In vitro histological and tetracycline staining properties of surface layer rat incisor enamel also reflect the cyclical nature of the maturation process. Histochem; 75:341-351.

DenBesten PK, Crenshaw MA and Wilson MH 1985 Changes in the fluoride-induced modulation of maturation stage ameloblasts of rats. J Dent Res, 64:1365-1370.

Drinkard C, Gibson L, Crenshaw MA and Bawden JW 1981 Calcium binding by organic matrix of developing bovine enamel. Archs Oral Biol, 26:483-485.

Ishige N, Ohya K and Ogura H 1987 A rapid cyclic modulation of ameloblasts during enamel maturation. J Dent Res (Abstract), 66:354.

Josephsen K 1983 Indirect visualization of ameloblast modulation in the rat incisor using calcium-binding compounds. Scand J Dent Res, 91:76-78.

Josephsen K and Fejerskov O 1977 Ameloblast modulation in the maturation zone of the rat incisor enamel organ. A light and electron microscopic study. J Anat, 124:45-70.

Karim A and Warshawsky H 1979 The effect of colcemid on the structure and secretory activity of ameloblasts in the ratincisor as shown by radioautography after injection of <sup>3</sup>H-proline. Anat Rec, 195:587-609.

Kashiwa HK and House CM Jr 1964 The glyoxal bis(2-hydroxyanil) method modified for localizing insoluble calcium salts. Stain Tech, 39:359-367.

Kashiwa HK and Sigman MD Jr 1966 - Calcium localized in odontogenic cells of rat mandibular teeth by the glyoxal bis(2-hydroxyanil) method. J Dent Res, 45:1796-1799.

Kopriwa BM and Leblond CP 1962 Improvement in the coating technique for radioautography. J Histochem Cytochem 10:269-284.

Kudo N 1975 Effect of colchicine on the secretion of matrices of dentine and enamel in the rat incisor: an autoradiographic study using <sup>3</sup>H-proline. Calcif Tiss Res, 18:37-46.

McKee MD and Warshawsky H 1986 Modification of the enamel maturation pattern by vinblastine as revealed by glyoxal bis(2-hydroxyanil) staining and <sup>45</sup>calcium radioautography. Histochemistry, 86:141-145.

Moe H and Mikkelsen H 1977 Light microscopical and ultrastructural observations on the effect of vinblastine on ameloblasts in vivo. I. Short-term effect on secretory ameloblasts. Acta Pathol Microbiol Scand, 85A:73-88.

Nanci A, Slavkin HC and Smith CE 1987 Immunocytochemical and radioautographic evidence for secretion and intracellular degradation of enamel proteins by ameloblasts during the maturation stage of amelogenesis in rat incisors. Anat Rec, 217:107-123.

Reith EJ and Boyde A 1981 Autoradiographic evidence of cyclical entry of calcium into maturing enamel of the rat incisor tooth. Archs Oral Biol, 26:983-987.

Reith EJ, Boyde A and Schmid MI 1982 Correlation of rat incisor ameloblasts with maturation cycles as displayed on the enamel surface with EDTA. J Dent Res, 61:1563-1573.

Reith EJ, Schmid MI and Boyde A 1984 Rapid uptake of calcium in maturing enamel of the rat incisor. Histochem, 80:409-410.

Robinson C, Hiller CR and Weatherell JA 1974 Uptake of <sup>32</sup>P labelled phosphate into developing rat incisor enamel. Calcif Tiss Res, 15:143-152.

Smith CE, McKee MD and Nanci A 1987 Cyclic induction and rapid movement of sequential waves of new smooth-ended ameloblast modulation bands in rat incisors as visualized by polychrome fluorescent labelling and GBHA-staining of maturing enamel. J Dent Res, In Press.

Suga S 1959 Amelogenesis: Some histological and histochemical observations. Int Dent J, 9:394-420.

Takano Y, Crenshaw MA, Bawden JW, Hammarström L and Lindskog S 1982 The visualization of the patterns of ameloblast modulation by the glyoxal bis(2-hydroxyanil) staining method. J Dent Res, 61(Sp. Iss.):1580-1586.

Takuma S, Sawada T and Yanagisawa T 1982 Ultrastructural changes of secreting rat-incisor ameloblasts following administration of vincristine and vinblastine. J Dent Res, 61(Sp Iss);1472-1478.

Warshawsky # 1985 Ultrastructural studies on amelogenesis. In: The Chemistry and Biology of Mineralized Tissues. Ed. Butler WT. Ebsco Media, Birmingham. pp. 33-45.

Warshawsky H and Smith CE 1974 Morphological classification of rat incisor ameloblasts. Anat Rec, 179:423-446.

### FIGURE LEGENDS: CHAPTER FOUR

Figure 1. GBHA-stained normal, control teeth. Darkly-stained bands run across the enamel. Interband regions contain an apical lightly-stained area and an incisal unstained area. The enamel in the secretion zone stains lightly with GBHA. The arrow indicates the notch made at the opaque boundary. X6.5.

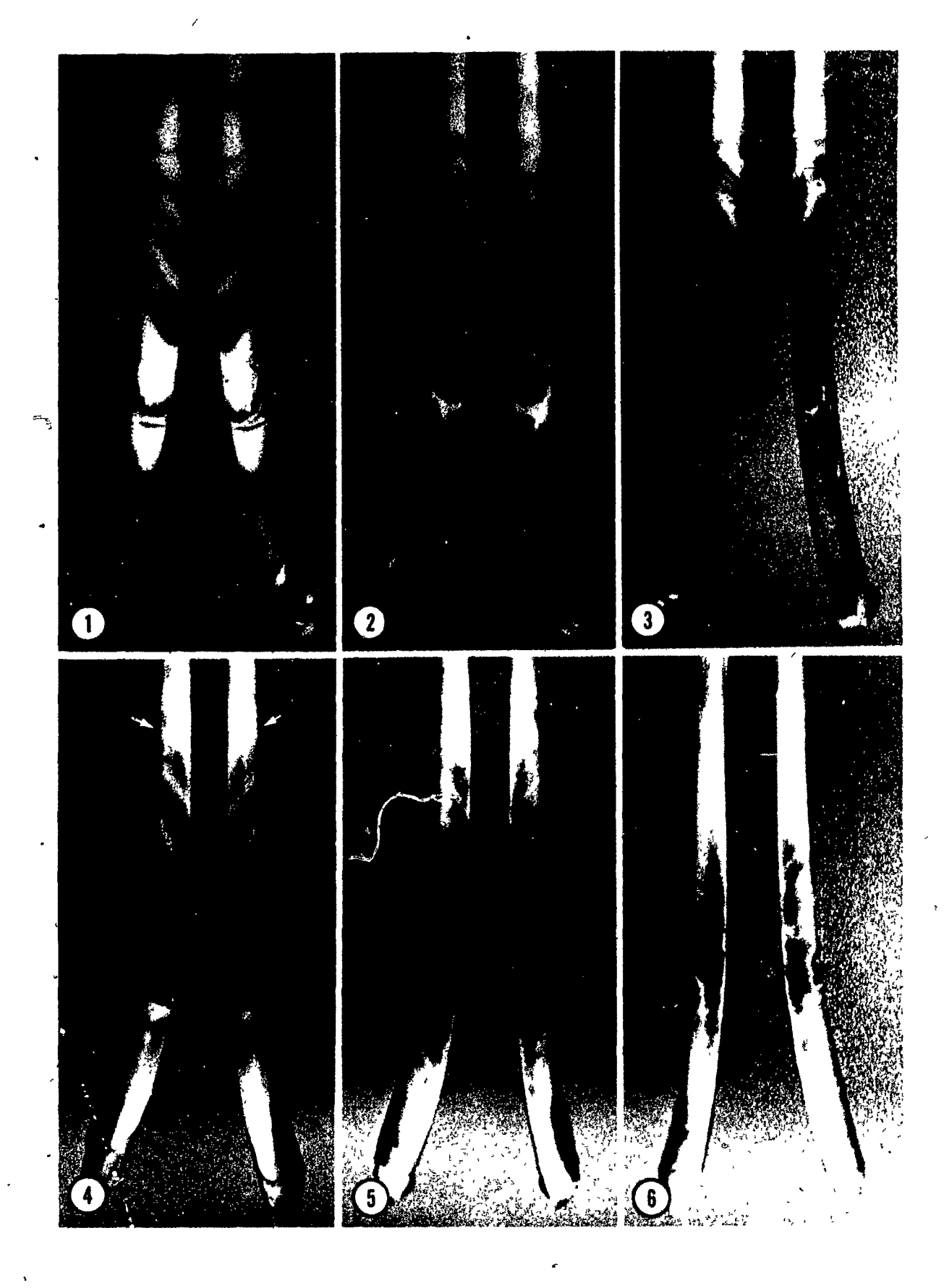
Figure 2. Incisors stained with GBHA 4 h after vinblastine injection. Note the modification of the banding pattern and the widening of the darkly-stained bands. Xb.5.

Figure 3. Incisors stained with GBHA 8 h after vinblastine injection. The staining is fairly continuous and no band or interband regions can be resolved. X6.5.

Figure 4. Radioautographs of normal, control teeth sacrificed 5 min after injection of <sup>45</sup>Ca. The radioautographic reaction consists of broad black bands separated by narrow white bands of unlabeled enamel. The arrow indicates the notch made at the opaque boundary. X6.5.

Figure 5. Radioautographs of incisors 4 h after vinblastine injection. Note that the banding of the maturation pattern is not as obvious when compared to Figure 4. X6.5.

Figure 6. Radioautographs of incisors 8 h after vinblastine injection. Very little radioautographic reaction is present. X6.5.



CHAPTER FIVE: USE OF BACKSCATTERED ELECTRON IMAGING ON DEVELOPED RADIOAUTOGRAPHIC EMULSIONS: APPLICATION TO VIEWING THE RAT INCISOR ENAMEL MATURATION PATTERN FOLLOWING 45CALCIUM INJECTION.

### **SYNOPSIS**

Backscattered electron 'imaging (BEI) can be used to obtain compositional contrast in biological structures because it detects differences in concentration of elements with different atomic number. Rat incisor enamel shows a banded pattern in the maturation zone when radioautography is used to reveal the location of injected <sup>45</sup>Ca at the enamel surface. The bands of developed silver grains in the photographic emulgion that coats the enamel surface are ideal for atomic number contrast. purpose of this study was to use BEI radioautographic pattern with SEM resolution. One-month-old rats were injected with 45Ca and sacrificed at early (1 min, 5 min, 30 min), intermediate (4 h, 8 h), and late (1 d, 4 d) time intervals after injection. Whole incisors were dissected, the enamel organs were removed, and the enamel surface was coated with photographic emulsion and processed for radioautography. radioautographed teeth were examined with a JEOL JSM-840 SEM equipped with a JEOL backscatter annular-type detector. early time intervals, light microscopic examination showed 5 or 6 broad black bands running across the teeth. These were separated by narrow white bands of unlabeled enamel. BEI resolved the presence of a delicate subbanding pattern within each dark band. At the intermediate time intervals, although the incisal bands persisted, only a diffusely-blackened apical area was seen by

light microscopy. BEI resolved bands in this apical region, but these showed no subbanding pattern. At the late time intervals, both light microscopy and BEI showed no banding, and the enamel was uniformly labeled. The significantly improved resolution obtained with BEI on surface radioautographs has revealed a previously undetected substructure in the <sup>45</sup>Ca-labeled banding pattern seen in enamel maturation.

### INTRODUCTION

The secondary electron imaging (SEI) mode of the scanning electron microscope (SEM) is unique in its ability to provide topographic images of surface features with high spatial resolution. As a high-energy electron beam passes through a specimen it produces many low-energy (typically less than 50 eV) "secondary" electrons within the material owing to electronelectron scattering (reviewed by Becker and Sogard, 1979; Becker and Geoffroy, 1981). Because the greatest density of secondary electrons is created by the primary beam before it has a chance to spread, there is high spatial resolution relative to other available signals. However, secondary electrons carry little information about the elemental composition of a sample, and their range is quite short, escaping from the specimen only if they are produced within a few nanometers of the surface (Becker and Geoffroy, 1981). In addition to secondary electrons, the interaction between an incidental electron beam and a specimen results in a variety of other signals such as X-rays, Auger electrons, and backscattered electrons. Backscattered electrons - are produced when incident electrons interact with atomic nuclei of the specimen and are scattered in any direction with little loss of energy (reviewed by Wells, 1977; Becker and Sogard, 1979; Becker and Geoffroy, 1981). If such an electron regains and leaves the surface of the specimen it is referred to as a backscattered electron. Backscattered electrons are more energetic than secondary electrons and so may escape from a greater depth within the specimen. The higher the energy of the

incident electron, the deeper it may penetrate while retaining the probability of regaining the surface. The number of backscattered electrons increases with the atomic number (Z) of the target hit by the incident beam (Wells, 1977). As a specimen 'is scanned, more dense or higher atomic number areas within the sample will produce more backscattering than less dense, lower The numerical differences between these atomic number regions. regions leads to an image that is said to show atomic number Such contrast differences can be produced by selectively staining biological structures with heavy metals that have relatively high atomic numbers. In this way cytochemical localizations (Soligo and de Harven, 1981; Soligo et al., 1983) and immunolocalizations (Hartman and Nakane, 1981; Ushiki et al., 1984; de Harven and Soligo, 1986), have been achieved by using backscattered electron imaging (BEI). Indeed, heavy metal staining has predominated as the best method to provide contrast in BEI (Abraham and DeNee, 1973, 1974; Becker and de Bruyn, 1976; Becker and Sogard, 1979; Becker and Geoffroy, 1981). al. (1982) used BEI of the silver particles in photographic films to enlarge their images. Boxde and Jones (1983) have used BEI to detect the level of mineralization in the dental tissues and bone with the aid of atomic number contrast provided by the calcium and phosphorous of hydroxyapatite. More recently, BEI has been to visualize cell surface receptors following radioautography of whole cells in vitro (Junger and Bachmann; 1980; Neugebauer et al., 1985; Salpeter, 1986).

Dental enamel of the rat incisor shows a banded maturation pattern as revealed by surface radioautography after 45Ca

The State of the S

injection (Reith and Boyde, 1981a; Reith et al., 1984). The bands of developed silver grains are ideal for providing regional differences in atomic number contrast relative to neighboring unlabeled areas. The purpose of this study was to apply backscattered electron imaging methods to analyses of surface radioautographs. Significant improvement in detecting substructures in the bands of the enamel maturation pattern has been achieved, clearly demonstrating the usefulness of BEI for viewing specimens processed for radioautography.

#### MATERIALS AND METHODS

## 45 Calcium radioautography

Male Sherman and Wistar rats weighing 100 ± 10 gm were used in this study. Each animal was injected via the external jugular vein with 100 uCi of  $^{45}$ calcium chloride (New England Nuclear) in 0.2 ml physiological saline. Two animals at each time interval were sacrificed by decapitation under ether anesthesia at 1 min, 5 min, 30 min, 4 h, 8 h, 1 d, and 4 d after injection. incisors were dissected from the surrounding alveolar bone and the enamel organs were wiped from the teeth with gauze moistened in saline. All incisors were air-dried at room temperature. position of the white opaque boundary (Robinson et al., 1974) was notched in the enamel with a scalpel. Following air-drying, all teeth were dipped in a 0.5% gelatin solution containing 0.05 gm chrome alum as a hardener for 20 sec at 40°C. The teeth then were dipped in Kodak NTB2 liquid emulsion, exposed for 5 or 6 days, and developed according to the method of Kopriwa and

Leblond (1962). All teeth were attached to a platform with plasticene and photographed.

## Backscattered electron imaging (BEI)

For BEI, the teeth were mounted on aluminum stubs with plasticene. The embedded incisal tips of the teeth were conductively coupled with the stub using conductive carbon paste (SPI Supplies, Toronto). The teeth used in this study were not carbon-coated since the specimens showed good conductance. preparations were examined with a JEOL JSM-840 scanning electron microscope fitted with a tungsten cathode and with a JEOL BEI backscatter divided annular-type detector. Optimum image quality was attained at an accelerating voltage of 10 kV. objective aperture was used, and the working distance was 34 mm with no stage tilt. The inverse signal polarity was chosen for the observations because it makes electron backscattering structures appear as black images, while nonbackscattering areas appear white. This inverse BEI image is similar to that usually seen with light and transmission electron microscopy, thus allowing for easier comparison. The backscattered electron images were recorded directly onto Type 55P/N Polaroid film.

#### RESULTS-

45 Calcium radioautography in routine preparations viewed by light microscopy

The teeth dipped for radioautography showed a smooth labial surface, which indicated that the enamel organs had been completely removed during the wiping procedure. At the apical

end of the incisors, the soft odontogenic tissues were removed, which left only the mineralized components of the teeth.

At the time intervals used in this study, three different radioautographic patterns were observed. At the early time intervals (1 min, 5 min and 30 min after 45Ca injection), the radioautographic emulsion on the tooth surface was blackened in a banded pattern (Fig. 1), presumably representing incorporation of <sup>45</sup>Ca into the enamel close to or at the surface. This pattern generally consisted of 5 or 6 broad black bands separated by narrow white bands of unlabeled enamel. The intensity of the radioautographic reaction in the heavily-exposed bands decreased incisally. At the early time intervals there was a suggestion of a subbanding pattern in the apical-most bands (Fig. 1). The central bands were the most oblique as the incisal-most bands became more transverse. At these early time intervals, the radioautographic banding patterns of each set of teeth were similar with regard to their position and number of bands. the intermediate times after injection (4 h and 8 h), the intensity of the reaction gradually increased. By 4 h (Fig. 5) and 8 h after injection, although the incisal bands could still be observed, the banding pattern was diffuse, and the apical bands had blended to form one blackened area. At the late time intervals, 1 d (Fig. 7) and 4 d after injection, most of the maturation zone enamel was uniformly blackened. At all time intervals, the pigmented enamel showed no radioautographic reaction. The enamel in the secretion zone showed practically no labeling at the early time intervals, but this increased slightly at the intermediate and late time intervals. The relationship of

the bands to the opaque boundary, marked with a scalpel in these preparations, was not consistent among animals, since a darkly-labeled band or a lighter or unlabeled region would appear immediately incisal to the opaque boundary. In the same animal, the banding patterns were generally symmetrical between the contralateral incisors.

## BEI of the 45 calcium radioautographs

The same teeth processed for radioautography could be observed, without any coating, by BEI. Incisors viewed by secondary electron imaging (SEI) showed smooth surface topography with only a slight indication of any banding (Fig. 2). viewing and aligning the axes of the teeth normal to the incident electron beam, BEI confirmed the presence of the radioautographic banding patterns at the labial surface of the teeth (Fig. 3). The position of the bands in BEI with inverse polarity (Fig. 4) corresponded exactly to those observed in the light microscope (Fig. 1). At the early time intervals, 1 min, 5 min (Figs. 3,4) and 30 min, a definite subbanding pattern of each dark apical band was observed. This subbanding was most noticeable in the apical bands of the maturation zone enamel. In the inverted image at 5 min (Fig. 4), the subbanding pattern was as follows in an apical to incisal direction: (1) a white unlabeled area, (2) a thin black stripe, (3) a thin unlabeled stripe and, (4) a broad black band of which the apical region was slightly darker. pattern could easily be determined in the first two apical bands, but became 'less distinct incisally' as the bands became more transversely oriented. Again, the notched enamel, indicating the

presence of the opaque boundary, was clearly visible in each of the teeth and was used as a reference point to compare banding patterns. At the intermediate time intervals, 4 h (Fig. 6) and 8 h after injection of <sup>45</sup>Ca injection, banding was still present at the surface of the teeth. The diffusely-darkened area shown in Figure 5 revealed its banded nature with BEI (Fig. 6). However, at these time intervals, no subbanding patterns were present within the dark bands. At the late times, 1 d (Fig. 8) and 4 d after <sup>45</sup>Ca injection, the banding pattern was barely visible by BEI. Exclusive of the pigmented enamel, all maturing enamel contained <sup>45</sup>Ca, and no unlabeled areas were found.

#### **DISCUSSION**

## BEI of developed radioautographic emulsions

The purpose of radioautography is to identify the presence of radioelements within tissues by the action of emitted radiation on photographic emulsions. The method consists of applying a photographic emulsion to a tissue, allowing sufficient time for the emitted radiation to act on the emulsion, and developing and fixing the preparation as in ordinary photography. The sites of radioactivity in the tissue can be identified by the accumulation of microscopic black silver grains adjacent to those areas in the tissue that contain the radioactive element (Gross et al., 1951; Nadler, 1951).

Backscattered electron imaging as used in this study relies on the presence of elemental silver (Ag) formed by the photographic process (James and Kornfeld, 1942; Mees, 1946):

Photographic emulsions in general consist of silver bromide crystals embedded in gelatin; the bromide concentration and mean diameter of the crystals vary with the different types of emulsion (reviewed by Gross et al., 1951). When the radiation that emanates from a radioactive source strikes and traverses a silver bromide crystal in a photographic emulsion, there is an excitation and release of electrons from some of the bromide ions (reviewed by Nadler, 1951). These electrons migrate within the crystal and are trapped at specific irregularities called ensitivity specks. By trapping the migrating electrons, these locations become negatively charged and attract neighboring positively charged silver ions. The silver ions (Ag+) are thereby reduced to elemental silver (Ag) to form latent images. During chemical development of the photographic emulsion, those crystals that have latent images undergo a weak chemical reduction of more silver ions, thus producing elemental silver that precipitates around each latent image. During fixation, the remaining silver bromide ions in which latent images were never formed are dissolved and washed away. The developed photographic grains that remain indicate the sites of radioactivity.

The atomic number contrast necessary for BEI resides, in this case, in the grains of elemental silver present in the developed photographic emulsion. The atomic number of silver is 47, and this is high enough to provide good regional atomic number contrast relative to the background emissions of calcium (Z = 20) and phosphorous (Z = 15) of hydroxyapatite. Owing to the differential distribution of silver, information was gained on regional differences in the incorporation of  $^{45}$ Ca into

developing enamel at resolutions well beyond the light microscope. It was thus shown that BEI can be successfully applied to resolve and analyze patterns in developed radioautographic emulsions that exceed the resolution obtained by light microscopy.

## The enamel maturation pattern

Backscattered electron imaging of developed radioautographic emulsions covering the labial surface of rat incisors showed good atomic number contrast in the form of bands of silver grains running across the enamel. This indicates that bands of newlyinjected 45Ca are present at or near the enamel surface. Immediately adjacent to this maturing enamel are the smooth-ended (SA) and ruffle-ended (RA) ameloblasts of maturation (Suga, 1959; Warshawsky and Smith, 1974; Boyde and Reith, 1976, Josephsen and Fejerskov, 1977). Several studies have demonstrated the band-like arrangement of SAs and RAs across the rat incisor (Takano and Ozawa, 1980; Reith and Boyde, 1981b; Warshawsky, 1985; Nanci et al., 1987). Other studies have correlated various stained banding patterns in rat incisor enamel with the distribution of the two types of maturation ameloblasts (Boyde and Reith, 1981, 1982; Reith and Boyde, 1981a; Reith et al., 1982; Takano et al., 1982). These correlations indicate that the banded maturation pattern is under the control of the overlying ameloblasts. The banded nature of the enamel maturation pattern can also be visualized by radioautography following 45Ca injection. This was first described by Reith and Boyde (1981a), and the regions that demonstrated most calcium

incorporation were shown to be those overlain by RAs (Reith and Boyde, 1981b; Takano et al., 1982).

This study has confirmed the results of Reith and Boyde (1981a), and Reith et al. (1984) in the maturation zone. addition, BEI has resolved a subbanding pattern within the broad bands at the early time intervals that was not obvious previously. A similar pattern has been abserved in enamel with following staining of calcium glyoxal hydroxyanil) (GBHA) (Takano et al., 1982). The radioautographic results confirm that 45 ca is present in the maturing enamel in some regions and is either completely or partly absent from other Presumably, differences in band intensity reflect differences in the extent of calcium incorporation. Consequently, this subbanding pattern predicts that there must be subpopulations of RAs within each band. Each subpopulation presumably has a different function, or degree of function, related to calcium processing during enamel maturation. differences in silver grain density reflect differences in calcium incorporation, these results suggest that RAs are directly or indirectly involved with allowing calcium to be incorporated into growing enamel crystallites. This differential calcium binding may reflect the ability of the enamel organ to or restrict, calcium passage the enamel. Alternatively, it may be determined by physicochemical properties of either the organic matrix or the growing crystallite surfaces. In any case, the exact mechanism by which calcium traverses the enamel organ to contribute to crystallite growth remains to be

#### determined.

#### Calcium dynamics

The uptake of 45Ca by mineralized tissues may be due to adsorption, exchange, and/or the new formation of stable calcium phosphate. Carlsson (1955) found that the fraction of the calcium taken up by the process of exchange was large in bone but was small or absent in the incisor tooth of the rat. concluded that calcium irreversibly entered the tooth and was used for crystal growth. Bauer and Shtacher (1968) compared the rate of deposition of the mineral precursor 85Sr to the rate of collagen synthesis measured by <sup>14</sup>C-proline uptake and concluded that there was mineral exchange in bone but not in teeth. Attempts to remove labile or free labeled calcium in dentin by injecting large amounts of unlabeled calcium were ineffective (Munhoz and Leblond, 1974), and it was concluded that in dentin, all or nearly all the labeled calcium entering the dentin is retained and may be considered as being added for crystal growth. However, these authors did not quantitate the effects that the unlabeled calcium had on the exchangeability of labeled calcium in the enamel.

Although conclusive evidence is lacking concerning the exchangeability of calcium in enamel, it appears that all or nearly all of the calcium that reaches the enamel is used for hydroxyapatite crystallite growth. As soon as 30 sec after <sup>45</sup>Ca injection, the entire thickness of secretory and maturing enamel is uniformly labeled (Munhoz and Leblond, 1974). This may be interpreted as indicating that the enamel matrix mineralizes

immediately after it is secreted (Nanci and Warshawsky, 1984) and continues to do so at about the same rate until the final degree of mineralization is achieved (Leblond and Warshawsky, 1979). the present study, although the apical banding pattern had blended as observed by light microscopy at 4 h after 45Ca injection, BEI revealed that the banding pattern was still present within that area. However, the subbands were no longer At 1 d and 4 d after injection, practically no detectable. banding was present, and the enamel was uniformly labeled. Therefore, at longer time intervals after injection, labeled calcium entered regions that were previously unlabeled. could occur by reutilization of calcium from the initial Several sources could supply labeled calcium to a injection. systemic pool for reutilization. First, the labeled calcium in the enamel itself could exchange with circulating unlabeled calcium. Second, assuming that the injected labeled calcium is irreversibly incorporated into enamel hydroxyapatite, then labeled calcium entering the enamel over longer time intervals may come from calcium exchange from bone. This possibility is strengthened by the fact that only 20% of the calcium incorporation in bone is attributable to stable, growth-related incorporation (Munhoz and Leblond, 1974). Therefore, even at long time intervals following injection of  $^{45}$ Ca there is a constant, but diminishing, supply of 45Ca available to the rat incisor. Consequently, cells that did not allow the entry of  $^{45}$ Ca to the enamel at the early time intervals had modulated to cells that did permit calcium entry. This is consistent with the observation that ameloblasts rapidly modulate from one cell type

to another during enamel maturation (Ishige et al., 1987; Smith et al., 1987). With time, the continuous availability of <sup>45</sup>Ca to the enamel would result in uniformly-labeled enamel, thus masking the delicate radioautographic pattern of the subbands and ultimately of the bands themselves.

#### REFERENCES

Abraham JL and DeNee PB 1973 Scanning electron microscope histochemistry using backscatter electrons and metal stains. Lancet, 1:1125-1127.

Abraham JL and DeNee PB 1974 Biomedical applications of backscattered electron imaging - One year's experience with SEM histochemistry. Scanning Electron Microscopy, pp. 251-258.

Bauer GCH and Shtacher G 1968 Incorporation and gelease of <sup>85</sup>Sr and <sup>14</sup>C-proline-hydroxyproline in mineral and collagen of bone and incisor teeth of growing rats. Calcif Tiss Res, 2:106-110.

Becker RP and de Bruyn PPH 1976 Backscattered electron imaging of exogenous peroxidase activity in rat bone marrow. Scanning Electron Microscopy, pp. 171-178.

Becker RP and Sogard M 1979 Visualization of subsurface structures in cells and tissues by backscattered electron imaging. Scanning Electron Microscopy, pp. 835-870.

Becker RP and Geoffroy JS 1981 Backscattered electron imaging for the life sciences: Introduction and index to applications - 1961 to 1980. Scanning Electron Microscopy, pp. 195-206.

Boyde A and Reith EJ 1976 Scanning electron microscopy of the lateral cell surfaces of rat incisor ameloblasts. J Anat, 122:603-610.

Boyde A and Reith EJ 1977 Scanning electron microscopy of rat maturation ameloblasts. Cell Tiss Res, 178:221-228.

Boyde A and Reith EJ 1981 Display of maturation cycles in rat incisor enamel with tetracycline labelling. Histochem, 72:551-561.

Boyde A and Reith EJ 1982 In vitro histological and tetracycline staining properties of surface layer rat incisor enamel also reflect the cyclical nature of the maturation process. Histochem, 75:341-351.

Boyde A and Jones SJ 1983 Backscattered electron imaging of dental tissues. Anat Embryol, 168:211-226.

Carlsson A 1955 On the mechanism of the skeletal turnover of lime salts. Acta Physiol Scand, 26:200-211.

de Harven E and Soligo D 1986 Scanning electron microscopy of cell surface antigens labeled with colloidal gold. Am J Anat, 175:277-288.

Frasca P, Galkin B, Feig S, Muir H, Soriano R and Kaufman H 1982 A new method of magnifying photographic images using the scanning

electron microscope in the backscattered electron detection mode. Scanning Electron Microscopy, pp. 917-923.

Gross J, Bogoroch R, Nadler NJ and Leblond CP 1951 The theory and methods of the radioautographic localization of radioelements in tissues. Am J Roentgenology Radium Ther, 65:420-458.

Hartman AL and Nakane PK 1981 Intracellular localization of antigens with backscatter mode of SEM using peroxidase labeled antibodies. Scanning Electron Microscopy, pp. 33-44.

Ishige N, Ohya K and Ogura H 1987 A rapid cyclic modulation of ameloblasts during enamel maturation. J Dent Res (Abstract), 66(Sp Iss):354.

James TH- and Kornfeld G 1942 Reduction of silver halides and the mechanism of photographic development. Chem Rev, 30:1.

Josephsen K 1983 Indirect visualization of ameloblast modulation in the rat incisor using calcium-binding compounds. Scand J Dent Res, 91:76-78.

Josephsen K and Fejerskov O 1977 Ameloblast modulation in the maturation zone of the rat incisor enamel organ. A light and electron microscopic study. J Anat, 124:45-70.

Junger E and Bachman L 1980 Methodological basis for an autoradiographic demonstration of insulin receptor sites on the surface of whole cells: A study using light- and scanning electron microscopy. J Microsc, 119:199-211.

Kopriwa BM and Leblond CP 1962 Improvement in the coating technique for radioautography. J Histochem Cytochem, 10:269-284.

Leblond CP and Warshawsky H 1979 Dynamics of enamel formation in the rat incisor tooth. J Dent Res, 58(B):950-975.

Mees CEK 1946 The Theory of the Photographic Process. The MacMillan Co., New York.

Munhoz COG and Leblond CP 1974 Deposition of calcium phosphate into dentin and enamel as shown by radioautography of sections of incisor teeth following injection of <sup>45</sup>calcium into rats. Calcif Tiss Res, 15:221-235.

Nadler NJ 1951 Some theoretical aspects of radioautography. Can J Med Sci, 29:182-194.

Nanci A and Warshawsky H 1984 Relationship between the quality of fixation and the presence of stippled material in newly formed enamel of the rat incisor. Anat Rec, 208:15-31.

Nanci A, Slavkin HC and Smith CE 1987 Immunocytochemical and radioautographic evidence for secretion and intracellular

degradation of enamel proteins by ameloblasts during the maturation stage of amelogenesis in rat incisors. Anat Rec, 217:107-123.

Neugebauer K, Salpeter MM and Podleski TR 1985 Differential responses of L5 and rat primary muscle cells to factors in rat brain extract. Brain Res, 346:58-69.

Reith EJ and Boyde A 1981a Autoradiographic evidence of cyclical entry of calcium into maturing enamel of the rat incisor tooth. Archs Oral Biol, 26:983-987.

Reith EJ and Boyde A 1981b The arrangement of ameloblasts on the surface of maturing enamel of the rat incisor tooth. J Anat, 133:381-388.

Reith EJ, Boyde A and Schmid MI 1982 Correlation of rat incisor ameloblasts with maturation cycles as displayed on the enamel surface with EDTA. J Dent Res, 61:1563-1573.

Reith EJ, Schmid MI and Boyde A 1984 Rapid uptake of calcium in maturing enamel of the rat incisor. Histochem, 80:409-410.

Robinson C, Hiller CR and Weatherell JA 1974 Uptake of <sup>32</sup>P labelled phosphate into developing rat incisor enamel. Calcif Tiss Res, 15:143-152.

Salpeter MM 1986 Electron microscopy in medical research and diagnosis: Present and future directions. V. EM autoradiography. J Electron Microsc Tech, 4:81-145.

Smith CE, McKee MD and Nanci A 1987 Cyclic induction and rapid movement of sequential waves of new smooth-ended ameloblast modulation bands in rat incisors as visualized by polychrome fluorescent labelling and GBHA-staining of maturing enamel. J Dent Res, In Press.

Soligo D and de Harven 1981 Ultrastructural cytochemical localizations by back-scattered electron imaging of white blood cells. J Histochem Cytochem, 29:1071-1079.

Soligo D, Pozzoli E, Nava MT, Polli N, Lambertenghi-Deliliers G and de Harven E 1983 Cytochemical methods for the backscattered electron imaging mode of scanning electron microscopy. Scanning Electron Microscopy, pp. 1795-1802.

Suga S 1959 Amelogenesis. Some histological and histochemical observations. Int Dent J, 9:394-420.

Takano Y and Ozawa H 1980 Ultrastructural and cytochemical observations on the alternating morphological changes of ameloblasts at the stage of enamel maturation. Arch Hist Jap, 43:385-399.

Takano Y, Crenshaw MA, Bawden JW, Hammarström L and Lindskog S 1982 The visualization of the patterns of ameloblast modulation by the glyoxal bis(2-hydroxyanil) staining method. J Dent Res, 61(Sp Iss):1580-1586.

Ushiki T, Yonehara K, Iwanaga TJ and Fujita T 1984 Application of backscattered electron image to immunocytochemistry in freeze-cracked tissues. Archs Hist Jap, 47:553-557.

Warshawsky H 1985 Ultrastructural studies on amelogenesis. In: The Chemistry and Biology of Mineralized Tissues. Ed. Butler WT. Ebsco Media, Birmingham. pp. 33-45.

Warshawsky H and Smith CE 1974 Morphological classification of rat incisor ameloblasts. Anat Rec, 179:423-446.

Wells OC 1977 Backscattered electron image (BSI) in the scanning electron microscope (SEM). Scanning Electron Microscopy, pp. 747-777.

#### FIGURE LEGENDS: CHAPTER FIVE

Figure 1. Light microscope radioautographs of the two lower incisors from a rat sacrificed 5 min after injection of <sup>45</sup>Ca. The teeth were processed for radioautography, and development of the photographic emulsion reveals the presence of the banded enamel maturation pattern that is due to <sup>45</sup>Ca incorporation at the surface of the teeth. The pattern consists of 5 or 6 broad black bands separated by narrow white bands of unlabeled enamel. The incisal pigmented enamel shows no banding. The scored enamel (arrows) represents the position of the opaque boundary. X10.

Figure 2. Scanning secondary electron image of the same pair of teeth as those shown in Figure 1. The smooth surface of the teeth indicates that the cells of the enamel organ are completely removed. The banding pattern is only barely visible. X12.

Figure 3. Backscattered electron image of the same teeth as those shown in Figure 1. The banded distribution of developed silver grains in the radioautographic emulsion produces good atomic number contrast relative to those areas with no silver, thus allowing for good resolution of the enamel maturation pattern. X12.

Figure 4. Backscattered electron image identical with that of Figure 3 except that the inverse signal polarity image was recorded. This "negative" image allows for easier comparison with the original light microscope radioautographs (compare with Fig. 1). Note that each dark band has a delicate subbanding pattern (1,2,3,4 as described in the text) that can only be clearly resolved using backscattered electron imaging. X12.

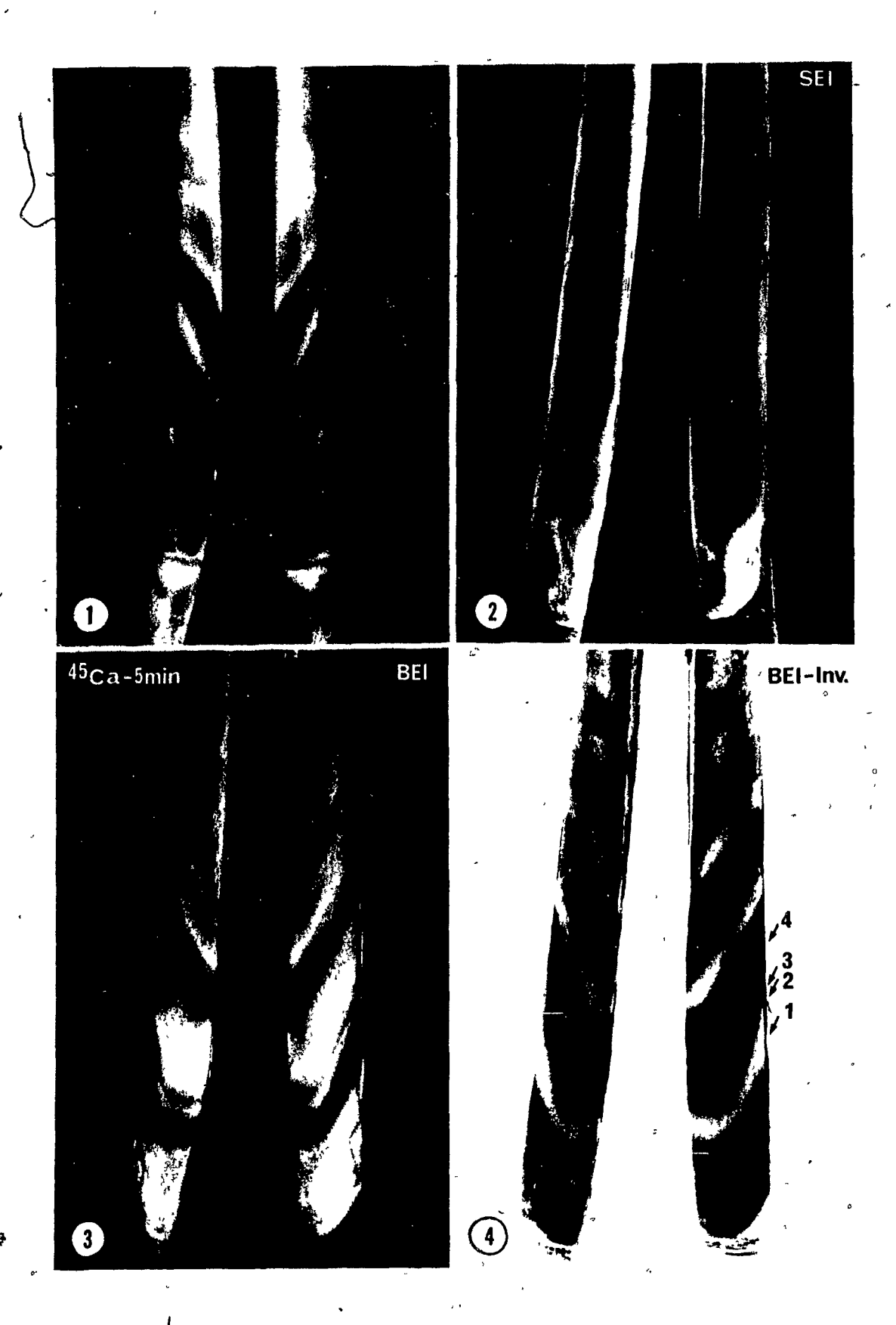
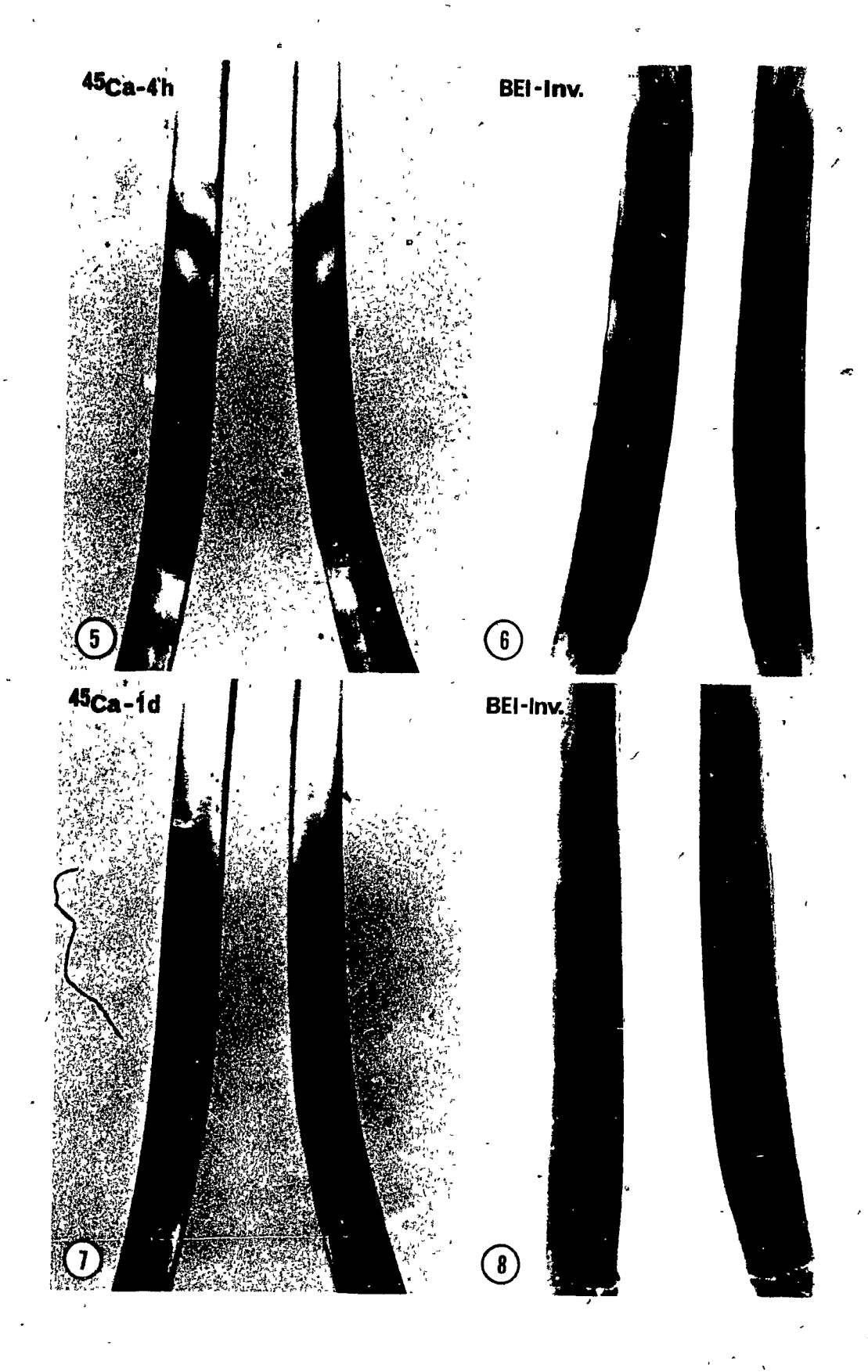


Figure 5. Light microscope radioautographs of the lower incisors from a rat sacrificed 4 h after injection of <sup>45</sup>Ca. The apical region of the maturation zone enamel is diffusely blackened, and only the incisal bands can be discerned. X10.

Figure 6. Inverse backscattered electron image of the teeth shown in Figure 5. This electron detection mode allows several bands to be resolved within the blackened area shown in Figure 5; however, no subbanding pattern can be observed at this time interval. X12.

Figure 7. Light microscope radioautographs of the lower incisors from a rat sacrificed 1 d after injection of <sup>45</sup>Ca. No banding is apparent, and only a diffuse labeling of the maturing enamel is observed. X10.

Figure 8. Inverse backscattered electron image of the teeth shown in Figure 7. The maturation zone enamel is uniformly grey, with only a very slight indication of banding. X12.



CHAPTER SIX: A RADIOAUTOGRAPHIC STUDY OF THE EFFECTS OF VINBLASTINE ON THE FATE OF INJECTED <sup>45</sup>CALCIUM AND <sup>125</sup>I-INSULIN IN THE RAT INCISOR.

## SYNOPSIS

In order to elucidate the effect of vinblastine on the movement of calcium and macromolecules through both the enamel organ in the zone of secretion and the odontoblast layer, <sup>45</sup>Ca and <sup>125</sup>I-insulin were used as radioautographic tracers. Vinblastine did not alter the radioautographic localization of both labeled calcium and insulin in the enamel organ and underlying enamel. On the other hand, the labeling with both <sup>45</sup>Ca and <sup>125</sup>I-insulin in the pulp, odontoblasts and dentin was eliminated after vinblastine injection. From these results, it is concluded that vinblastine has no effect on the passage of calcium and macromolecules in the enamel organ and secretory ameloblast layers, whereas the effect on the pulp and odontoblasts was to prevent the passage of these tracers into the predentin and dentin.

#### INTRODUCTION

Ameloblasts and odontoblasts have been shown to be directly responsible for forming the organic matrix of the enamel and dentin, respectively. However, the cells have only been indirectly implicated in the mineralization of these matrices. The effect of anti-microtubular agents such as colchicine; colcemid and vinblastine on these cells has been studied both ultrastructurally and functionally from the viewpoint of the synthesis and secretion of the organic matrix (Moe and Mikkelsen, 1977; Karim and Warshawsky, 1979; Miake et al., 1982; Takuma et There is no report of vinblastine's effect on the passage of ions or molecules to the enamel and dentin. the observations that 45Ca enters the enamel and dentin within seconds after injection (Munhoz and Leblond, 1974), and that  $^{125}$ I-insulin enters the dentin and predentin within minutes (Martineau-Doizé et al., 1986), we have attempted to elucidate the effects of vinblastine on the passage of calcium and large molecules such as insulin through the cellular layers overlying enamel and dentin. Radioautography was used to visualize these tracers after vinblastine-treated rats were injected with 45Ca and <sup>125</sup>I-labeled insulin.

## MATERIALS AND METHODS

Male Sherman rats weighing  $100 \pm 10$  gm were used in this study. Experimental rats were anesthetized and injected with 5 mg of vinblastine sulphate (Sigma Chemicals) in 0.3 ml of physiological saline via the external jugular vein. Control rats

were injected with 0.3 ml of normal saline.

## 45 Calcium experiment

At one hour after vinblastine injection, experimental and control animals were injected with 10 µCi/gm body weight of 45Ca (as calcium chloride, specific activity 10 µCi/µg, New England Nuclear) via the contralateral external jugular vein. perfused through the left ventricle 2 min later with Ringer's lactate for 30 sec to rinse out free tracer. This was followed by 5% glutaraldehyde in 0.05 M cacodylate buffer, pH 7.3, for about 10 min. The upper and lower incisors were dissected, postfixed with 1% osmium 'tetroxide in 0.1 M cacodylate buffer (pH' 7.3) for 1 h, dehydrated through graded acetones, and embedded in Throughout these procedures, both experimental and control teeth were treated identically to equalize any potential loss of water soluble labeled calcium from Experimental and control incisor were embedded in a common block (see Fig. 1) and one-micrometer-thick sections were cut on ethylene glycol and mounted on glass slides. They were processed for light microscope radioautography (Kopriwa and Leblond, 1962). After radioautographic exposure, the slides were developed and stained with 1% toluidine blue.

## 125 T-insulin experiment

At 1 h after vinblastine injection, experimental and control animals were injected with 0.15 ml (approximately 250 x  $10^6$  cpm) of freshly-prepared  $^{125}$ I-porcine insulin (2.5  $\mu$ g/100 gm body weight, specific activity 165  $\mu$ Ci/ $\mu$ g) via the contralateral external jugular vein. The  $^{125}$ I-insulin was prepared by the

Chloramine T method as previously described (Hunter and Greenwood, 1962; Posner et al., 1978). Five minutes after the injection of the labeled insulin, the rats were rinsed and sacrificed by perfusion of fixative as described above. The upper and lower jaws were removed and immersed in the same fixative for 2 h. After decalcification with 4.13% isotonic disodium EDTA (Warshawsky and Moore, 1967) for 16 d at 4°C, the jaws were cut into cross-sectional segments which were postfixed in osmium, dehydrated, and embedded in Epon. One-micrometer-thick sections mounted on glass slides were stained with iron hematoxylin and processed for light microscope radioautography.

#### RESULTS

## Localization of 45 calcium

In the control incisors the radioautographic reaction was identical to the results reported by Munhoz and Leblond (1974). Numerous silver grains were located over the entire thickness of the enamel and dentin (Figs. 1,2). The calcification front of the dentin was heavily labeled whereas the deeper portion of the dentin showed less labeling (Fig. 2). Silver grains seemed uniformly distributed over the enamel (Fig. 2). Few grains were present over the pulp, odontoblast bodies, and the predentin. The enamel organ, including the ameloblasts was also weakly labeled (Fig. 2).

In the vinblastine-injected rats, the radioautographic reaction over the enamel organ and the underlying enamel was not different from the control rats (Fig. 3). However, no labeling

was seen over the predentin and dentin after the vinblastine injection (Fig. 3).

## Localization of 125 I-insulin

In the control rats, a heavy reaction was present over the predentin and the adjacent dentin (Fig. 4) as previously reported (Martineau-Doizé et al., 1986). There was a moderate radioautographic reaction over the pulp and the enamel organ. Only background labeling was observed over the enamel.

The distribution of silver grains over the enamel organ in the vinblastine-injected animals was similar to that of the control rats. However, no labeling was observed over the pulp, predentin and dentin after vinblastine injection (Fig. 5).

## **DISCUSSION**

In the secretory ameloblast and odontoblast, vinblastine causes disappearance of microtubules and a dramatic disorganization of cell organelles related to the synthesis and secretion of organic matrix (Moe and Mikkelsen, 1977; Miake et al., 1982; Takuma et al., 1982). Consequently, the secretory activity of these cells is disrupted and no new matrix is released at their respective growth sites. This inhibitory effect of vinblastine on secretory activity could have important functional implications regarding the passage or binding of calcium to mineralizing enamel and dentin.

Vinblastine significantly alters the incorporation of labeled calcium into the enamel of the maturation zone (McKee and Warshawsky, 1986; Chapter Four). In the same study, the binding

state of calcium, as revealed by glyoxal bis(2-hydroxyanil)(GBHA) staining, was also affected by vinblastine. However, in the secretion zone, it was difficult to detect any changes. The present study, using light microscope radioautography, was undertaken to look more closely at the effects of vinblastine on the movement of calcium during enamel and dentin secretion. Furthermore, insulin was used as a large molecular-weight tracer (McKee et al., 1986; Chapter Two) to determine extracellular access of solutes to the enamel and dentin across the enamel organ in the secretion zone and odontoblast layers in normal and vinblastine-treated rats, respectively.

Vinblastine did not affect the normal distribution of labeled calcium in the enamel of the secretion zone, nor did it change the ability of the enamel organ and the ameloblast layer to prevent the passage of insulin to the enamel. Presumably then, this indicates that the passage of calcium to the enamel in the secretion zone is not dependent on a mechanism which involves an intact network of microtubules. Furthermore, it indicates that contrary to previous conclusions (Eisenmann et al., 1979), enamel mineralization in the secretion zone is functionally separate from the pathway of synthesis and secretion of the organic matrix.

In the pulp, predentin and dentin, vinblastine prevented radioautographic reactions after injection of both <sup>45</sup>Ca and <sup>125</sup>I-insulin. In the rat incisor, specific binding sites for insulin, presumably receptor sites, are present only on the endothelial cells of fenestrated capillaries in the papillary layer of the maturation zone, whereas nonspecific binding was described in

predentin and dentin (Martineau-Doizé ét al., 1986). the binding observed in this 125I-insulin experiment may be designated as nonspecific, it reflects the ability of this molecule to act as an intercellular tracer. Because negligible radioautographic reactions were found over the pulp, odontoblast bodies, predentin and dentin, it is possible that vinblastine prevented the movement, from the bloodstream to the tissue fluid of the pulp, of both small molecules and ions, such as calcium, and larger molecules like insulin. If vinblastine treatment creates a barrier to these molecules, then presumably it would occur at the level of the endothelial cells of the capillaries in the pulp and the odontoblast layer. It is possible that the anti-microtubular action of vinblastine may transendothelial exchange either through modification or removal of fenestrae or by interruption of transcytosis. However, it has been postulated that vesicle movement through endothelium occurs by pure diffusion or Brownian movement (reviewed by Simionescu, 1983), a mechanism not requiring the presence of microtubules. It is also unlikely that vinblastine alters insulin binding in endothelial cells since no insulin receptors were detected in the capillaries of the pulp and odontoblast layer (Martineau-Doizé et al., 1986). In addition, Pringault et al. (1985) have shown that insulin binding in hepatocytes remains high for up to 4 h after vinblastine treatment, and only decreases thereafter as a result in reutilization of insulin receptors. interruption Alternatively, the mineralization which occurs calcification front that converts predentin to dentin has been

postulated to require the presence of a noncollagenous protein (Butler et al., 1985). Presumably, the odontoblasts are responsible for elaborating such a protein. If vinblastine prevents this molecule from being secreted into the predentin, then perhaps the mineralization that requires its presence cannot Thus, there would be no binding of calcium at the occur. predentin-dentin border. However, this does not explain the absence of binding in the more mature mineralized dentin. Although the exact site and mode of action of vinblastine on the odontoblasts and the pulp remains to be clarified, these results suggest that pathways for entry of calcium for mineralization in dentin may differ from those of enamel.

#### REFERENCES

Butler WT, Sato S, Rahemtulla F, Prince CW, Tomana M, Bhown M, DiMuzio MT and Bronckers ALJJ 1985 Glycoproteins of bone and dentin. In: The Chemistry and Biology of Mineralized Tissues. Ed. Butler WT. Ebsco Media, Birmingham, pp. 107-112.

Eisenmann DR, Ashrafi S and Nieman A 1979 Calcium transport and the secretory ameloblast. Anat Rec, 193:403-422.

Hunter WM and Greenwood FC 1962 Preparation of iodine-131 labeled human growth hormone of high specific activity. Nature, 194:495-496.

Karim A and Warshawsky H 1979 The effect of colcemid on the structure and secretory activity of ameloblasts in the rat incisor as shown by radioautography after injection of  $^3\mathrm{H}$ -proline. Anat Rec, 195:587-610.

Kopriwa BM and Leblond CP 1962 Împrovement in the coating technique for radioautography. J Histochem Cytochem, 10:269-284.

Martineau-Doizé B, McKee MD, Warshawsky H and Bergeron JJM 1986 In vivo demonstration by radioautography of binding sites for insulin in liver, kidney, and calcified tissues of the rat. Anat Rec, 214:130-140.

McKee MD and Warshawsky H 1986 Modification of the enamel maturation pattern by vinblastine as revealed by glyoxal bis(2-hydroxyanil) staining and <sup>45</sup>calcium radioautography. Histochemistry, 86:141-145.

McKee MD, Martineau-Doizé B and Warshawsky H 1986 Penetration of various molecular-weight proteins into the enamel organ and enamel of the rat incisor. Archs Oral Biol, 31:287-296.

Miake Y, Yanagisawa T and Takuma S 1982 Electron microscopic study on the effects of vinblastine on young odontoblasts in the rat incisor. J Biol Buccale, 10:319-330.

Moe H and Mikkelsen H 1977 Light microscopical and ultrastructural observations on the effect of vinblastine on ameloblasts of the rat incisor in vivo. I. Short-term effects on secretory ameloblasts. Acta Pathol Microbiol Scand, 85A:73-88.

Munhoz COG and Leblond CP 1974 Deposition of calcium phosphate into dentin and enamel as shown by radioautography of sections of incisor teeth following injection of  $^{45}$ Ca into rats. Calcif Tiss Res. 15:221-235.

Posner BI, Josefsberg Z and Bergeron JJM 1978 Intracellular polypeptide hormone receptors: Characterization of insulin binding sites in Golgi fractions from the liver of female rats. J Biol Chem, 253:4067-4073.

Pringault E, Plas C, Desbuquois B and Clauser H 1985 Reutilization of insulin receptor and hormonal response in cultured foetal hepatocytes: the effects of chloroquine and vinblastine. Biol Cell, 52:13-22.

Simionescu N 1983 Cellular aspects of transcapillary exchange. Physiol Rev, 63:1536-1579.

Takuma S, Sawada T and Yanagisawa T 1982 Ultrastructural changes of secreting rat-incisor ameloblasts following administration of vincristine and vinblastine. J Dent Res, 61(Sp Iss):1472-1478.

Warshawsky H and Moore G 1967 A technique for the fixation and decalcification of rat incisors for electron microscopy. J Histochem Cytochem, 15:543-549.

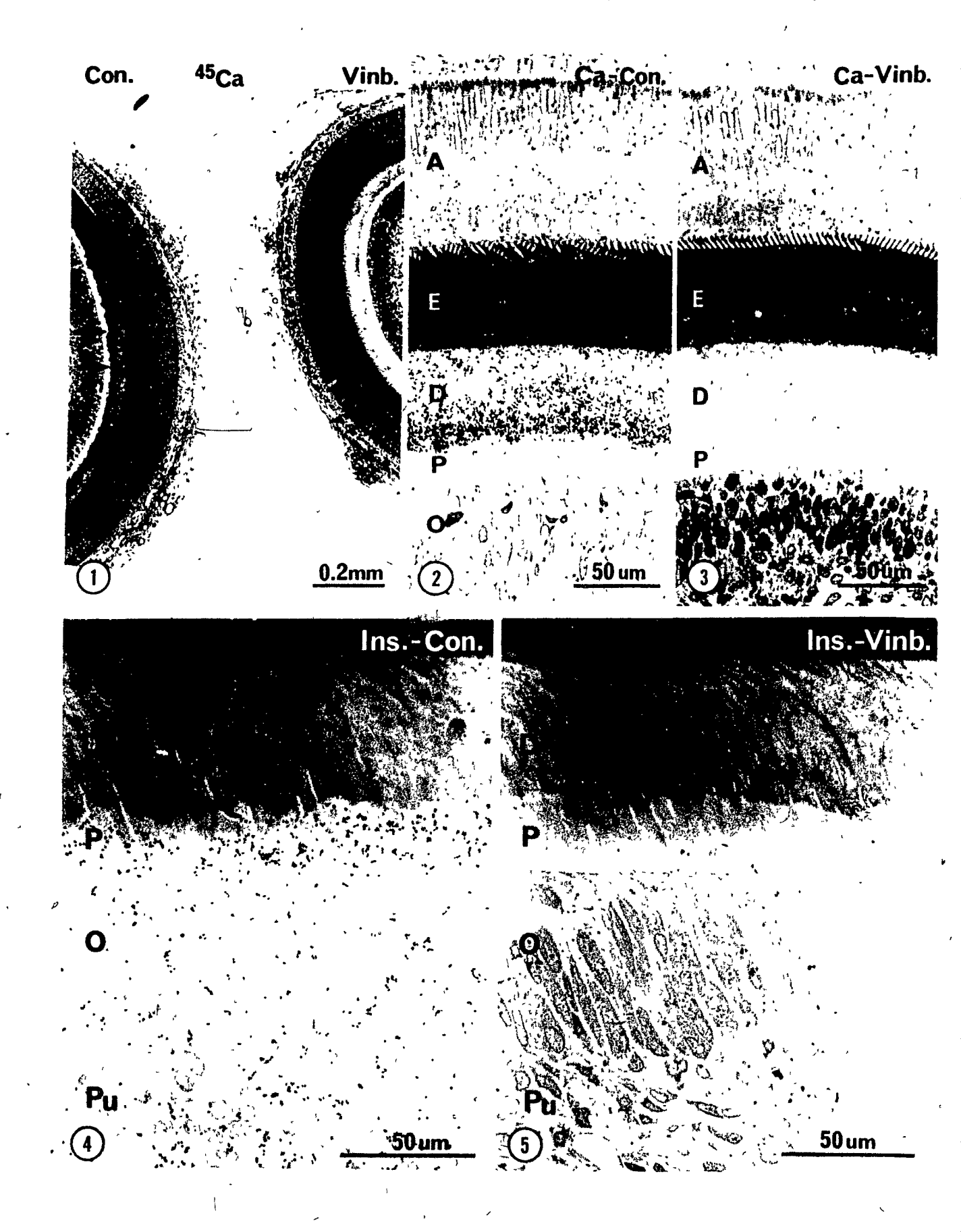
#### FIGURE LEGENDS: CHAPTER SIX

Figure 1. Low power light microscope radioautograph of the <sup>45</sup>Ca experiment. A control incisor (Con., left side) and an experimental incisor (Vinb., right side) are embedded together in the same block. An intense reaction is seen over the dentin of the control incisor (arrows). X60.

Figure 2. Higher magnification of a region of the calcium-control incisor shown in Figure 1. Numerous silver grains are present over the dentin (D) and enamel (E). An enhanced reaction appears over the dentin side of the calcification front. A, ameloblasts; P, predentin; O, odontoblasts. X300.

Figure 3. Higher magnification of a region of the calcium-vinblastine treated incisor shown in Figure 1. Reactions over enamel (E) and ameloblasts (a) are identical to those of control rats. No grains are seen over dentin (D), predentin (P) or odontoblasts (O). X300.

Figures 4.5. Light microscope radioautographs of the <sup>125</sup>I-insulin experiment show dentin (D), predentin (P), odontoblasts (O), and pulp (Pu) from a control rat (Ins.-Con., Fig. 4) and a vinblastine-treated rat (Ins.-Vinb., Fig. 5). The reactions seen over the dentin, predentin, odontoblasts, and pulp in the control rat (Fig. 4) are eliminated in the vinblastine-treated animal. (Fig. 5). X450.



CHAPTER SEVEN: IN VITRO STAINING OF ENAMEL USING HISTO-CHEMICAL COMPLEXING METHODS FOR CALCIUM

#### SYNOPSIS

Characteristic patterns can be visualized at the surface of the rat incisor in the maturation zone by staining with glyoxal bis(2-hydroxyanil)(GBHA). Similar patterns can be obtained with certain histological and fluorochrome stains. and radioautography following  $^{45}$ Ca injection. In this study, several histochemical reagents known to complex with different states of calcium, were used to stain enamel and to compare the resulting enamel maturation patterns. Rat incisors were quickly dissected and immediately immersed in solutions containing the following calcium-binding reagents: GBHA, Arsenazo III, Calmagite, Murexide, N, N-Naphthaloylhydroxylamine and Calcein. one contralateral lower incisor from each pair was counterstained with GBHA in order to relate the staining patterns to the classical maturation pattern known to reveal the position of smooth-ended ameloblasts. Each of the stains showed a similar, but not identical, pattern consisting of a series of broad or narrow bands running transversely and obliquely across the Some of the reagents also stained enamel in the enamel. secretion zone. The appearance and distribution of the staining patterns appears to be controlled on a time scale related to the rapid modulation of maturation ameloblasts. Since the different stains revealed differences in ionic or complexed states of calcium from one region of enamel to another, it is proposed that the enamel organ controls the entry, distribution and processing of calcium within maturing enamel.

#### INTRODUCTION

Enamel formation consists of several stages of which the Phenomena occur within this maturation stage is the longest. stage in a cyclical manner as shown by repetitive banding. The banded nature of the cyclical pattern can be visualized in the light microscopy of enamel organ and the enamel by means of: ameloblasts (Josephsen and Fejerskov, 1977; Reith and Boyde, 1981b), scanning electron microscopy of ameloblasts (Boyde and Reith, 1976, 1977; Skobe et al., 1985), radioautography of enamel (Reith and Boyde, 1981a; Takano et al., 1982a; Reith et al., 1984; McKee and Warshawsky, 1986a; Chapter Four; McKee et al., 1987; Chapter Five), horseradish peroxidase penetration patterns in dissected enamel organs (Takano and Ozawa, 1980), different molecular-weight protein penetration patterns (McKee et al., 1986; Chapter Two), tetracycline and fluorochrome labeling of enamel (Takano and Ozawa, 1980; Boyde and Reith, 1981; Josephsen, 1983; DenBesten et al., 1985; Ishige et al., 1987; Smith et al., 1987), EDTA etching of enamel during perfusion (Reith et al., 1982) and GBHA staining of enamel (Takano et al., 1982b; McKee and Warshawsky, 1986a,b; Chapters Three and Four). These studies all demonstrated that functional subpopulations of ameloblasts exist within the maturation zone of amelogenesis. functional subdivisions presumably are related to differences in a variety of activities including secretion, absorption, permeability, diffusion, and transport of substances to and from the enamel.

The banded nature of the patterns observed during enamel maturation must be due to biochemical and physicochemical differences in the organic and inorganic phases of enamel. inorganic phase of enamel consists of growing hydroxyapatite crystallites, putative calcium-phosphate complexes (reviewed by Glimcher, 1976), and transient mineral ions (Robinson et al., As observed in previous studies (Reith and Boyde, 1981a; 1979). Takano et al., 1982b; Reith et al., 1984; McKee and Warshawsky, 1986b; Chapter Three; McKee and Warshawsky, 1986a; Chapter Four; McKee et al., 1987; Chapter Five), the amount of calcium that reaches and enters the enamel, and the state of the calcium, is different from one region to another within the maturation zone. The repetitive banded nature of these differences is commonly referred to as the maturation pattern. Similarly, since organic matrices presumably act as templates for initiating, organizing and directing crystal growth in mineralized tissues (reviewed by Glimcher, 1976; Veis, 1985), it seems reasonable to predict that the organic matrix of enamel may also be differentially distributed in conformation with the maturation pattern. Indeed, Boyde and Reith (1982), using several histological stains, found evidence of banding in the maturation zone. It therefore seems probable that the distribution of certain enamel matrix components may be associated with a similar distribution of different ionic or binding states of calcium. The purpose of this study was to use various histochemical complexing methods for different chemical states of calcium to detect the presence and distribution of banding patterns within the enamel.

## MATERIALS AND METHODS

## Animal and tissue handling procedures prior to staining

Sherman and Sprague-Dawley rats weighing 100 ± 20 gm were used in this study. Animals were sacrificed by decapitation under ether anesthesia and the lower incisors were quickly dissected from the surrounding alveolar bone. Enamel organs were wiped from the teeth with gauze moistened in cold saline. Dissected wet incisors were transferred immediately to the staining solutions.

## GBHA staining of incisors

Freshly-dissected lower incisors were stained with glyoxal bis(2-hydroxyanil)(GBHA) to reveal the basic maturation pattern at the surface of the teeth as described previously (Takano et al., 1982b). The incisors were immersed for 30 sec at room temperature in 100 ml of a 75% ethanol solution containing 0.875 gm of GBHA (Sigma Chemicals) and 0.35 gm NaOH. After staining, the incisors were rinsed briefly in absolute ethanol and allowed to air dry at room temperature. Contralateral teeth were mounted as pairs and photographed.

# Histochemical complexing stains for calcium applied to incisor enamel

Chemicals were obtained from the Sigma Chemical Company (St. Louis) and freshly-dissected lower incisors were immersed in the following aqueous solutions under constant agitation: (1) 0.1% Arsenazo III (sodium salt; 2,7- bis(2-arsonophenylazo)-1,8-dihydroxynaphthalene-3,6-disulfonic acid) for 30 sec, (2) 0.1%

(triethanolammonium salt; [1-(1-hydroxy-4-methyl-2-Calmagite phenyl-azo)-2-naphthol-4-sulfonic acid) for 40 sec, (3) 0.1% Murexide ammonium (ammonium purpurate; salt nitrilodibarbaturic acid) for 2 min, (4) N, N-Naphthaloylhydroxylamine (sodium salt; N-Hydroxynaphthalimide) for 2 min (5) 0.15% Calcein (2'7'-[(bis[carboxymethyl]and, amino) methyl]fluorescein) in a 2.0% sodium bicarbonate solution for 20 sec. In all cases, both lower incisors from the same animal were stained with the same stain and the lower left incisors were then counterstained with GBHA. Contralateral incisors were air-dried, mounted as pairs in plasticene, and photographed. The Calcein-stained teeth were photographed under a B-100A "Blak-Ray" lamp having an ultraviolet range of 320-400 nm with peak excitation at 365 nm (Ultraviolet Products Inc.).

### RESULTS

Lower incisors showed a banding pattern on the surface of the enamel after GBHA staining (Fig. 1) as previously described by Takano et al. (1982b). The location of the individual bands of this pattern varied slightly on incisors from different animals, but were generally symmetrical in contralateral incisors from the same animal. The staining pattern consisted of up to six dark red bands running across the enamel, separated by interband regions. The staining intensity of the bands decreased incisally and no bands were observed in the pigmented enamel. The interband regions contained a lightly-stained pink area apically, and an incisal unstained area. The secretion zone enamel apical to the first band stained lightly.

Arsenazo III formed a blue complex with calcium that stained the enamel in broad bands that ran transversely and obliquely across the enamel of the incisor (Fig. 2). Occasionally a finer striping was observed in the stained regions. The broad bands decreased in staining intensity in an incisal direction and were separated by narrow bands of unstained enamel. The pigmented enamel and the enamel in the secretion zone was not stained. The contralateral lower left incisor, counterstained with GBHA to reveal the position of smooth-ended ameloblasts (Takano et al., 1982b; Smith et al., 1987), allowed the distribution of both stains to be observed. The dark red GBHA-stained bands of enamel corresponded exactly with the narrow bands of enamel left unstained by Arsenazo III.

Calmagite formed a red complex with calcium that stained enamel in broad bands in a pattern similar to that observed after Arsenazo III staining (Fig. 3). Broad red Calmagite-stained bands of enamel were separated by narrow bands of unstained enamel. Although the pigmentation zone of enamel was not stained, the secretion zone enamel stained darkly. Staining of the contralateral incisor with GBHA masked or altered (changed to a blue color) some of the Calmagite staining but it was still possible to observe that the darkly-stained GBHA bands were found in thin regions of enamel unstained by Calmagite.

Murexide staining of enamel showed broad pink bands alternating with narrower bands of darkly- and lightly-stained enamel, and unstained areas (Fig. 4). The repeating pattern, in an apical to incisal direction, consisted of a broad darkly-

stained area, a narrow lightly-stained band, a narrow darkly-stained band, and an unstained area. The enamel in the secretion zone was lightly-stained and the pigmented enamel was not stained. Counterstaining with GBHA showed that the darkly-stained GBHA bands were in the narrow bands of enamel unstained by Murexide.

N,N-Naphthaloylhydroxylamine showed a banded pattern that stained enamel either dark yellow or a light blotchy yellow, alternating with unstained areas (Fig. 5). Typically the darkly-stained regions and blotchy yellow-stained regions were observed just apical and incisal to the unstained areas, respectively. A slight indication of striping was observed in the stained enamel. Superimposed GBHA staining showed that the unstained regions following N,N-Naphthaloylhydroxylamine were darkly stained with GBHA.

Calcein formed yellow-orange complexes with calcium in visible light that caused enamel to fluoresce a yellow-green color under ultraviolet light (Fig. 6). The most heavily stained areas appeared as broad bands across the enamel similar to those observed previously with the other stains. Staining with GBHA showed that the less-stained Calcein areas corresponded with the dark GBHA bands (seen as yellow-green bands in ultraviolet light).

#### DISCUSSION

### Calcium dynamics

In vertebrates, the major inorganic solid phase of mineralized tissues is calcium and inorganic phosphate. In

mammalian enamel, this extracellular mineral phase consists of highly-crystalline, ribbon-like crystallites in close association with certain structural components of the organic matrix (Bai and Warshawsky, 1985). Presumably, crystal growth in enamel occurs as the organic matrix creates a favorable local environment around the hydroxyapatite crystallites. At these sites the constituents of the mineral phase in solution are induced to form a solid phase in relation to specific constituents of the organic matrix (Glimcher, 1976). The formation of enamel hydroxyapatite requires a solid-phase transformation of inorganic ions from constituents initially existing as ions or ion complexes in solution (reviewed by Glimcher, 1976). This phase transformation involves the initiation and formation of the first particles of the solid phase and the subsequent growth of the solid-phase particles (crystals). Each of these processes is governed by physicochemical laws that are probably regulated by separate biological control mechanisms defined by the amelogenins and enamelins of the organic matrix of enamel. It is therefore necessary to establish exactly how the enamel proteins are associated with the growing crystallites and how these proteins serve to distribute, process and regulate the solid-phase transformation of inorganic minerals from solution.

### Staining reactions

Since numerous colorimetric and photometric methods have been developed for the detection of soluble and insoluble metal ions and ion complexes, several of these were chosen to visualize calcium at the surface of rat incisor enamel. Previously, certain metal substitution methods such as the von Kossa silver nitrate procedure, been identify have used to tissue mineralization. These methods demonstrate the anion, such as phosphate and carbonate, rather than the cation. Of particular interest during enamel maturation is the pathway(s) taken by the predominant cation, calcium, since this mineral precursor differentially enters maturing enamel in a banded pattern (Reith and Boyde, 1981a; Takano et al., 1981a; Reith et al., 1984; McKee and Warshawsky, 1986a; Chapter Four; McKee et al., 1987; Chapter A selection of reagents capable of complexing with calcium in various ways was chosen so as to provide some insight into the histochemistry of calcium at the enamel surface.

Glyoxal bis(2-hydroxyanil)(GBHA) has been used demonstrate soluble and insoluble calcium salts in tissue sections (Kashiwa and Atkinson, 1963; Kashiwa and House, 1964; Kashiwa, 1966; Kashiwa and Sigman, 1966). More recently, GBHA was used to effectively demonstrate the enamel maturation pattern on whole-mount teeth (Takano et al., 1982b). GBHA chelates calcium by both electrovalent and covalent bonds to the oxygen and nitrogen atoms of GBHA in an alkaline medium to form a red complex (Goldstein and Stark-Mayer, '1958). The reagent undergoes base-catalyzed hydrolysis at the necessary high pH to yield glyoxal and the amine; the glyoxal rearranges to glycolate anion and precipitates calcium glycolate from the alcoholic medium needed to keep the reagent in solution (Lindstrom and Milligan, 1967). Chelation of calcium by GBHA is dependent on the presence of ionic calcium and, therefore, on the solubility of calcium

salts (Kashiwa and House, 1964). The alcoholic and highly. alkaline (pH 13.1) nature of the staining solution acts to minimize the diffusion and loss of calcium, and interference from other cations, thus contributing to the sensitivity of the method (Milligan and Lindstrom, 1972). The failure of GBHA to stain some regions of enamel following whole-mount staining, and its ability to darkly and lightly stain other areas of enamel, indicates differences in the chemical state of calcium at the surface and within maturing enamel. Since GBHA relies on the availability of ionizable calcium, the results indicate that different calcium-phosphate complexes may exist in different regions of maturing enamel. The darkly-stained enamel corresponds to regions overlaid by smooth-ended ameloblasts (Takano et al., 1982b), thus indicating that these cells either directly or indirectly control the complexing of calcium within the enamel.

Arsenazo III is a metallophilic dye that reacts 1:1 with calcium to form a blue complex, and in the pH range of 3-10 (neutral pH was used in this study), has excellent sensitivity for calcium, even when present with large excesses of magnesium and manganese (Michaylova and Ilkova, 1971). It forms stable complexes with calcium and selects Ca<sup>2+</sup> over Mg<sup>2+</sup> by about 50-fold (Weissmann et al., 1976; Weidner and Byrd, 1982). Incisors stained with Arsenazo III show a dramatic blue banding pattern at the surface of the maturing enamel. A contralateral incisor, having GBHA staining superimposed on the Arsenazo III staining, reveals that Arsenazo III stains calcium in enamel related to ruffle-ended ameloblasts. Consequently, the fact that calcium

(including that incorporated into hydroxyapatite) present in regions of enamel related to smooth-ended ameloblasts does not stain, reveals that Arsenazo III selectively complexes with ionic calcium solubilized from certain specific calcium salts. The origin of this calcium has yet to be determined.

Calmagite was first introduced by Lindstrom and Diehl (1960) as an indicator for the titration of calcium and magnesium. It forms a 1:1 complex with calcium and stains red at the neutral pH used in this study. GBHA counterstaining of Calmagite-stained incisors shows that Calmagite complexes with calcium in regions of enamel related to ruffle-ended ameloblasts.

Murexide is a metallophilic dye that combines with calcium in basic solution to form complexes ranging in color from yellow-orange to red and has been used for histochemical detection of calcium by Kaufman and Adams (1957) and Jurgensonn (1971). Murexide is a chelating agent which binds to calcium in situ without precipitation, thus minimizing diffusion and dislocation artifacts (Chaplin and Grace, 1976). Counterstaining with GBHA shows heaviest Murexide staining in the apical regions of enamel related to ruffle-ended ameloblasts.

N,N-Naphthaloylhydroxylamine was first used by Beck (1951) and later was applied to the demonstration of calcium oxalate (Voigt, 1957; Macaluso and Berg, 1959; Roscher, 1971), as a marker for bone deposition (Foldes et al., 1971), and as an electron microscopic marker for calcium in muscle cells (Zechmeister, 1979). Superimposition of GBHA staining reveals that the heaviest N,N-Naphthaloylhydroxylamine staining at pH 8.5

is in the incisal regions of enamel related to ruffle-ended ameloblasts.

Calcein was first described as a fluorochromic cation indicator by Diehl and Ellingboe (1956). Commercially available Calcein is often a 50:50 mixture of two fluorescent materials from which two types of complexes are formed with calcium (Wallach and Steck, 1963; Chiu and Haynes, 1977). GBHA staining superimposed on Calcein staining reveals that calcium is available to complex with Calcein in regions of enamel related to ruffle-ended ameloblasts.

### Interpretation of staining patterns

The amount of histochemical information gained from staining of biological material usually is limited by the fact that most often the tissue has been chemically altered by fixation. The inorganic mineral phase of enamel investigated in this study was not chemically fixed, was not aqueously treated prior to staining (other than the wiping procedure to remove the enamel organ), and was performed almost immediately following sacrifice of the animal. Other than by rapid freezing, the quick dissection procedure followed by immediate in situ staining may be the most sensitive way to gain histochemical information about the surface layer of enamel.

Various calcium salts occur in animal tissues in a variety of normal and pathological conditions. Calcium in tissues may be present in the form of soluble salts as chlorides, sulfates or lactates, or in an ionized, ionizable, or masked form with proteins (proteinates), or it may occur in the form of insoluble

deposits within tissues as phosphates, carbonates or oxalate salts. Experimental data gained from the use of suitable histochemical reactions for calcium might make it possible to identify and differentiate various forms of calcified material. However, frequently the exact nature of the calcium binding mechanism is not clear, and this makes identification and interpretation of histochemical reactions rather difficult. In any case, regional differences in the state of calcium may be observed and these in turn can be related to the cellular components of the tissue. In this way, information was gained on the distribution and state of calcium within the enamel and its relation to the type and distribution of maturation ameloblast within the enamel organ.

With the development of in vitro chemical modeling techniques it has been observed that apatite formation in aqueous solutions is often preceded by the transitory appearance of other calcium-phosphate phases (reviewed by Brown and Chow, 1976; Boskey, 1985; Eanes, 1985). The calcium salts most often suggested to be possible mineral precursor phases to apatite in aqueous preparations at physiological pH are octacalcium phosphate (OCP; Brown, 1966; Eanes and Meyer, 1977; Brown et al., 1981; Cheng, 1987), amorphous calcium phosphate (ACP; Eanes and Posner, 1965; Eanes et al., 1965; Termine et al., 1967; Posner and Betts, 1975; Boskey and Posner, 1976), and dicalcium phosphate dihydrate (DCPD; Francis and Webb, 1971). The discovery of these precursor phases in synthetic preparations suggests that in vivo, apatite may not necessarily form directly from constituent ions in solution via classical heterogenous

nucleation and growth mechanisms, although the existence of these precursors is still a matter of much controversy (Grynpa's et al., 1984; Bonar et al., 1985). It is interesting to note that in synthetic preparations under physiological conditions, the lifetime of ACP and OCP is 6 and 20 minutes, respectively, before converting by hydrolysis to apatite (Eanes and Reddi, 1979; Eanes, 1985). It therefore seems likely that if indeed precursor phases do exist, then they may not accumulate to an extent sufficient enough to be easily detected by physical means. The histochemical methods used in this study are specific and sensitive enough to detect small changes in the state of calcium in the surface layer of enamel. It is possible that the observed staining patterns, and the differences between staining patterns using different calcium-specific stains, may reflect the presence of a precursor calcium-phosphate phase(s) prior to conversion to apatite. A single incisor can be dissected, wiped and stained to reveal the staining pattern in the maturation zone in less than 2 minutes after sacrifice of the animal. Presumably, the rapidity and low temperature (4°C) of these experimental procedures would act only to minimize any possible conversion of precursor to apatite. Alternatively, the process by which calcium and phosphorous are sequestered from the surrounding extracellular milieu is a dynamic one whereby calcium and phosphorous and calcium-phosphate complexes are gradually converted from ions and complexes in solution to poorly-crystalline hydroxyapatite. turn converts to the highly-ordered, crystalline hydroxyapatite characteristic of mineralized tissues.

the process whereby enamel crystallites are formed may not necessarily include distinct and extensive layers of the above-mentioned mineral precursors, but may instead involve a slow but constant dynamic reorganization of mineral ions and complexes at the surface of the crystals. It should be stressed however, that direct, physical identification of these putative complexes is necessary in order to validate the potential of the histochemical reagents used in this study to bind to calcium derived from specific calcium-phosphate complexes in the enamel.

An alternative explanation for the observed staining patterns may be hypothesized from knowledge of the matrix-mineral relationship. One suggestion for the role of organic matrices in mineralized tissues is that they may serve to nucleate and direct mineralization. Calcium binding sites have been identified in enamel proteins (Drinkard et al., 1981; Traub et al., 1985), dentin phosphophoryns (Lee et al., 1977; Stetler-Stevenson and Veis, 1987), bone osteocalcin (Hauschka, 1985) and osteonectin (Romberg et al., 1983), cartilage chondrocalcin (Boskey, 1985), alkaline phosphatase (de Bernard et alí, 1985; Wuthier and Register, 1985) and lipids (Boyan, 1985). Synthetic calciumphosphate solutions with concentrations of these ions similar to those of serum may contain, in addition to free calcium and phosphate ions, a variety of Ca-P and Ca-P-x complexes (where x = a variety of organic or inorganic ligands; reviewed by Glimcher, 1976). It may be that enamel proteins in solution act as Ca or Ca-P ligands; this is in agreement with the calcium binding properties of enamel proteins (Drinkard et al., 1981; Traub et 1981) and the fact that quanidine extraction of enamel

proteins completely prevents staining of enamel with GBHA (McKee and Warshawsky, 1986b; Chapter Three). It is possible that the calcium stains used in this study visualize different Ca-P-ligand complexes (where the ligands are enamel proteins) within the enamel, a relationship mediated by the overlying maturation ameloblasts.

At present, these two hypotheses describing possible mechanisms for the differential staining of the enamel maturation. pattern can be considered only as tentative. investigation is necessary to clarify the exact nature of the calcium-stain complex. What can be emphasized, however, is that the staining patterns formed by each of the histochemical reagents are slightly different, yet each reflects the intimate association and distribution of the overlying ruffle-ended and smooth-ended ameloblasts of the maturation zone. Undoubtedly, bands of each cell type exert control over selected, underlying areas of enamel such that the ionic or complexed states of calcium are different from one region of enamel to another. Another important consideration related to these staining differences is that overlying ameloblasts are rapidly modulating between ruffle-ended and smooth-ended morphologies (Ishige et al., 1987; Smith et al., 1987). An implication of this rapid modulation phenomenon is that the ability of calcium to complex with the histochemical reagents used in this study changes in a matter of hours, and changes back again, such that a complete cycle of complexing and non-complexing occurs within 8 hours. this way, ameloblasts exert both spatial and temporal control over enamel mineralization.

#### REFERENCES

Bai P and Warshawsky H 1985 Morphological studies on the distribution of enamel matrix proteins using routine electron microscopy and freeze-fracture replicas in the rat incisor. Anat Rec, 212:1-16.

Beck G 1951 Mikrochemie 36/37, 245 (Cited in: Voigt, 1957).

Bonar LC, Grynpas MD, Roberts JE, Griffin RG and Glimcher MJ 1985 Physical and chemical characterization of the development and maturation of bone mineral. In: The Chemistry and Biology of Mineralized Tissues. Ed. Butler WT. Ebsco Media, Birmingham. pp. 226-233.

Boskey AL 1985 Overview of cellular elements and macromolecules implicated in the initiation of mineralization. In: The Chemistry and Biology of Mineralized Tissues. Ed. Butler WT. Ebsco Media, Birmingham. pp. 335-343.

Boskey AL and Posner AS 1976 The formation of hydroxyapatite at low supersaturations. J Phys Chem, 80:40-46.

Boyan BD 1985 Proteo ipid-dependent calcification. In: The Chemistry and Biology of Mineralized Tissues. Ed. Butler WT. Ebsco Media, Birmingham. pp. 125-131.

Boyde A and Reith EJ 1976 Scanning electron microscopy of the lateral cell surfaces of rat incisor ameloblasts. J Anat, 122:603-610.

Boyde A and Reith EJ 1977 Scanning electron microscopy of rat maturation ameloblasts. Cell Tiss Res, 178:221-228.

Boyde A and Reith EJ 1981 Display of maturation cycles in ratincisor with acute tetracycline labelling. Histochem, 72:551-561.

Boyde A and Reith EJ 1982 In vitro histological and tetracycline staining properties of surface layer rat incisor enamel also reflect the cyclical nature of the maturation process. Histochem, 75:341-351.

Brown WE 1966 Crystal growth of bone mineral. Clin Orthop Rel Res, 44:205-220.

Brown WE and Chow LC 1976 Chemical properties of bone mineral. Annual Rev Material Sci, 6:213-236.

Brown WE, Mathew M and Tung MS 1981 Crystal chemistry of octacalcium phosphate. Prog Crystal Growth Charact, 4:59-87.

Chaplin AJ and Grace SR 1976 An evaluation of some complexing methods for the histochemistry of calcium. Histochem, 47:263-269.

Cheng P-K 1987 Formation of octacalcium phosphate and subsequent transformation to hydroxyapatite at low supersaturation: A model for cartilage calcification. Calcif Tiss Int, 40:339-343.

Chiu VCK and Haynes DH 1977 High and low affinity Ca<sup>2+</sup> binding to the sarcoplasmic reticulum. Use of a high-affinity fluorescent calcium indicator. Biophys J, 18:3-22.

deBernard B, Gherardini M, Lunazzi GC, Modricky C, Moro L,/Panfili E, Pollesello P, Stagni N and Vittur F 1985 Alkaline phosphatase of matrix vesicles from preosseous cartilage is a Ca++ binding glycoprotein. In: The Chemistry and Biology of Mineralized Tissues. Ed. Butler WT. Ebsco Media, Birmingham. pp. 142-145.

DenBesten PK, Crenshaw MA and Wilson MH 1985 Changes in the fluoride-induced modulation of maturation stage ameloblasts of rats. J Dent Res, 64:1365-1370.

Diehl H and Ellingboe JL 1956 Indicator for titration of calcium in presence of magnesium with disodium dihydrogen ethylenediaminetetraacetate. Anal Chem, 28:882.

Drinkard C, Gibson L, Crenshaw MA and Bawden JW 1981 Calcium binding by organic matrix of developing bovine enamel. Archs Oral Biol, 26:483-485.

Eanes ED 1985 Dynamic aspects of apatite phases of mineralized tissues. Model studies. In: The Chemistry and Biology of Mineralized Tissues. Ed. Butler WT. Ebsco Media, Birmingham. pp. 213-220.

Eanes ED and Posner AS 1965 Kinetics and mechanism of conversion of noncrystalline calcium phosphate to crystalline hydroxyapatite. Trans NY Acad Sci, 28:233-241.

Eanes ED, Gillessen IH and Posner AS 1965 Intermediate states in the precipitation of hydroxyapatite. Nature, 208:365-367.

Eanes ED and Meyer JL 1977 The maturation of crystalline calcium phosphates in aqueous suspension at physiologic pH. Calcif Tiss Res, 23:259-269.

Eanes ED and Reddi AH 1979 The effect of fluoride on bone mineral apatite. Metab Bone Dis Rel Res, 2:3-10.

Foldes I, Modis L, Petko M, Gyurko M and Josza A 1970 Comparative study of morphological methods for the determination of calcium salts. Acta Histochem (Jena), 37:397-409.

Francis MD and Webb NC 1971 Hydroxyapatite formation from a hydrated calcium monohydrogen phosphate precursor. Calcif Tiss Res, 6:335-342.

Glimcher MJ 1976 Composition, structure and organization of bone and other mineralized tissues and the mechanism of calcification. In: Handbook of Physiology and Endocrinology. Williams and Wilkins, Baltimore. pp. 25-116.

Goldstein D and Stark-Mayer C 1958 New specific test for calcium. Anal Chim Acta, 19:437-439.

Grynpas MD, Bonar LC and Glimcher MJ 1984 Failure to detect an amorphous calcium-phosphate solid phase in bone mineral: A radial distribution function study. Calcif Tiss Int, 36:291-301.

Hauschka P 1985 Osteocalcin and its functional domains. In: The Chemistry and Biology of Mineralized Tissues. Ed. Butler WT. Ebsco Media, Birmingham. pp. 149-158.

Ishige N, Ohya K and Ogura H 1987 A rapid cyclic modulation of ameloblasts during enamel maturation. J Dent' Res (Abstract), 66(Sp Iss):354.

Josephsen K 1983 Indirect visualization of ameloblast modulation in the rat incisor using calcium-binding compounds. Scand J Dent Res, 91:76-78.

Josephsen K and Fejerskov O 1977 Ameloblast modulation in the maturation zone of the rat incisor enamel organ. A light and electron microscopic study. J Anat, 124:45-70.

Jurgensonn HB von 1971 Histologischer Calciumnachweis mit der Metallindikatoren Murexid Calcon und Calcein. Histochemie, 28:23-32.

Kashiwa HK 1966 Calcium in cells of fresh bone stained with glyoxal bis(2-hydroxyanil). Stain Tech, 41:49-55.

Kashiwa HK and Atkinson WB 1962 The applicability of a new Schiff base, glyoxal bis(2-hydroxyanil), for the cytochemical localization of ionic calcium. J Histochem Cytochem, 11:258-264.

Kashiwa HK and House CM Jr 1964 The glyoxal bis(2-hydroxyanil) method modified for localizing insoluble calcium salts. Stain Tech, 39:359-367.

Kashiwa HK and Sigman MD Jr 1966 Calcium localized in odontogenic cells of rat mandibular teeth by the glyoxal bis(2-hydroxyanil) method. J Dent Res, 45:1796-1799.

Kaufman HE and Adams EC 1957 Murexide: another approach to the histochemical staining of calcium. Lab Invest, 6:275-283.

Lindstrom F and Diehl H 1960 Indicator for the titration of calcium plus magnesium with (Ethylenedinitrilo) tetraacetate. Anal Chem: 32:1123-1127.

Lindstrom F and Milligan CW 1967 Mechanisms of color fading in the direct spectrophotometric method for calcium using glyoxal bis(2-hydroxyanil). Anal Chem, 39:132-133.

Lee SL, Veis A and Glonek T 1977 Dentin phosphoprotein: An extracéllular calcium-binding protein. Biochém, 16:2971-2979.

Macaluso MP and Berg NO 1959 Calcium oxalate crystals in kidneys in acute tubular nephrosis and other renal diseases. Acta Path Microbiol Scand, 46:197-205.

McKee MD and Warshawsky H 1986a Modification of the enamel maturation pattern by vinblastine as revealed by glyoxal bis(2-hydroxyanil) staining and 45 calcium radioautography. Histochemistry, 86:141-145.

McKee MD and Warshawsky H 1986b Effects of various agents on staining of the maturation pattern at the surface of rat incisor enamel. Archs Oral Biol, 9:577-585.

McKee MD, Martineau-Doizé B and Warshawsky H 1986 Penetration of various molecular weight proteins into the enamel organ and enamel of the rat incisor. Archs Oral, Biol, 31:287-296.

McKee MD, Warshawsky H and Nanci A /1987 Use of backscattered electron imaging on developed radioautographic emulsions: Application to viewing rat incisor enamel maturation pattern following <sup>45</sup>calcium injection. J Electron Microsc Tech, 5:357-365.

Mikhailova V and Ilkova P 1971 Photometric determination of micro amounts of calcium with arsenazo III. Anal Chim Acta, 53:194-198.

Milligan CW and Lindstrom F 1972 Colorimetric determination of calcium using reagents of the glyoxal bis(2-hydroxyanil) class. Anal Chem, 44:1822-1829.

Posner AS and Betts F 1975 Synthetic amorphous calcium phosphate and its relation to bone mineral structure. Accounts Chem Res, 8:273-281.

Reith EJ and Boyde A 1981a Autoradiographic evidence of cyclical entry of calcium into maturing enamel of the rat incisor tooth. Archs Oral Biol, 26:983-987.

Reith EJ and Boyde A 1981b The arrangement of ameloblasts on the surface of maturing enamel of the rat incisor tooth. J Anat, 133:381-388.

Reith EJ, Boyde A and Schmid MI 1982 Correlation of rat incisor ameloblasts with maturation cycles as displayed on enamel surface with EDTA. J Dent Res, 61:1563-1573.

Reith EJ, Schmid MI and Boyde A 1984 Rapid uptake of calcium in maturing enamel of the rat incisor. Histochem, 80:409-410.

Robinson C, Briggs HD, Atkinson PJ and Weatherell JA 1979 Matrix and mineral changes in developing enamel. J Dent Res, 58 (Sp Iss B):871-880.

Romberg RW, Werness PG, Riggs BL and Mann KG 1983 Isolation of native osteonectim. Calcif Tiss Int (Abstract), 35:664.

Roscher AA 1971 A new histochemical method for the demonstration of calcium oxalate in tissues following ethylene glycol poisoning. Amer J Clin Path, 55:99-104.

Skobe Z, LaFrazia F and Prostak M 1985 Correlation of apical and lateral membrane modulations of maturation ameloblasts. J Dent Res, 64:1055-1061.

Smith CE, McKee MD and Nanci A 1987 Cyclic induction and rapid movement of sequential waves of new smooth-ended ameloblast modulation bands in rat incisors as visualized by polychrome fluorescent labelling and GBHA-staining of maturing enamel. J Dent Res, In Press.

Stetler-Stevenson WG and Veis A 1983 Bovine dentin phosphophoryn: Composition and molecular weight. Biochem, 22:4326-4335.

Takano Y and Ozawa H 1980 Ultrastructural and cytochemical observations on the alternating morphological changes of the ameloblasts at the stage of enamel maturation. Archs Histol Jap, 43:385-399.

Takano Y, Crenshaw MA and Reith EJ 1982a Correlation of  $^{45}$ Ca incorporation with maturation ameloblast morphology in the ratincisor. Calcif Tiss Int, 34:211-213.

Takano Y, Crenshaw MA, Bawden JW, Hammarström L and Lindskog S 1982b The visualization of the patterns of ameloblast modulation by the glyoxal bis(2-hydroxyanil) staining method. J Dent Res 61(Sp Iss):1580-1586.

Termine JD, Wuthier RE and Posner AS 1967 Amorphous-crystalline mineral changes during endochondral and periostial bone formation. Proc Soc Exp Biol Med, 125:4-9.

Traub W, Jodaikin A and Weiner A 1985 Diffraction studies of enamel protein-mineral structural relations. In: The Chemistry and Biology of Mineralized Tissues. Ed. Butler WT. Ebsco Media, Birmingham. pp. 221-225.

Veis A 1985 Phosphoproteins of dentin and bone. Do they have a role in matrix mineralization. In: The Chemistry and Biology of / Mineralized Tissues. Ed. Butler WT. Ebsco Media, Birmingham. pp. 170-176.

Voigt GT 1957 Ein never histotopochemischer Nachweis des Calciums (mit Nachtalylhydroxamsäure). Acta Histochem (Jena), 4:122-131.

Wallach DFH and Steck TL 1963 Fluorescence techniques in the microdetermination of metals in biological materials. Anal Chem, 35:1035-1046.

Weidner E and Byrd W 1982 The microsporidian spore invasion tube. II. Role of calcium in the activation of invasion tube discharge. J Cell Biol, 93:970-975.

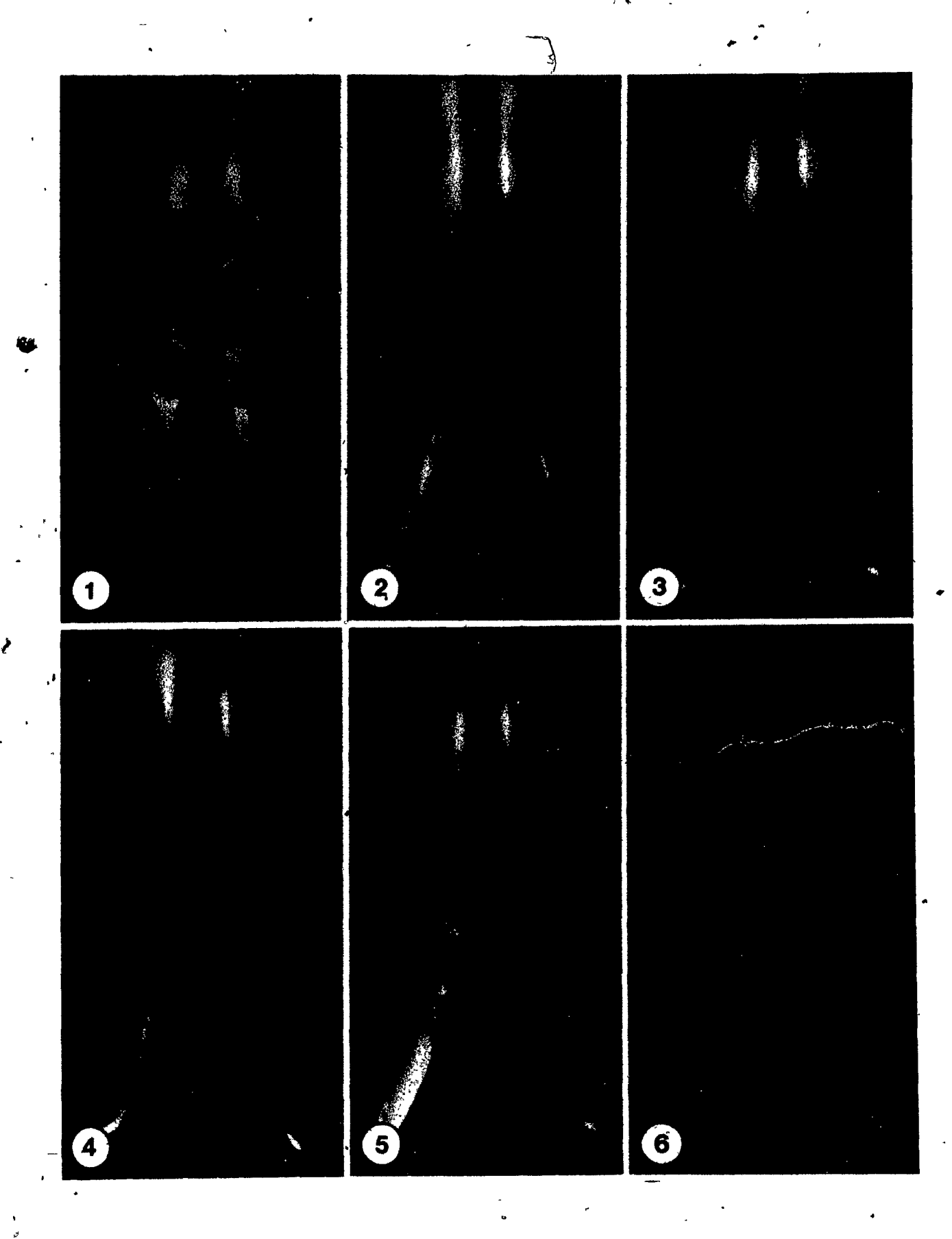
Weissmann G, Collins T, Evers A and Dunham P 1976 Membrane perturbation: Studies employing a calcium-sensitive dye, arsenazo III, in liposomes. Proc Natl Acad Sci USA, 73:510-514.

Wuthier RE and Register TC 1985 Role of alkaline phosphatase, a polyfunctional enzyme, in mineralizing tissues. In: The Chemistry and Biology of Mineralized Tissues. Ed. Butler WT. Ebsco Media, Birmingham. pp. 113-124.

Zechmeister A 1979 A new selective ultrahistochemical method for the demonstration of calcium using N,N-Naphthaloylhydroxylamine. Histochem, 61:223-232.

### FIGURE LEGENDS: CHAPTER SEVEN

- Figure 1. Contralateral lower incisors stained with glyoxal bis(2-hydroxyanil)(GBHA). Darkly-stained bands run tranversely and obliquely across the enamel in the maturation zone and indicate the positions of bands of smooth-ended ameloblasts (Takano et al., 1982b). Interband regions contain an apical lightly-stained area and an incisal unstained area, both of which correspond to bands of ruffle-ended ameloblasts. The enamel in the secretion zone stains lightly. X6.5.
- Figure 2. Arsenazo III-stained incisors show broad blue bands running across the enamel in the maturation zone separated by narrower bands of unstained enamel (at left). The staining intensity of the bands decreases in an incisal direction. The enamel in the pigmentation zone and secretion zone does not stain. Counterstaining of the contralateral incisor with GBHA (at right) reveals that the dark red GBHA bands correspond to the narrow white areas left unstained by Arsenazo III. X6.5.
- Figure 3. Calmagite-stained incisors show broad red bands running across the enamel in the maturation zone separated by narrower bands of unstained enamel (at left). The staining intensity of the bands decreases in an incisal direction. The pigmented enamel does not stain but the enamel in the secretion zone stains a dark red color. Superimposed GBHA staining of the contralateral incisor (at right) shows that the narrow areas left unstained by Calmagite stain with GBHA. X6.5.
- Figure 4. Murexide-stained incisors show broad pink bands alternating with harrower bands of darkly- and lightly-stained enamel, and unstained enamel in the maturation zone (at left). The staining intensity of the bands decreases in an incisal direction. The enamel in the secretion zone is stained a light pink and the pigmented enamel is unstained. Counterstaining with GBHA (at right) shows the dark red GBHA bands in the narrow areas left unstained by Murexide. X5.5.
- Figure 5. N,N-NaphthaloylNydroxylamine-stained incisors show bands of dark and light blotchy yellow running across the enamel in the maturation zone (at left). The staining intensity of the bands decreases in an incisal direction. Secretion zone enamel is lightly stained and the pigmented enamel shows no staining. Narrow bands of enamel left unstained by N,N-Naphthaloyl-hydroxylamine stain dark red with GBHA (at right). X6.5.
- Figure 6. Calcein-stained incisors show yellow-orange bands in normal white light that fluoresce a yellow-green color under ultraviolet light (at left). The most heavily stained areas appear as broad bands across maturing enamel similar to those observed after staining with Arsenazo III and Calmagite (Figs. 2 and 3). Staining with GBHA (at right) shows that the less-stained Calcein areas correspond to the dark red GBHA bands, here seen as yellow-green bands due to ultraviolet light. X6.5.



CHAPTER EIGHT: IN VITRO STAINING OF ENAMEL PROTEINS USING SEVERAL COMMON HEAVY METAL AND HISTOLOGICAL STAINS.

#### SYNOPSIS

The staining pattern in the enamel of the maturation zone of the rat incisor represents cyclical phenomena occurring within the enamel that presumably are controlled by the ruffle-ended and smooth-ended ameloblasts of the overlying enamel organ. Various experimental techniques have revealed that the staining pattern in the enamel reflects the banded distribution of maturation The present study has investigated the possibility ameloblasts. that certain enamel matrix components may be unevenly distributed \Dissected lower rat according to the maturation pattern. incisors were wiped free of their enamel organs and immediately immersed in fixative containing one of the following heavy metal and histological stains commonly used to reveal proteins: uranyl acetate, lead citrate, Coomassie Blue, Alcian Blue and Ruthenium Red. Other animals were injected with 35s-methionine as a precursor to enamel proteins and the incisors were dissected and wiped of their enamel organs and processed as whole mounts for radioautography. Teeth stained by heavy metals were also viewed by backscattered electron imaging. Both radioautography and protein staining in vitro revealed that proteins are distributed in bands and stripes across the enamel in the maturation zone. \* Correlation of this pattern with maturation ameloblast morphology demonstrates the intricate control exerted by the enamel organ over the cyclical events that occur during enamel maturation.

### INTRODUCTION

. Ruffle-ended and smooth-ended maturation ameloblasts in the rat incisor enamel organ are arranged as bands that overlie the maturing enamel at either a transverse or oblique angle relative to the long axis of the incisor (Takano and Ozawa, 1980; Reith and Boyde, 1981a; Warshawsky, 1985; Nanci et al., 1987). In the maturation zone, these ameloblasts rapidly modulate between being ruffle-ended or smooth-ended such that as many as 45 modulation waves may pass over a given area of enamel (Smith et al., 1987). The distribution of these cells affects the enamel in such a way which imparts to it the characteristic staining with qlyoxal bis(2-hydroxyanil) (Takano et al., 1982b; McKee and Warshawsky, 1986a,b; Chapters Three and Four; Chapter Seven) described as the This maturation pattern can be enamel maturation pattern. visualized in the enamel at any given point in time by the following methods: radioautography (Reith and Boyde, 1981b; Takano et al., 1982a; Reith et al., 1984; McKee and Warshawsky, 1986a; Chapter Four; McKee et al., 1987; Chapter Five), different molecular weight protein penetration patterns (McKee et al., 1986; Chapter Two), tetracycline and fluorochrome labeling (Takano and Ozawa, 1980; Boyde and Reith, 1981; Josephsen, 1983; DenBesten et al., 1985; Ishige et al., 1987; Smith et al., 1987), EDTA etching by perfusion (Reith et al., 1982), and staining by other histochemical reagents that bind calcium (Chapter Seven). These studies have demonstrated that each type of ameloblast is related to a differentially reactive band of enamel and consequently must have a different function with regard to enamel

The ultimate effect of the alternating ameloblast maturation. morphologies is to produce the enamel maturation pattern, and to do this they must effect changes in the organic or inorganic Cyclical changes in the inorganic mineral phases of enamel. phase of enamel can be inferred and correlated with ameloblast morphology principally using radioautography by administration of 45 calcium and various histochemical complexing methods for calcium (references as above). On the other hand, documented cyclical changes in the organic matrix of enamel and correlation to cell type are relatively few (Boyde and Reith, 1982; McKee and Warshawsky, 1986b; Chapter Three). Since mineral entry and binding occurs in a cyclical manner, and since organic matrices commonly act to initiate, organize and direct crystal growth in mineralized tissues (reviewed by Glimcher, 1976; Veis, 1985), it seems reasonable to predict that certain components of the organic phase of enamel may also be differentially distributed in a maturation pattern. The purpose of this study was to use various stains to investigate the distribution of organic components at the enamel surface, and to correlate this distribution with overlying ameloblast morphology.

# MATERIALS AND METHODS

# Animal and tissue handling prior to staining

Sherman, Sprague-Dawley and Wistar rats weighing 100 ± 20 gm were used in this study. Animals were sacrificed by decapitation under ether anesthesia and the lower incisors were quickly dissected from the surrounding alveolar bone. Enamel organs were wiped from the teeth with gauze moistened in cold saline. The

dissected wet incisors were transferred immediately to the staining solutions.

## Staining procedures

All stains were prepared in fixative containing 2% glutaraldehyde, 0.1 M sodium cacodylate and 0.05% CaCl2. Staining solutions were prepared immediately before use and were filtered through number 50 filter paper. Stains were obtained through Sigma Chemical Co. (St. Louis) or JBEM Services (Montreal) and were prepared at the following concentrations: (1) - 4.0% uranyl acetate (preparation and staining procedures performed in the dark), (2) 4.0% lead citrate, (3) 0.1% Coomassie Brilliant Blue G, (4) 0.01% Alcian Blue 8GX and, (5) 0.01% Ruthénium Red (ruthenium oxychloride ammoniated). In all cases, both incisors from the same animal were stained at room temperature with the same stain, were rinsed vigorously in distilled water after staining and were air-dried at room temperature. While drying, some incisors were scored with a scalpel at the position of the narrow translucent bands (Takano Before drying, some stained teeth were et al., 1982b) ... transferred to the same fixative solution but without the respective stain; these incisors were soaked for 2 to 6 h in order to evaluate the possibility of simple diffusion of stain into the enamel. Other teeth were stained with aqueous solutions of the stains without fixative and some inclisors were fixed prior to staining. Contralateral incisors were mounted as pairs in plasticene and photographed. Uranyl acetate-stained teeth were " photographed with a Wratten No. 47 blue filter to enhance

# Backscattered electron imaging of stained incisors

For backscattered electron imaging (BEI), the teeth were mounted on aluminum stubs with plasticene and carbon-coated. preparations were examined with a JEOL JSM-840 scanning electron microscope fitted with a tungsten cathode and with a JEOL BEI backscatter divided annular-type detector. Optimum image quality: was attained at an accelerating voltage of 10 kV. A 110 um objective aperture was used and the working distance was 34 mm The inverse signal polarity was recorded with no stage tilt. which makes electron backscattering structures appear as dark images while nonbackscattering structures appear as lighter This inverse BEI image is similar to that usually seen with normal light photography, thus allowing for easier The backscattered electron images were recorded comparison. directly onto Type 55P/N Polaroid film

# 35s-methionine injection and radioautography

Wistar rats were injected via the external jugular vein with 0.5 mCi <sup>35</sup>S-methionine (S.A. = 1134 Ci/mMol; New England Nuclear) in 0.2 mls PBS, pH 7.4. At 6 min after injection of the radioactive tracer, the animal was injected via the contralateral jugular vein with a large excess of "cold" nonradioactive methionine (Sigma Chemicals) in 0.2 ml PBS, pH 7.4. At 1 h after the initial injection the animals were sacrificed by decapitation and the lower incisors were quickly dissected and the enamel organs were removed. Both teeth were then immediately immersed in

2% glutaraldehyde containing 0.1 M sodium cacodylate buffer, pH 7.4, for 30 min at room temperature. The incisors were then washed vigorously in distilled water for several minutes and airdried at room temperature. Following air-drying the teeth were dipped in a 0.5% gelatin solution containing 0.05 gm chrome alum as a hardener for 20 sec at 40°C. The incisors were dipped in Kodak NTB2 liquid emulsion, exposed for 14 d, and developed according to the method of Kopriwa and Leblond (1962).

#### RESULTS

# Staining patterns

enamel surface with uranyl acetate, lead citrate, Coomassie Blue, Alcian Blue and Ruthenium Red. Although enamel was stained in simple aqueous solutions, the staining patterns were most distinct when the stains were prepared in solution with fixative and the results reported below describe incisors stained in sodium cacodylate-buffered glutaraldehyde. Each of these stains produced a repetitive but slightly different staining pattern.

Incisors stained with uranyl acetate for 3 h at room temperature showed darkly-stained enamel in the secretion zone and 4 or 5 narrow stained bands of enamel in the maturation zone (Fig. 1). Staining for shorter time intervals showed the same, kut less intense, pattern. The bands were for the most part obliquely oriented relative to the long axis of the incisor, but became more transverse incisally. Soaking of a fresh incisor

for 1 h in physiological saline at room temperature prior to staining with uranyl acetate in fixative removed the staining pattern (Fig. 2). Backscattered electron imaging of uranylstained teeth relied on differences in the quantity of \ backscattered electrons produced by the high atomic number of uranium (Z=92) relative to the background backscattering caused by calcium (Z=20) and phosphorous (Z=15). BEI of the same teeth shown in Figure 1 demonstrated the differential distribution of uranium into 4 bands (Fig. 3). During drying after staining with uranyl acetate, the enamel showed narrow translucent bands which appeared to dry more slowly than adjacent broad areas. incisors were scored along these translucent bands and BEI revealed that the enamel bands stained by uranyl acetate were located just apical to the score marks representing the translucent bands (Fig. 4). Frequently observed in the interband regions were narrower parallel stripes that laterally, followed the same orientation as the bands, but mesially lost this orientation as the stripes abruptly hooked incisally (Fig. 4). The stripes were most obvious in the first few interband regions.

Incisors stained for 3 h at room temperature with lead citrate showed a pattern similar to staining with uranyl acetate (Fig. 5). Since lead citrate did not produce a color reaction suitable for normal light photography, BEI was employed to visualize the enamel maturation pattern by utilizing the high atomic number provided by lead (Z=82). The pattern again consisted of 4 to 5 darkly-stained bands with interband regions containing narrow parallel stripes (Fig. 5). Scoring of the

translucent bands during drying showed that again the stained bands were immediately apical to the score marks.

Incisors stained with Coomassie Blue (Fig. 6) and Alcian Blue (Fig. 7) for 2 h at room temperature were more effective in showing the repeated parallel narrow stripes. These stripes began immediately adjacent to the darkly-stained secretion zone enamel and continued uninterrupted along the enamel maturation zone, only decreasing in staining intensity as they approached the pigmented enamel. The stripes maintained the orientation throughout each tooth. In addition, faint staining of broader bands was observed superimposed on the stripes. broad bands were oriented differently from the stripes and the pattern was similar to that seen after staining with uranyl and lead. Observation of Coomassie Blue-stained and Alcian Bluestained incisors while drying revealed that the bands were present just apical to the translucent bands, exactly as observed after uranyl and lead staining.

Incisors stained with Ruthenium Red for 1 h at room temperature also showed a pattern at the surface of the enamel (Fig. 8). This pattern consisted of 4 or 5 narrow bands of stained enamel in the maturation zone. These bands had the same orientation as those previously described but determination of their position during drying revealed that unlike the other stains they were located just incisal to the translucent bands. The bands decreased in staining intensity incisally. The enamel in the secretion zone was heavily stained and the pigmented enamel did not stain.

In all cases, and with each stain, additional and prolonged

soaking in fixative without stain did not diminish, alter or remove the staining pattern.

# Radioautography after 35s-methionine injection

Whole mount radioautography 1 h after <sup>35</sup>S-methionine injection showed a repetitive distribution of radioactivity at the surface of the tooth (Fig. 9). Most prominent in this pattern was the presence of narrow stripes in the apical region of the maturation zone. The enamel in the secretion zone was also heavily labeled. Some unlabeled areas appeared as white bands and may correspond to regions of enamel normally overlaid by smooth-ended ameloblasts.

### **DISCUSSION**

### Staining reactions

The stains used in this study are common histological stains used to reveal proteins in histological sections and in polyacrylamide gels. The stains were selected either for their ability to produce a color reaction when bound to proteins in situ or for their intrinsic property of having a high atomic number, thus making the staining patterns suitable for backscattered electron imaging (McKee et al., 1987; Chapter Five). In all cases, the stains bound to constituents of the enamel to produce a repetitive pattern. The reactions were considered to represent true binding of stain to protein since the staining patterns were not diminished or altered during prolonged immersion in the same aquéous fixative solution but without the staining agent. Whether the stains were coupled

directly to the protein, or via the fixative was uncertain. However, since staining occurred in aqueous solutions, it seems likely that direct complexing had occurred between the dye and the protein.

Most heavy metal ions are known to form coordination complexes with various chemical groups having nitrogen, oxygen, sulfur or phosphorous atoms (reviewed by Zobel and Beer, 1965). Watson (1958a) tested various uranium salts as electron dense stains and found that uranyl acetate gave superior results. Uranyl acetate is commonly used as a histological stain and has a high affinity for the phosphate groups of nucleic acids (Huxley and Zubay, 1961; Zobel and Beer, 1965) and a slightly lesser affinity for the carboxyl (Stoeckenius, 1961) and free amino (Lombardi et al., 1971) groups of proteins. When uranyl acetate is employed en bloc, it also has a fixative effect (Glauert, 1974) giving good structural preservation of DNA filaments (Ryter and Kellenberger, 1958; Nass et al., 1965), membranous structures and cell junctions (Terzakis, 1968; Goodenough and Revel, 1970) and ground proteins, myofibrils and mitochondria (Hayat, 1969). From the evidence on the binding abilities of uranyl acetate, and since all cellular components of the enamel organ are removed prior to staining, it seems reasonable to conclude that the staining reveals proteins and not nucleic acids, and that these proteins are distributed in a pattern resembling the enamel maturation pattern given by GBHA. The bands of enamel showing uranyl staining are just apical to the translucent bands observed during drying, a region shown to be overlaid by ruffle-ended

ameloblasts in vivo (Takano et al., 1982b; Smith et al., 1987). Since the uranyl-stained stripes are found throughout most of the maturation zone, they would be overlaid by either ruffle-ended or smooth-ended ameloblasts.

Histological staining using lead was introduced by Watson (1958b) and preferentially stains RNA (Dalton and Zeigel, 1960) and carbohydrates such as glycogen (Reynolds, 1963). The mechanism(s) for these binding reactions are not well understood but may be due to polymeric cations arising from complex lead compounds formed by divalent lead salts in alkaline solutions (Reynolds, 1963). The staining of carbohydrates may depend upon the formation of a stable lead-carbohydrate complex through hydrogen bonding (Reynolds, 1963). In any case, the visualization and distribution of the lead-stained pattern in enamel by BEI is identical to that following uranyl staining, and may also reflect a differential distribution of protein at the surface of the tooth.

Coomassie Blue presently is widely used for the demonstration of protein in acrylamide gels (Diezel et al., 1972; Fishbein, 1972) and appears to bind solely and reliably to protein. Furthermore, good results have been obtained using Coomassie Blue for the staining of proteins in histological sections (Feder and O'Brien, 1968; Fisher, 1968; Cawood et al., 1978). Little is known of the chemistry of the binding of Coomassie Blue to protein; nevertheless, all Coomassie Bluebinding biological material is sensitive to nonspecific protease (Cawood et al., 1978). Like other stains, it is probable that Coomassie Blue does not bind in identical quantities with all

proteins. Consequently, regional accumulations of some proteins may take up more stain than other proteins in neighboring areas. The increased staining of the narrow stripes relative to the broader bands of the enamel maturation pattern observed in this study may indicate stripes of an accumulated specific protein at the surface of the tooth capable of binding more Coomassie Blue relative to the protein in the bands. The Coomassie Blue-stained bands of enamel correlate to regions overlaid by ruffle-ended ameloblasts whereas the stripes correlate to both ameloblast morphologies.

Alcian Blue is a cationic dye commonly used to demonstrate the glycosaminoglycans (GAGs) associated with proteoglycans, It is well known from the literature that conventional methods of fixation prior to staining eliminate and/or translocate GAGs (reviewed by Goldberg et al., 1987). the addition of a cationic dye to the fixative reduces the mobility and precipitates and retains these components in situ (Scott, 1972). Alcian Blue has at least two, and up to four positive charges which react via salt linkages with the intense negative electrostatic field generated by GAGs to produce insoluble precipitates (Scott et al., 1964). Alcian Blue staining in fixative solution, as used in \*this study to prevent extraction and translocation of GAGs, revealed a faint staining of the enamel maturation pattern, but an especially intense staining of the narrow stripes associated with it. The staining pattern observed after Alcian Blue was practically identical to that after Coomassie Blue, possibly indicating that the general

protein accumulated in the narrow stripes and bands as revealed by Coomassie Blue may in fact be PGs. Furthermore, it is noteworthy that this pattern is similar to that observed following staining by the periodic acid-Schiff (PAS) reaction (McKee and Warshawsky, 1986b; Chapter Three) used to visualize glycoproteins.

Ruthenium Red is an inorganic cationic dye commonly used in solution with fixative to demonstrate GAGs (reviewed by Luft, 1971a; Goldberg and Septier, 1986). Furthermore, Ruthenium Red precipitates a large variety of polyanions by ionic interaction and its classical reaction with GAGs is typical rather than specific (Luft, 1971a). Also noted was that Ruthenium Red is intensely reactive towards certain lipids (Luft, 1971a,b). pattern observed after Ruthenium Red staining was different from the other stains used in this study in that the stained areas were found incisal to the translucent bands (in areas normally overlaid by smooth-ended ameloblasts). This was the only reagent to stain in a pattern identical to the calcium stain glyoxal bis(2-hydroxyanil)(GBHA). The reason for the dramatic difference between the staining patterns observed after Ruthenium Red and the similar cationic stain-Alcian Blue is not clear at present. In any case, it appears that each stain is selective for specific organic constituents of enamel that relate to specific and different maturation ameloblast morphologies.

Radioautography of fixed and routinely-sectioned incisors after injection of radiolabeled methionine revealed that this amino acid is incorporated into proteins that are secreted in

both the secretion and maturation zones of amelogenesis (Nanci et al., 1987). Whole mount radioautography, as used in this study, confirmed the presence of material containing 35S-methionine at or very close to the enamel surface and further demonstrated the presence of a pattern in the maturation zone consisting of narrow labeled stripes presumably representing newly-secreted protein at the surface of the tooth.

### <u>Interpretation of staining patterns</u>

Staining of certain organic constituents of enamel \_and confirmation of synthesis and release of newly-formed, 35smethionine-containing proteins by maturation zone ameloblasts, all in the form of a pattern previously known to exist during enamel maturation, emphasizes the cyclical nature of phenomena occurring in the maturation zone of amelogenesis. The cyclical nature of enamel maturation is now well-documented, especially with regards to the inorganic phase of enamel. correlations with overlying ameloblast morphology are possible using certain calcium-binding compounds (especially GBHA; Takano et al., 1982b; Smith et al., 1987) and the scoring method for the translucent bands (Takano et al., 1982b). Taken together, these techniques allow interpretation of the enamel maturation pattern as the functional consequence of the rapid modulation of maturation ameloblasts between their ruffle-ended and smoothended morphologies (Ishige et al., 1987; Smith et al., 1987). Apparently, this modulation profoundly affects the distribution of both the mineral and matrix phases of enamel.

This study was undertaken as an attempt to visualize the distribution of proteins at the surface of teeth and to correlate this distribution with ameloblast morphology. Prior to this, Boyde and Reith (1982) provided some evidence of the cyclical distribution of protein but no attempt was made to correlate the stained regions with the enamel organ. The present study has provided clear and direct evidence of protein banding and striping in the surface layer of enamel using different stains and direct correlations have been made to ruffle-ended and smooth-ended ameloblasts.

of great importance to the understanding of enamel maturation is determination of the significance and relationship between bands and stripes of matrix constituents and bands and stripes of different calcium states within the enamel. Evidently, the enamel organ controls this matrix-mineral relationship to such an extent that interference with the wave of modulation by vinblastine, caused by preventing smooth-ended ameloblasts from reverting back to ruffle-ended ameloblasts, predictably alters the maturation pattern in the enamel (McKee and Warshawsky, 1986a; Chapter Four).

The stains used in this study all demonstrated that protein was differentially distributed at the surface of the tooth. Biochemical investigations have shown that the organic matrix of enamel contains glycoproteins (Stack, 1954, 1956; Elgydi and Stack, 1956; Seyer and Glimcher, 1969; Elwood and Apostolopoulos, 1975; Belcourt and Gillmeth, 1979; Belcourt et al., 1982). Using "histochemistry and radioautography, glycoproteins have been identified in the enamel (Scheinmann et

al., 1962; Suga and Gustafson, 1963; Reith and Butcher, 1967; Weinstock and Leblond, 1971; Goldberg et al., Warshawsky, 1979; Warshawsky and Josephsen, 1981; Goldberg and Septier, 1986; McKee and Warshawsky, 1986b; Chapter Three). Similar histochemical and radioautographic identification of GAGs in the enamel has been reported (Belanger, 1955; Bevelander and Johnson, 1955; Leblond et al., 1955; Kennedy and Kennedy, 1957; Quintarelli and Dellova, 1963; Weill and Tassin, 1965; Lennox and ' Provenza, 1970; Yoshiki and Umeda, 1972; Nagai and Takuma, 1973; Blumen and Merzel, 1976; Goldberg et al., 1976, 1978, 1979a,b; Nakata et al., 1982; Goldberg and Septier, 1986). these studies ultrastructurally localized these molecules within sections of enamel. The present study has visualized proteins in general, and possibly proteoglycans, at the sufface of rat incisor enamel. The technique for rapid dissection and staining in fixative is useful in that it allows simultaneous fixation and staining of the matrix before the enamel proteins have a chance to significantly translocate, a procedure probably not sensitive enough for ultrastructural analysis but definitely adequate for whole mount staining. The dissection procedure must nevertheless be performed rapidly since unfixed enamel proteins (rapidly diffuse freely out of the enamel (Warshawsky, 1985; Smith and unpublished). Additional evidence diffusability of protein out of the enamel was demonstrated in this study by the removal of enamel stainability by prior soaking of a tooth in normal saline (Fig. 2).

The purpose of this study was not so much to substantiate and detect specific classes of proteins within the enamel, but rather to demonstrate with common histological stains that there is a specific distribution of proteins at the surface of the tooth. To this end, it has been shown that enamel proteins are distributed in a pattern similar to that observed following the use of certain caltium stains (Chapter Seven). It is probable that following identification of the specific proteins found within each of the bands and stripes it may be possible to gain information on their individual calcium-binding properties and how such organic components contribute to the processing of calcium within the enamel.

#### **REFERENCES**

Belanger LF 1955 Autoradiographic detection of radiosulfate incorporation by the growing enamel of rats and hamsters. J Dent Res, 34:20-27.

Belcourt AB and Gillmeth S 1979 EDTA soluble protein of human mature normal enamel. Calcif Tiss Int, 28:227-231.

Belcourt AB, Fincham AG and Termine JD 1982 Ethylenediamine tetracetic acid insoluble protein in adult human enamel. Caries Res, 16:72-76.

Bevelander G and Johnson PL 1955 The localization of polysaccharides in developing teeth. J Dent Res, 34:123-131.

Blumen G and Merzel J 1976 Autoradiographic study with <sup>35</sup>S-sodium sulphate of loss of sulfated glycosaminoglycans during amelogenesis in the guinea pig. Archs Oral Biol, 21:513-521.

Boyde A and Reith EJ 1981 Display of maturation cycles in ratincisor with acute tetracycline labelling. Histochem, 72:551-561.

Boyde A and Reith EJ 1982 In vitro histological and tetracycline staining properties of surface layer rat incisor enamel also reflect the cyclical nature of the maturation process. Histochem, 75:341-351.

Cawood AH, Potter U and Dickson HG 1978 An evaluation of Coomassie Brilliant Blue as a stain for quantitative microdensitometry of protein in section. J Histochem Cytochem, 26:645-650.

Dalton AJ and Ziegel RF 1960 J Biophys Biochem Cytol, 7:409.

DenBesten PK, Crenshaw MA and Wilson MH 1985 Changes in the fluoride-induced modulation of maturation stage ameloblasts of rats. J Dent Res, 64:1365-1370.

Diezel W, Kopperschlager G and Hofmann E 1972 An improved procedure for protein staining in polyacrylamide gels with a new type of Coomassie brilliant blue. Anal Biochem, 48:617-620.

Elgyedi H and Stack MV 1956 The carbohydrate content of enamel. Resume of findings. NY Dent J, 22:286.

Elwood WK and Apostolopoulos AX 1975 Analysis of developing enamel of the rat. III. Carbohydrate, DEAE-Sephadex and immunological studies. Calcif Tiss Res, 18:337-347.

Feder N and O'Brien TP 1968 Plant microtechnique, some principles and new methods. Ann J Bot, 55:123.

Fishbein WN 1972 Quantitative densitometry of 1-50 µg protein

in acrylamide gel slabs with Coomassie Blue. Anal Biochem, 46:388-401.

Fisher DB 1968 Protein staining of ribboned Epon sections for light microscopy. Histochemie, 16:92-96.

Glauert AM 1974 The fixation, dehydration and embedding of biological specimens. In: Practical Methods in Electron Microscopy. Ed. Glauert AM. North-Holland, Amsterdam. pp. 1-301.

Glimcher MJ 1976 Composition, structure and organization of bone and other mineralized tissues and the mechanism of calcification. In: Handbook of Physiology and Endocrinology. Williams and Wilkins, Baltimore. pp. 25-116.

Goldberg M, Triller M, Escaig F, Genotelle-Septier D and Weill R 1976. Detection sur coupes ultrafines de mucopolysaccharides acides par le bleu alcian dans des tissues dentaires inclus en Epon. J Biol Buccalé, 4:155-165.

Goldberg M, Genotelle-Septier D, Molon-Noblot M and Weill K 1978 Ultrastructural study of the proteoglycans in enamel from rat incisors during late enamel maturation. Archs Oral Biol, 23:1007-1011.

Goldberg M, Genotelle-Septier D and Weill R 1979a Ultrastructural study of the protein-polysaccharides distribution in enamel from rat incisors. J Dent Res, 58(B):1006-1007.

Goldberg M, Septier D, Escaig F and Weill R 1979b Histochemical electron microscopic comparisons between developing and nearly mature rat incisor enamel. J Dent Res, 58(B):2253.

Goldberg M and Septier D 1986 Ultrastructural location of complex carbohydrates in developing rat incisor enamel. Anat Rec, 216:181-190.

Goldberg M, Septier D and Escaig-Haye F 1987 Glycoconjugates in dentinogenesis and dentine. Prog Histochem Cytochem, 17:1-112.

Goodenough DA and Revel JP 1970 A fine structural analysis of intercellular junctions in the mouse liver. J Cell Biol, 45:272-290.

Hayat MA 1969 Uranyl acetate as a stain and fixative for heart tissue. Proc 27th Ann Conf EMSA, p. 412.

Huxley HE and Zubay G 1961 Preferential staining of nucleic acid-containing structures for electron microscopy. J Biophy Biochem Cytol, 11:273.

Ishige N, Ohya K and Ogura H 1987 A rapid cyclic modulation of ameloblasts during enamel maturation. J Dent Res (Abstract), 66(Sp Iss):354.

Josephsen K 1983 Indirect visualization of ameloblast modulation in the rat incisor using calcium-binding compounds. Scand J Dent Res, 91:76-78.

Kennedy JS and Kennedy GDC 1957 Sulphated mucopolysaccharides in rodent teeth. J Anat, 91:398-408.

Kopriwa BM and Leblond CP 1962 Improvement in the coating technique for radioautography. J Histochem Cytochem, 10:269-284.

Leblond CP, Belanger LF and Greulich RC 1955 Formation of bones and teeth as visualized by radioautography. Ann NY Acad Sci, 60:631-659.

Lennox DW and Provenza DV 1970 Mucopolysaccharides in odontogenesis. Histochemical and autoradiographic study. Histochemie, 23:328-341.

Lombardi L, Prenna G, Okolicsanyi L and Gautier A 1971 Electron staining with uranyl acetate. Possible role of free amino groups. J Histochem Cytochem, 19:161-168.

Luft JH 1971a Ruthenium red and violet. I. Chemistry, purification, methods of use for electron microscopy and mechanism of action. Anat Rec, 171:347-368.

Luft JH 1971b Ruthenium red and violet. II. Fine structural localization in animal tissues. Anat Rec, 171:369-416.

McKee MD and Warshawsky H 1986a Modification of the enamel. maturation pattern by vinblastine as revealed by glyoxal bis(2-hydroxyanil) staining and 45 calcium radioautography. Histochemistry, 86:141-145.

7

McKee MD and Warshawsky H 1986b Effects of various agents on staining of the maturation pattern at the surface of rat incisor enamel. Archs Oral Biol, 31:577-585.

McKee MD, Martineau-Doizé B and Warshawsky H 1986 Penetration of various molecular-weight proteins into the enamel organ and enamel of the rat incisor. Archs Oral Biol, 31:287-296.

McKee MD, Warshawsky H and Nanci A 1987 Use of backscattered electron imaging on developed radioautographic emulsions: Application to viewing rat incisor enamel maturation pattern following <sup>45</sup>calcium injection. J Electron Microsc Tech, 5:357-365.

Nagai N and Takuma S 1973 Electron probe and electron microscope studies of acid mucopolysaccharides in developing ratimolar. J Dent Res, 52:386.

Nakata T, Yamamoto K, Matsuo S, Nishimoto T, Kitano E and Akai M 1982 Nature and distribution of mucosubstances in human mature enamel identified by enzyme electron microscopy. Archs Oral Biol, 27:431-433.

Nanci A, Slavkin HC and Smith CE 1987 Immunocytochemical and radioautographic evidence for secretion and intracellular degradation of enamel proteins by ameloblasts during the maturation stage of amelogenesis in rat incisors. Anat Rec, 217:107-123.

Nass MMK, Nass S and Afzelius BA 1965 The general occurrence of mitochondrial D.N.A. Expl Cell Res, 37:516.

Quintarelli G and Dellovo MC . 1963 Mucopolysaccharide histochemistry of rat tooth germs. Histochemie, 3:195-207.

Reith EJ and Butcher EO 1967 Microanatomy and histochemistry of amelogenesis. In: Structural and Chemical Organization of Teeth. Ed. Miles AEW. Academic Press, New York. pp. 371-397.

Reith EJ and Boyde A 1981a The arrangement of ameloblasts on the surface of maturing enamel of the rat incisor tooth. J Anat, 133:381-388.

Reith Ed and Boyde A 1981b Autoradiographic evidence of cyclical entry of calcium into maturing enamel of the rat incisor tooth. Archs Oral Biol, 26:983-987.

Reith EJ, Boyde A and Schmid MI 1982 Correlation of rat incisor ameloblasts with maturation cycles as displayed on enamel surface with EDTA. J Dent Res, 61:1563-1573.

Reith EJ, Schmid MI and Boyde A 1984 Rapid uptake of calcium in maturing enamel of the rat incisor. Histochem, 80:409-410.

Reynolds ES 1963 The use of lead citrate at high pH as an electron-opaque stain in electron microscopy. J Cell Biol, 17:208-212.

Ryter A and Kellenberger E 1958 Etude au microscope électronique de plasmas contenant de l'acide désoxyribonucléique. Z. Naturf, 13:597.

Scheinmann E, Weinreb MM and Wolman M 1962 Histochemical study of the ameloblasts and the enamel matrix in rat molars. J Dent Res, 41:1293-1303.

Scott JE 1972 Histochemistry of Alcian Blue. III. The molecular biological basis od staining by Alcian Blue 8GX and analogous phthalocyanins. Histochemie, 32:191-212.

Scott JE, Quintarelli G and Dellovo MC 1964 The chemical and histochemical properties of Alcian Blue. I. The mechanism of Alcian Blue staining. Histochemie, 4:73-85.

Sever J and Glimcher MJ 1969 The content and nature of the carbohydrate components of the organic matrix of embryonic bovine

enamel. Biochim Biophys Acta, 18:410-418.

Smith CE, McKee MD and Nanci A 1987 Cyclic induction and rapid movement of sequential waves of new smooth-ended ameloblast modulation bands in rat incisors as visualized by polychrome fluorescent labelling and GBHA-staining of maturing enamel. J Dent Res, In Press.

Stack MV 1954 Organic constituents of enamel. J Am Dent Assoc, 48:297-306.

Stack MV 1956 The carbohydrate content of human dental enamel, J Dent Res, 35:966.

Stoeckenius W 1961 Electron microscopy of DNA molecules "stained" with heavy metal salts. J Biophys Biochem Cytol, 11:297.

Suga S and Gustafson G 1963 Studies on the development of rat enamel by means of histochemistry, microradiography and polarized light microscopy. In: Advancement of Fluorine Research and Dental Caries Prevention. Ed. Hardwick JL. Pergamon Press, Oxford. pp. 223-244.

Takano Y and Ozawa H 1980 Ultrastructural and cytochemical observations on the alternating morphological changes of the ameloblasts at the stage of enamel maturation. Archs Histol Jap, 43:385-399.

Takano Y, Crenshaw MA and Reith EJ 1982a Correlation of 45Ca incorporation with maturation ameloblast morphology in the ratincisor. Calcif Tiss Int, 34:211-213.

Takano Y, Crenshaw MA, Bawden JW, Hammarström L and Lindskog S 1982b The visualization of the patterns of ameloblast modulation by the glyoxal bis(2-hydroxyanil) staining method. J Dent Res, 61(Sp Iss):1580-1586.

Terzakis JA 1968 Uranyl acetate, a stain and a fixative. J Ultrastr Res, 22:168-184.

Veis 1985 Phosphoproteins of dentin and bone. Do they have a role in matrix mineralization. In: The Chemistry and Biology of Mineralized Tissues. Ed. Butler WT. Ebsco Media, Birmingham. pp. 170-176.

Warshawsky H 1979 Radioautographic studies of amelogenesis. J Biol Buccale, 7:105-126.

Warshawsky H 1985 Ultrastructural studies on amelogenesis. In: The Chemistry and Biology of Mineralized Tissues. Ed. Butler WT. Ebsco Media, Birmingham. pp. 33-45.

Warshawsky H and Josephsen K 1981 The behavior of substances labeled with  $^3\mathrm{H}\text{-}\mathrm{proline}$  and  $^3\mathrm{H}\text{-}\mathrm{fucose}$  in the cellular processes

of odontoblasts and ameloblasts. Anat Rec, 200:1-10.

Watson ML 1958a Staining of tissue sections for electron microscopy with heavy metals. J Biophys Biochem Cytol, 4:475.

Watson ML 1958b Staining of tissue sections for electron microscopy. II. Application of solutions containing lead and barium. J Biophys Biochem Cytol, 4:727.

Weill R and Tassin MT 1965 Etude histochimique de la matrice de l'émail histogénèse chez le rat. Acta Histochem, 22:259-285.

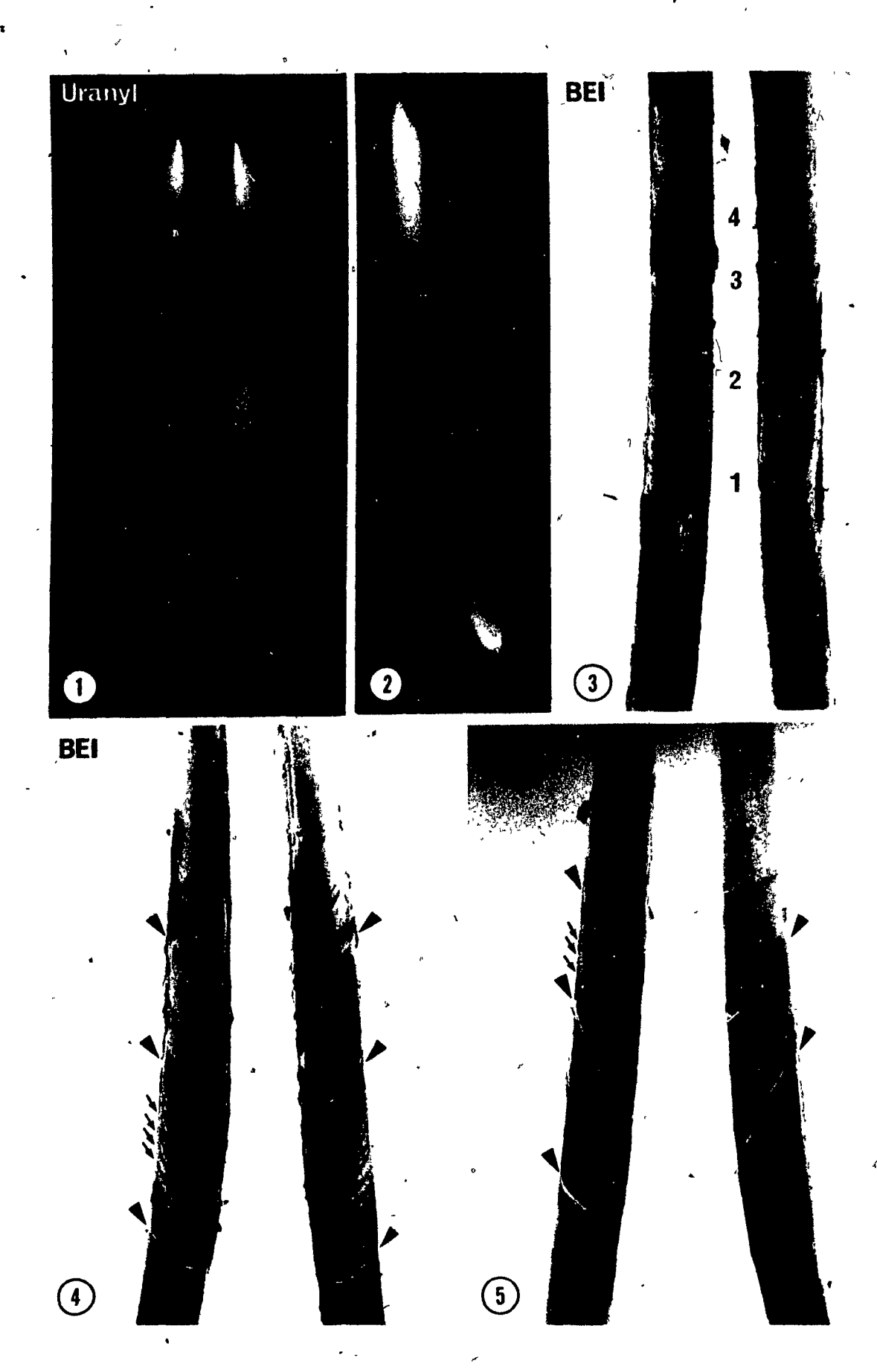
Weinstock A and Leblond CP 1971 Elaboration of the matrix glycoprotein of enamel by secretory ameloblasts of the rat incisor as revealed by radioautography after galactose <sup>3</sup>H injection. J Cell Biol, 51:26-51.

Yoshiki S and Umeda T 1972 Histochemical demonstration of acid mucopolysaccharides in rat enamel matrix at the stage of matrix formation after treatment with proteases. Archs Oral Biol, 17:1765-1770.

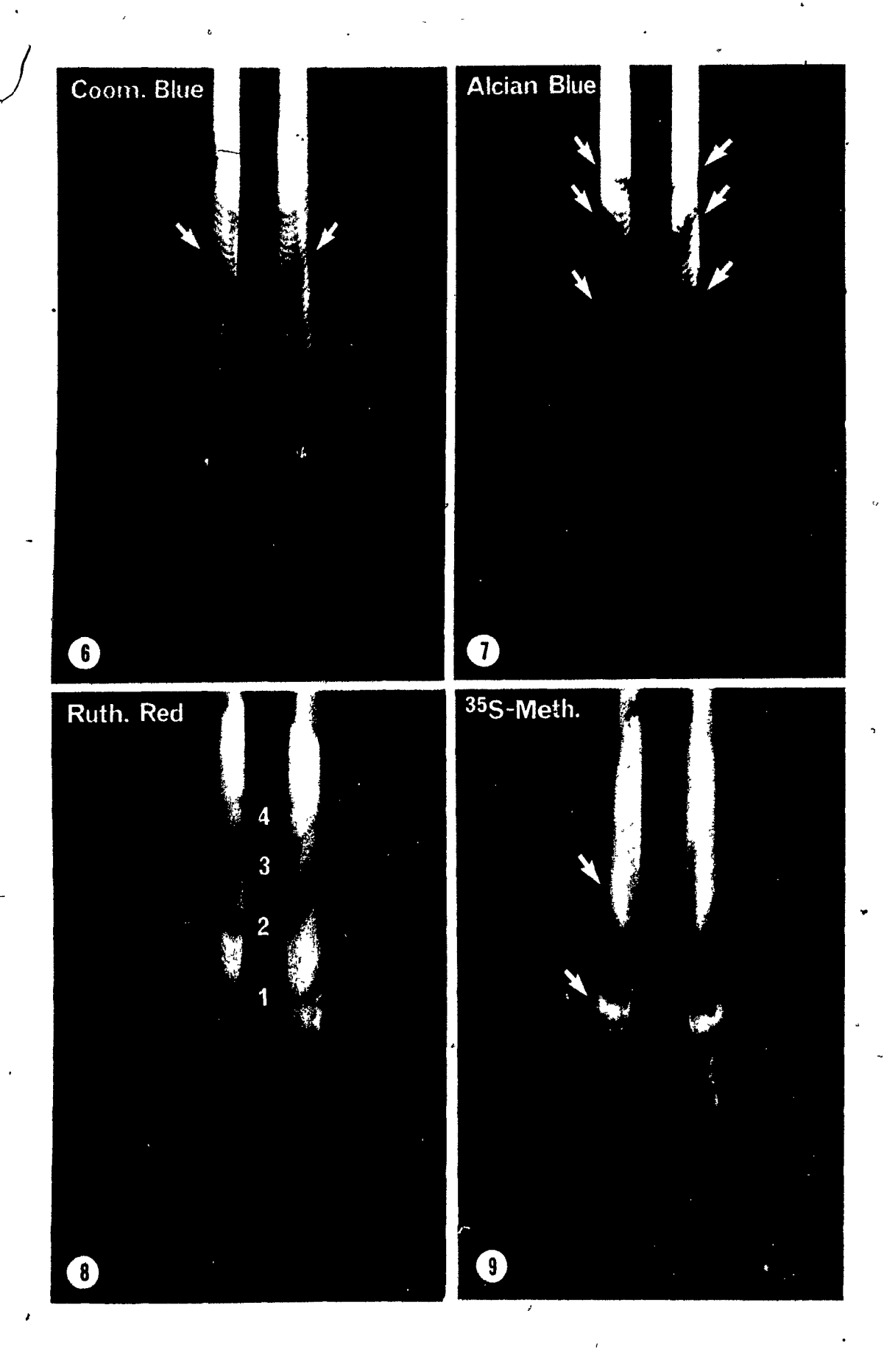
Zobel RR and Beer M 1965 The use of heavy metal salts as electron stains. Int Rev Cytol, 18:363-399.

#### FIGURE LEGENDS: CHAPTER EIGHT

- Figure 1. Contralateral lower rat incisors wiped free of their enamel organs and stained with uranyl acetate in fixative for 3 h. The enamel in the secretion zone is darkly-stained and in the maturation zone, 4 bands of stained enamel run obliquely across the teeth that resembles the enamel maturation pattern. Staining intensity decreases incisally. X6.5.
- Figure 2. An incisor soaked for 1 h in physiological saline at room temperature prior to staining with uranyl acetate as in Figure 1. Note the removal of the staining pattern presumably due to diffusion of enamel proteins out of the enamel and into the saline. X6.5.
- Figure 3. Inverse backscattered electron image of the same teath shown in Figure 1. This electron detection mode relies on the relatively high atomic number of the uranium in the stained areas of enamel relative to the background backscattering produced by the calcium and phosphorous in the unstained areas. Again, the presence of 4 narrow bands of stained enamel can be observed in the enamel maturation zone. X12.
  - Figure 4. Inverse backscattered electron image of another contralateral pair of teeth stained with uranyl acetate. In this animal, the finer stripes (small arrows) can be observed in the interband regions. Scoring of the translucent bands during drying (arrowheads) indicates that the uranyl-stained bands are found in regions of enamel normally overlaid by ruffle-ended ameloblasts. X12.
  - Figure 5. Inverse backscattered electron image of incisors stained with lead citrate in fixative for 3 h at room temperature. The staining pattern again consists of 4 to 5 darkly-stained bands just apical to the scored translucent bands (arrowheads) and interband regions containing narrow stripes (small arrows). X12.



- Figure 6. Contralateral lower incisors stained with Coomassie Blue in fixative for 2 h at room temperature. The enamel in the secretion zone is darkly-stained and in the maturation zone, the staining pattern consists of bands (white arrows) and stripes (black arrows). This stain is particularly effective in demonstrating the narrow stained stripes which continue uninterrupted and without changing orientation along the maturation zone. X6.5.
- Figure 7. Alcian Blue staining of incisors shows a pattern similar to that after staining with Coomassie Blue. The pattern consists of bands (white arrows) and stripes (black arrows) of stained enamel in the maturation zone. In the secretion zone, the enamel is darkly stained. Staining intensity diminishes in an incisal direction. X6,5.
- Figure 8. Ruthenium Red staining of incisors also shows a banding pattern at the surface of the teeth. The pattern consists of 4 bands of stained enamel running transversely and obliquely across the enamel in the maturation zone. The enamel in the secretion zone is darkly stained. The position of the bands with this stain is different from the other stains in that these areas of enamel are normally overlaid by smooth-ended ameloblasts. X6.5.
- Figure 9. Radioautographs of the lower incisors of an animal injected with <sup>35</sup>S-methionine 1 h prior to sacrifice. The enamel in the secretion zone is heavily labeled and in the maturation zone, narrow parallel stripes (black arrows) of radioactivity probably represent incorporation of <sup>35</sup>S-methionine into newly-synthesized enamel protein released at the surface of the tooth. Unlabeled areas (white arrows) may correspond to enamel related to smooth-ended ameloblasts. X6.5.



CHAPTER NINE: SPECIFIC BINDING SITES FOR TRANSFERRIN ON AMELOBLASTS OF THE ENAMEL MATURATION ZONE IN THE RAT INCISOR.

# SYNOPSIS

During enamel maturation in rodents, an iron-containing pigment is deposited into the surface layer of the enamel. Maturation zone ameloblasts presumably are responsible for this The presence of large amounts of ferritin in the deposition. cytoplasm of these cells suggests that they receive iron, presumably from circulating transferrin. radioautographic binding assay (Bergeron et al., 1977) iodinated transferrin was used to determine if indeed maturation ameloblasts possess transferrin receptors at their cell surfaces. Experimental rats received systemic injections of labeled transferrin, while control rats received injections of labeled transferrin plus a large excess of unlabeled transferrin in order to compete with the labeled transferrin for available specific Light microscope radioautography showed that ruffleended ameloblasts (RAs) of the enamel maturation zone had a high density of specific receptors for transferrin relative to smoothended ameloblasts (SAs). Electron microscopy and energy dispersive X-ray spectroscopy confirmed the presence of ferritin and iron, respectively, within these cells. It is postulated that the iron responsible for enamel pigmentation is transported by transferrin to maturation ameloblasts and is bound to specific transferrin receptors found mostly on RAs, and that the modulation of these cells into SAs results in alloss of most of these receptors.

#### INTRODUCTION

In the rodent incisor, the enamel maturation process includes deposition of an iron-containing pigment into the surface layer of mature enamel (Halse, 1972b; Halse and Selvig, 1974). Furthermore, the amount of iron in the enamel increases progressively with the age of the rat (Addison and Appleton, 1915; Pindborg et al., 1946; Schour and Massler, 1949; Lindemann, 1970; Halse, 1972b). Schmidt and Keil (1971) determined that the iron-containing compound in rodent enamel is an iron oxede, and it has been further proposed that the iron may in some way be associated with the hydroxyapatite crystallites of enamel (Selvig and Halse, 1975).

Almost all the ameloblasts in the entire maturation zone incorporate exogenously-injected radiolabeled iron as visualized by radioautography (Karim and Warshawsky, 1984; Ogura et al., 1984). Numerous other techniques have been used to identify iron both within this cellular layer as well as in the enamel. These include histochemical staining (Pindborg, 1947; Reith, 1959), electron microprobe analysis (Boyde et al., 1961; Halse, 1972a), polarizing microscopy (Schmidt and Keil, 1971) and electron microscopy (Reith, 1961; Jessen, 1968; Kallenbach, 1970). Electron microscopy has shown that ferritin is present within these cells (Reith, 1961; Jessen, 1968; Kallenbach, 1970). The ferritin is found either as free ferritin particles within the cytoplasm of the ameloblasts or in membrane-bounded pigment granules. The ferritin particles appear first within the cytoplasm, and then decrease as the number of pigment granules

containing ferritin particles increases (Kallenbach, 1970). Finally, mostly membrane-bounded granules with ferritin are found. Ameloblasts with many pigment granules appear orange-brown and are called "pigmented" ameloblasts. Ferritin is a protein containing about 23% iron in the ferric state (Granick and Michaelis, 1943), and is considered to be one of the storage forms of iron.

Most of the iron in foods occurs in the ferric (Fe3+) state, either as ferric hydroxide or as ferric organic compounds. acid medium, these compounds are broken down into free ferric ions or loosely-bound organic iron. Reducing substances may then convert ferric iron to the ferrous (Fe<sup>2+</sup>) state. In this form, iron is more soluble and is therefore more readily absorbed. Once ferrous iron enters the blood plasma it is, oxidized and combines with the metal-binding, glycoprotein apotransferrin. This complex, known as transferrin, transports iron in the blood plasma and crosses cell membranes by transferrin-receptormediated endocytosis (Seligman, 1983). Transferrin has a molecular weight of 88,000 daltons and binds two iron stoms per molecule (Pollycove, 1966; Harper, 1971). Presumably the transferrin then releases the iron to the cell where it combines with the protein apoferritin, to form ferritin (Granick, 1946, '1951; Farrant, 1954; Pollycove, 1966; Harper, 1971). presence of large amounts of ferritin in the cytoplasm of ameloblasts in the enamel maturation zone suggests that these cells receive iron from blood-borne transferrin found within the tissue fluid. In our-study, an in vivo radioautographic binding assay (Bergeron et al., 1977) using iodinated transferrin was

used to determine if indeed maturation ameloblasts possess transferrin receptors at their cell surfaces.

### MATERIALS AND METHODS

# Charging of transferrin with iron

Diferric transferrin was charged and saturated by a modified method of Klausner et al. (1983). Six mg of rat transferrin (Jackson Immuno Research Laboratories) were dissolved in 1 ml of 0.25 M Tris-HCl, pH 8.0, with 10 µM sodium bicarbonate. To this solution 20 µl of 100 mM disodium nitrilotriacetate and 12.5 mM of FeCl<sub>3</sub> were added. The solution was left at room temperature for 3 h and then was eluted through a Sephadex G-25 column which was equilibrated with 0.15 M NaCl/0.02 M Tris-HCl, pH 7.4. The amount of iron bound by the transferrin was estimated from the A<sub>465</sub> nm/A<sub>280</sub> nm ratio. Samples showing 90% saturation were collected and kept frozen at -20°C.

#### Iodination of transferrin

Iodination of transferrin with Na<sup>125</sup>I (New England Nuclear) was performed by a modification of the Chloramine T method (Hunter and Greenwood, 1962). The charged transferrin (6 mg/0.2 ml) was placed into a polystyrene tube and mixed with 5 mCi (50 ll) Na<sup>125</sup>I. The following reagents (all in 0.05 M phosphate buffer, pH 7.5) were then added: Chloramine T (10 mg in 1 ml), sodium metabisulphite (50 mg / 1 ml) and potassium iodide (60 mg in 1 ml). The reaction mixture was then purified on a Sephadex G-50 column that was equilibrated with 25 mM Tris-10 mM MgCl<sub>2</sub> buffer (pH 7.5). The <sup>125</sup>I-transferrin was freshly prepared

before each experiment and its integrity was evaluated by trichloroacetic acid (TCA) precipitation which showed 95% incorporation.

### Animal procedures

Male Sherman rats weighing approximately 100 gm were used in this study. Under pentobarbital anesthesia, experimental rats were injected via the jugular vein with 0.15 ml of iodinated transferrin (approximately 200 x 106 cpm). Control rats received the same amount of iodinated transferrin plus a large excess of unlabeled transferrin in order to compete with the "hot" transferrin for available specific receptors (Bergeron et al., 1977). At 2.5 min after injection of the transferrin, the animals were perfused through the left ventricle with lactated Ringer's solution for 15 sec followed by a 10 min fixation with 2.5% glutaraldehyde in 0.1 M sodium cacodylate buffer containing .0.05% calcium chloride, pH 7.3. The mandibles were dissected, immersed in fixative overnight and washed extensively in 0.1 M cacodylate buffer. The mandibles were decalcified in 4.13% disodium EDTA for 2 wks at 4°C (Warshawsky and Moore, 1967). The hemimandibles were then cut into segments, postfixed in 2% osmium, dehydrated through graded acetones and embedded in Epon One-micrometer-thick longitudinal sections were stained 812. with iron hematoxylin and processed for radioautography according to the method of Kopriwa and Leblond (1962). The sections were exposed for 8 wks and quantitative analysis of silver grains was performed. Silver grains over ruffle-ended ameloblasts (RAs) and smooth-ended ameloblasts (SAs) throughout the entire maturation zone were counted in longitudinal sections of the incisor. In the experimental animals, 190,164  $\mu m^2$  of RAs and 101,972  $\mu m^2$  of SAs were counted and in the control animals, 206,700  $\mu m^2$  of RAs and 107,484  $\mu m^2$  of SAs were counted.

# Electron microscopy and X-ray microanalysis

Following identification of RAs by light microscopy, the areas containing these cells were trimmed for thin sectioning. Thin sections were cut with a diamond knife on a Reichert OM-U2 ultramicrotome, mounted on copper grids and stained with uranyl acetate and lead citrate. Electron micrographs were taken with a JEOL 2000FX operated at 80 kV. For energy-dispersive X-ray analysis, an X-ray detector system (Link AN 10,000) was used on unstained sections from the same blocks. The system was operated at 80 kV in the transmission mode using 100 sec of counting time. The width of the analysed area was approximately 5 µm in diameter, and X-rays were generated from the supranuclear cytoplasm shown in Figure 5.

#### RESULTS

# Light microscope radioautography

In the experimental rats, the enamel organ and the enamel in the zones of presecretion and secretion showed few silver grains. In the maturation zone, numerous silver grains were found over all regions of RAs and the periodontal connective tissue adjacent to the enamel organ (Fig. 1). The SAs and the papillary layer showed only weak labeling (Figs. 1,3). In the control animals (Figs. 2,4), numerous grains were found over the periodontal

connective tissue, but only weak labeling was present over RAs (Fig. 2), SAs (Fig. 4) and the rest of the enamel organ. the concomitant administration of an excess of unlabeled transferrin together with the labeled transferrin given to the control animals did not produce a competitive inhibition of the labeling in the periodontal connective tissue, and experimental values never exceeded the control, it was concluded that the reaction represented nonspecific binding to highcapacity sites. Table 1 shows the grain counts obtained over RAs in the experimental versus the control animals. Grain counts over the RAs in the experimental rats significantly exceeded the counts in control rats (p<0.001). Therefore, these RA reactions represented binding of labeled transferrin to specific sites (Fig. 1). Table 2 shows grain counts obtained over SAs in the experimental versus the control animals. Although qualitatively the SA reaction appeared similar in the experimental versus the control, quantitation revealed a difference that was much less significant (p<0.021). The RA reaction was 5 times greater than the SA reaction, and since only 20% of the maturation zone was SAs, the sample size was substantially smaller.

# Electron microscopy

Electron microscopy of maturation ameloblasts showed free ferritin particles homogeneously dispersed throughout the cytoplasm as well as membrane-bounded pigment granules in the supranuclear cytoplasm of both RAs (Fig. 5) and SAs. The pigment granules were irregular in shape and surrounded by an often ill-defined membrane.

# Energy-dispersive X-ray spectroscopy (EDX)

Figure 6 shows the X-rays generated by an unstained area in a RA similar to that shown in Figure 5. The presence of iron within the specimen was demonstrated by the appearance of the Kanand KB, X-ray peaks marked Fe in Figure 6. Presumably this iron was related to the ferritin particles found either free and homogeneously dispersed in the cytoplasm, or in the pigment granules. The copper peaks (Cu, Fig. 6) were generated by the copper grid.

#### DISCUSSION

All living cells require iron for the processes of cellular respiration (Weinberg, 1978). The density of transferrin receptors appears to be related to the iron requirement of the cell (Trowbridge and Omary, 1981; Sutherland et al., 1981). Furthermore, transferrin receptors are numerous on the basal cells of various epithelia (Gatter et al., 1983; Salonen and Kallajoki, 1986) and on epithelial cells which have undergone malignant transformation (Lloyd et al., 1984). These findings are consistent with the view that the expression of transferrin receptors is also related to cell proliferation (Trowbridge and Omary, 1981; Sutherland et al., 1981). The presence of a high density of transferrin receptors on RAs in this study experiment was obviously not related to proliferation, since these cells do not divide. Since other cells also have a metabolic requirement for iron, but lack detectable receptors, it seemed likely that the high density of specific receptors for transferrin on RAs reflected their unique ability to accumulate iron-containing

pigment.

It has been shown that iron is incorporated by ameloblasts very early in the enamel maturation zone (at 1.5 mm into the zone; Karim and Warshawsky, 1984), although no ferritin is obvious within the cells at this point. Incisal to this point, all ameloblasts of the maturation zone incorporate iron and show the presence of intracellular ferritin until they become reduced ameloblasts at the incisal end of the tooth (Karim and Warshawsky, 1984). Thus, concomitant with iron incorporation into maturation ameloblasts is the appearance of ferritin. Ferritin first occurs as free particles within the cytoplasm and is then incorporated into membrane-bounded granules (Kallenbach, 1970; Karim and Warshawsky, 1984). A similar pathway is known to occur in hepatocytes (Kerr and Muir, 1960; Harris, 1963). Pigmentation of ameloblasts is a result of iron-containing On the other hand, pigmentation of enamel is not ferritin. caused by ferritin, but by some unknown low-molecular-weight iron compound (Schmidt and Keil, 1971) or by iron in some association with the hydroxyapatite crystallites (Selvig and Halse, 1975). The iron-containing pigment eventually leaves the ameloblasts to enter the enamel by some as yet unknown mechanism. It has been postulated that pigment granules in ameloblasts represent a lysosomal mechanism for the removal and breakdown of ferritin (Kallenbach, 1970; Takano and Ozawa, 1981) as these structures are acid phosphatase positive (Takano and Ozawa, Therefore, the normal pathway of iron from the blood to the enamel can be visualized as follows: ingested or stored iron is solubilized as ferrous iron and passes to blood plasma where it is oxidized and combined with the plasma protein apotransferrin to become diferric transferrin. It then leaves the capillaries of the enamel organ to enter the tissue fluid where it binds to specific transferrin receptors at the cell surfaces of the ameloblasts. After receptor-mediated-endocytosis the iron is uncoupled from the transferrin and transferred to apoferritin to form ferritin within the ameloblasts. The intracellular processing of iron in ameloblasts may involve binding to low-molecular-weight intermediates prior to incorporation into ferritin as evidenced in other cell types (Charley et al., 1960; Stitt et al., 1962; Primosigh and Thomas, 1968). By some further mechanism, the iron is released from the ferritin and enters the surface layer of the enamel.

Karim and Warshawsky (1984) have shown that most of the maturation zone ameloblasts incorporate 55Fe, however, no careful distinction was made between RAs and SAs. An important mediator in the transport of the iron to the enamel appears to be In our study, there were indeed high levels of transferrin. specific transferrin receptor sites at the surface of RAs. reason for the reduction in transferrin binding to SAs remains to be clarified, particularly in view of the fact that these cells also show ferritin particles, pigment granules and uptake of radiolabeled, iron (Karim and Warshawsky, 1984). It is possible that most of the iron is transported directly into RAs which then modulate into SAs (Josephsen, 1983; Ishige et al., 1987; Smith et Modulation of these cells to SAs appears to result al., 1987)'. in a loss of most of the transferrin receptors.

TABLE 1

Grain counts over RAs of rats injected with 125I-transferrin

,	Experimental	Control
Area of one sample	2756 μm <sup>2</sup>	2756 µm²
Number of samples	69.	7.5
Average number of grains/2756µm <sup>2</sup>	112.1 <u>+</u> 13.1	$75.1 \pm 9.2$
Student's t-test	p<0.001	
•	•	•

TABLE 2

Grain counts over SAs of rats injected with 125I-transferrin

	Experimental	Control
Area of one sample	2756 µm <sup>2</sup>	2756 µm²
Number of samples	137	39 -
Average number of grains/2756µm²	$22.0 \pm 5.7$	19.2 ± 3.3
Student's t-test*	p<0.021	

### REFERENCES

Addison WHG and Appleton JI 1915 The structure and growth of the incisor teeth of the albino rat. J Morphol, 26:43-96.

Bergeron JJM, Levine G, Sikstrom R, O'Shaughnessy D, Kopriwa BM, Nadler NJ and Posner BI 1977 Polypeptide hormone binding sites in vivo: Initial localization of 125I-labeled insulin to hepatocyte plasmalemma as visualized by electron microscope radioautography. Proc Natl Acad Sci USA, 74:5051-5055.

Boyde A, Switzur VR and Fearnhead RV 1961 Application of the scanning electron-probe X-ray microanalyser to dental tissues. J Ultrastruct Res, 5:201-207.

Charley P, Rosenstein M, Shore E and Saltman P 1960 The role of chelation and binding equilibria in iron metabolism. Archs Biochem Biophys, 88:222-226.

Farrant JL 1954 An electron microscopic study of ferritin. Biochim Biophys Acta, 13:569-576.

Gatter KC, Brown G, Trowbridge IS, Woolston R-E and Mason YD 1983 Transferrin receptors in human tissues: Their distribution and possible relevance. J Clin Path, 36:539-545.

Granick S 1946 Ferritin: Increase of protein apoferritin in gastrointestinal mucosa as direct response to iron feeding. J Biol Chem, 164:737-746.

Granick S 1951 Structure and physiological functions of ferritin. Physiol Rev, 31:489-511.

Granick S and Michaelis L 1943 Ferritin. II. Apoferritin of horse spleen. J Biol Chem USA, 147:91-97.

Halse H 1972á An electron microprobe investigation of the distribution of iron in incisor enamel. Scand J Dent Res, 80:26-39.

Halse H 1972b Location and first appearance of rat incisor pigmentation. Scand J Dent Res, 80:428-433.

Halse H and Selvig KA 1974 Incorporation of iron in ratincisor enamel. Scand  $\hat{J}_{\gamma}$ Dent Res, 82:47-56.

Harper HA 1971 Water and mineral metabolism. In: Review of Physiological Chemistry. Lange Med. Publications, Los Altos, California. p. 406.

Harris JW 1963 The Red Cell. Harvard University Press, Cambridge, Massachusetts. pp. 31-57.

Hunter WM and Greenwood FC 1962 Preparation of iodine-131 labeled human growth hormone of high specific activity. Nature, 194:495-496.

Ishige  $N_{\nu}$  Ohya K and Ogura H 1987 A rapid cyclic modulation of ameloblasts during enamel maturation. J Dent Res (Abstract), 66:354.

Jessen H 1968 The morphology and distribution of mitochokdria in ameloblasts with special reference to a helix-containing type. J Ultrastruct Res, 22:120-135.

Josephsen K 1983 Indirect visualization of ameloblast modulation in the rat incisor using calcium-binding compounds. Scand J Dent Res, 91:76-78.

Josephsen K and Fejerskov O 1977 Ameloblast modulation in the maturation zone of the rat incisor enamel organ. A light and electron microscopic study. J Anat, 124:45-70.

Kallenbach E 1970 Fine structure of rat incisor enamel organ during late pigmentation and regression stages. J Ultrastruct Res, 30:38-63.

Karim A and Warshawsky H 1984 A radioautographic study of the incorporation of iron 55 by the ameloblasts in the zone of maturation of rat incisors. Am J Anat, 169:327-335.

Kerr DHS and Muir AR 1960 A demonstration of the structure and disposition of ferritin in the human liver cell. J Ultrastruct Res, 3:313-319.

Klausner RD, Van Renswoude JV, Ashwell G, Kempf C, Schechter AN, Dean A and Bridges KR 1983 Receptor mediated endocytosis of transferrin in K562 cells. J Biol Chem, 258:4715-4724.

- Kopriwa BM and Leblond CP 1962 Improvement in the coating technique of radioautography. J Histochem Cytochem, 10:259-284.

Lindemann G 1970 Rat incisor pigmentation. Tandlaegebladet, 74:662-670.

Lloyd JM, O'Dows T and Tee D 1984 Demonstration of an epitope of the transferrin receptor in human cervical epithelium-a potentially useful cell marker. J Clin Path, 37:131-135.

Ogura H, Ohya K, Mataki S, Hashimoto K and Kubota M 1984 Experimental studies on the transport mechanism of iron in rat incisors using 55Fe and colchicine. In: Tooth Enamel IV. Eds. Fearnhead RW and Suga S. Elsevier Science Publishers, Amsterdam. pp. 256-260.

Pindborg JJ 1947 Studies on incisor pigmentation in relation to liver iron and blood picture of the white rat. V. Histochemical demonstration of the embedding of the pigment in the enamel. Odont Tidsk, 55:443-446.

Pindborg EV, Pindborg JJ and Plum CM 1946 Studies on incisor pigmentation in relation to liver iron and blood picture of the white rat. I. The effect of iron deficiency on the pigmentation of the incisors in the rat. Acta Pharmacol, 2:285-293.

Pollycove M 1966 Iron metabolism and kinetics. Seminars in Hematology, 3:235-298.

Posner BI, Josefsberg Z and Bergeron JJM 1978 Intracellular polypeptide hormone receptors: Characterization of insulin binding sites in Golgi fractions from the liver of female rats. J Biol Chem, 253:4067-4073.

Primosigh JT and Thomas ED 1968 Studies on the partition of iron in bone marrow cells. J Clin Invest, 47:1473-1482.

Reith EJ 1959 The enamel organ of the rat's incisor, its histology and pigment. Anat Rec, 133:75-90.

Reith EJ 1961 The ultrastructure of ameloblasts during matrix formation and the maturation of enamel. J Biophys Biochem Cytol, 9:825-840.

Salonen J and Kallajoki M 1986 Immunohistochemical localization of transferrin receptors in junctional and sulcular epithelium of human gingiva. Archs Oral Biol, 31: 345-349.

Schmidt WJ and Keil JA 1971 Polarizing Microscopy of Dental Tissues. Permagon Press, Oxford.

Schour I and Massler M 1949 The teeth. In: The Rat in Laboratory Investigation. Eds. Farris, EJ and Griffith JQ Jr. Lippincott, Philadelphia. pp. 104-165.

Seligman PA 1983 Structure and function of the transferrin receptor. Prog Hemat, 8:131-147.

Selvig KA and Halse H 1975 The ultrastructural localization of iron in rat incisor enamel. Scand J Dent Res, 83:88-95.

Smith CE, McKee MD and Nanci A 1987 Cyclic induction and rapid movement of sequential waves of new smooth-ended ameloblast modulation bands in rat incisors as visualized by polychrome fluorescent labelling and GBHA-staining of maturing enamel. J Dent Res, In Press.

Stitt C, Charley P, Butt EM and Saltman P 1962 Rapid induction of iron deposition in spleen and liver

with an iron-ferritin chelate. Proc Soc Exp Biol Med, 110:70-71.

Sutherland R, Delia D, Schneider C, Newman R, Kemshead J and Graves M 1981 Ubiquitous cell-surface glycoprotein on tumor cells is proliferation associated receptor for transferrin. Proc Natn Acad Sci USA, 78:4515-4519.

Takano Y and Ozawa H 1981 Cytochemical studies on the ferritin-containing vesicles of the rat incisor ameloblasts with special reference to the acid phosphatase activity. Calcif Tiss Int, 33:51-55.

Trowbridge IS and Omary B 1981 Human cell surface glycoprotein related to cell proliferation is the receptor for transferrin. Proc Natn Acad Sci USA, 78:3039-3043.

Warshawsky H and Moore G 1967 A technique for the fixation and decalcification of rat incisors for electron microscopy. J Histochem Cytochem, 15:542-549.

Weinberg ED 1978 Iron and infection. Microbiol Rev, 42:45-66.

Figure 1. Light microscope radioautograph of the enamel organ of an experimental animal injected with \$125I\$-transferrin. Ruffle-ended ameloblasts (RAs) and the connective tissue of the periodontal space (ps) show numerous silver grains. The papillary layer (pl) is only weakly labeled. X400.

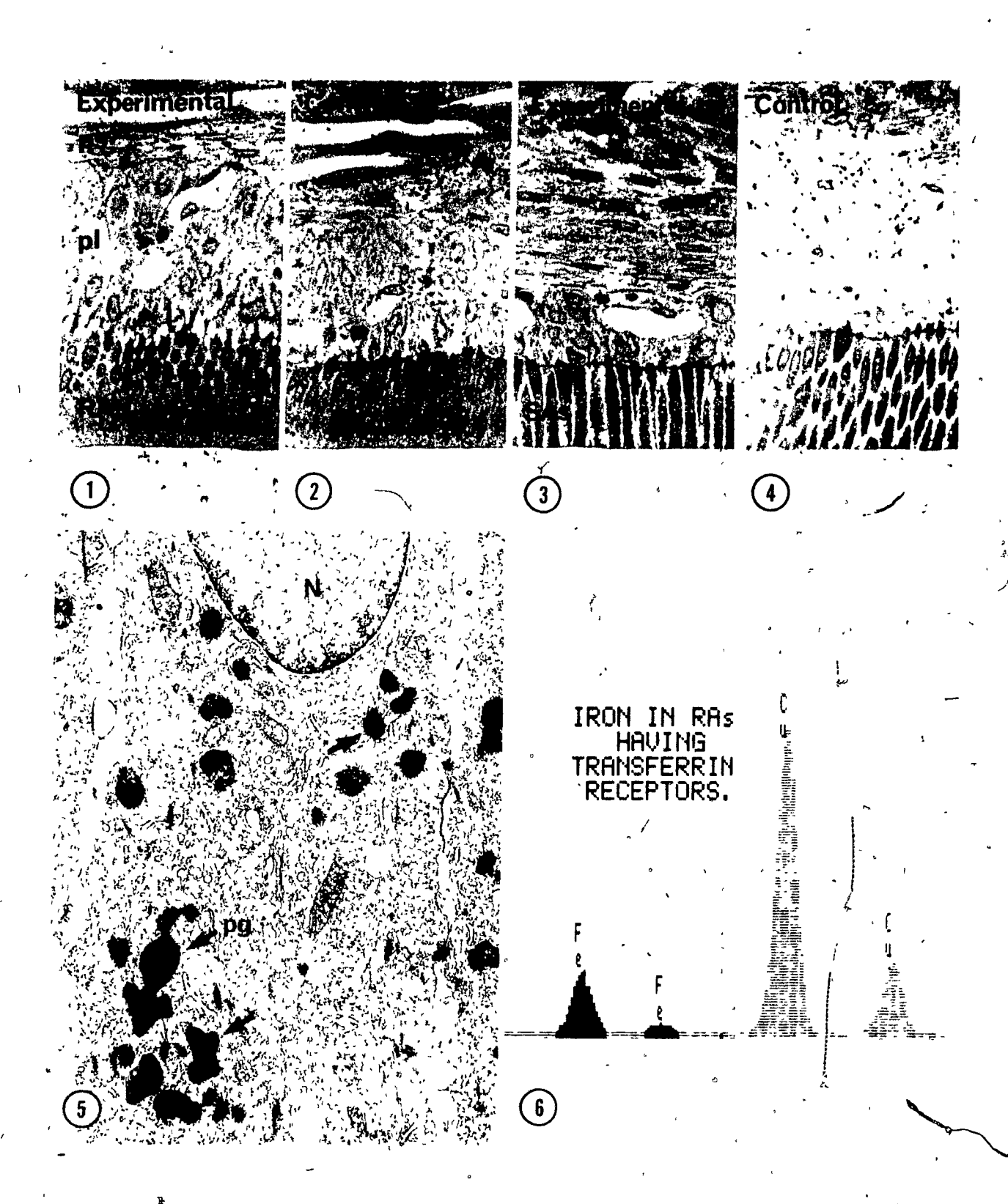
Figure 2. Light microscope radioautograph of the enamel organ of a control animal injected with a large excess of unlabeled transferrin together with the labeled transferrin. Note that only weak labeling is present over ruffle-ended ameloblasts (RAs) and the papillary layer. Although the periodontal connective tissue still shows a strong reaction, the diminished number of silver grains over RAs is due to the competitive binding for specific transferrin receptors by the unlabeled transferrin. X400

Figure 3. Light microscope radioautograph of the enamel organ of an experimental animal injected with \$125\text{I-transferrin.}\$ Smoothended ameloblasts (SAs) and the rest of the enamel organ show only a few silver grains. X400.

Figure 4. Light microscope radioautograph of the enamel organ of a control animal injected with a large excess of unlabeled transferrin together with the labeled transferrin. The low level of labeling appears qualitatively similar to the experimental (Fig. 3). X400.

Figure 5. Electron micrograph of the supranuclear region of the same RAs shown in Figure 1 that possess transferrin receptors. The supranuclear cytoplasm contains ferritin particles in pigment granules (pg, arrows) as well as numerous free ferritin particles that are homogeneously dispersed throughout the cytoplasm. N, nucleus. X12,000.

<u>Figure 6.</u> X-ray spectrum of the  $K_{\infty}$  and  $K_{\beta}$  peaks of iron (Fe) generated from an area similar to that in Figure 5. The iron is presumably present as ferritin within pigment granules or as free ferritin particles within the cytoplasm. The copper peaks (Cu) are from the copper specimen grid.



CHAPTER TEN: USE OF ISOLATED ENAMEL CRYSTALLITES IN LATTICE IMAGING BY HIGH RESOLUTION ELECTRON MICROSCOPY

#### SYNOPSIS

The inorganic phase of enamel is composed of hydroxyapatite crystallites that are unique in biological calcification. needle-shaped crystals of bone and dentin, Their large crystallites are ribbon-like and extremely long. size and length was exploited for high resolution imaging of lattice fringes by developing a technique for isolation of separated crystallites. These preparations yielded crystallites with a known orientation relative to the axis of the electron The results reported here present lattice fringes from crystallites which were oriented with their long axes perpendicular to the axis of the electron beam. This orientation was achieved by isolating and dispersing rat enamel crystallites in suspension and plating them onto coated specimen grids. the crystallites were not surrounded by embedding media, were not sectioned and were isolated from other crystallites. fringe measurements and selected area electron diffraction on numerous or single crystallites revealed data consistent with an apatitic system. Major diffraction reflections corresponded to the hkl planes of (002) and (110), and these correlated with the 0.344 nm and 0.472 nm d-spacings observed by transmission In addition, these isolated crystallite electron microscopy. preparations were advantageous in analyzing the moiré patterns formed by overlapping crystallites.

#### INTRODUCTION

The inorganic phase of enamel consists of crystallites of calcium and phosphate in the form of a regularly-substituted hydroxyapatite (Young, 1974). Enamel crystallites are unique in biological calcification because, unlike the needle-shaped, small crystallites of bone and dentin, they are ribbon-like, flat and extremely long (Daculsi et al., 1984; Menanteau et al., 1984). These flat ribbons are packed together to form either the enamel rods or the interrod enamel which separates the rods and is formed by similar crystallites oriented in a different direction.

Lattice fringes were first seen on hexagonal profiles of resin-embedded enamel crystallites in sections by Nylen and Omnell (1962). The fringes had an 0.82 nm periodicity and were always parallel to one of the pairs of edges of the elongated were then observed These same fringes hexagon. longitudinally-oriented enamel crystals (Nylen, 1964). Subsequently, lattice fringes of many periodicities were observed in enamel crystallites with different orientations.

The results reported here show lattice fringes from crystallites which were oriented with their longitudinal axes generally perpendicular to the axis of the electron beam. In order to achieve this orientation, isolated enamel crystallites from rat incisor enamel were prepared by a simplification of the method used on boyine enamel by Menanteau et al. (1984). By plating these crystallites onto coated specimen grids, they are not surrounded by embedding media, they are not sectioned and are isolated from other crystallites. Such preparations have three

distinct advantages: (1) they are the thinnest possible specimens (being only as thick as the crystallite's thickness), thus satisfying one requirement of high resolution electron microscopy (Bres et al., 1985), (2) they are in a known plane of orientation which precludes any profiles other than those in longitudinal orientation, and (3) the overlapping of crystallites can easily be identified. Furthermore, the preparations used in this study allow the moiré patterns commonly produced by overlapping enamel crystallites to be better interpreted.

In addition, very high magnification enlargements were made by a method similar to Frasca et al. (1982). Scarning electron microscopy in the backscattered electron detection mode was used to take advantage of the silver in the negative. For these enlargements, copies of the original negatives obtained by transmission electron microscopy were used.

### MATERIALS AND METHODS

# Preparation of isolated enamel crystallites

Samples of rat enamel were obtained from the lower incisors of male Sherman rats weighing approximately 100 gm. Following dissection of the incisors from the surrounding alveolar bone, the enamel organs were removed with wet gauze. The teeth were scored along the cemento-enamel junctions and the enamel in the late secretion zone and early maturation zone was removed from the dentin.

Proteins were extracted from the enamel sample by the method of Termine et al. (1980) using 4.0 M guanidine-HCl in 0.05 M Tris-HCl buffer at 4°C for 3 days. The enamel was washed in 0.05

M Tris-HCl buffer at 4°C. The pieces of extracted enamel were placed in a porcelain spot plate in a few drops of buffer. A glass rod was used to crush the enamel which dissociated easily to form a suspension in the buffer. The suspension was transferred to a small glass vial and the volume was made up to 2 ml with buffer. After sonication for 20 sec, a gold loop was used to transfer a drop of the solution to 0.4% formvar and carbon-coated 1000 mesh copper grids. Grids were blotted on number 50 filter paper and dessicated for 10 min.

# Electron optical analyses

The specimens were examined at 200 kV in a JEOL 2000FX electron microscope. A large objective aperture (80 µm) was used and electron micrographs were taken at magnifications ranging between  $2-4 \times 10^5$ . A liquid-nitrogen-cooled anticontamination device was used to decrease specimen contamination. area electron diffraction was performed on large areas of the specimen containing many crystallites or on single isolated crystallites utilizing a 20 µm diffraction aperture. Diffraction patterns were interpreted using evaporated aluminum as a calibration standard. For backscattered electron imaging (BEI) of the photographic film, a method similar to that of Frasca et al. (1982) was used. Copies were made from the original negatives onto contrast process ortho film (Kodak). interest were cut from the film, mounted on aluminum stubs and coated by evaporation of carbon. These specimens were examined with a JEOL JSM-840 scanning electron microscope fitted with a backscatter divided annular-type detector. Optimum image quality

was obtained at an accelerating voltage of 15 kV. A 70 µm objective aperture was used and the working distance was 14 mm with no stage tilt. The backscattered electron images were taken with normal signal polarity and recorded directly onto Type 55 P/N Polaroid film.

#### RESULTS

The crystallites isolated from pieces of guanidine-extracted enamel were intrinsically electron opaque and did not require staining. The long axes of the enamel crystallites lay parallel to the grid surface but they were otherwise at random. Densely-packed clumps or dispersed criss-crossing patterns were found (Fig. 1). The crystallites were extremely long and fairly constant in width. They were uniform in electron density except for irregular dark bands which were observed across the width of the crystallites (small arrows, Fig. 1). Tilting of the specimen caused these electron dense bands to widen, disappear or move along the long axes of the crystallites, thus indicating that these areas represented slight bends or waviness of the crystallites. Often moiré patterns, were clearly visible where crystallites overlapped (large arrows, Fig. 1).

### Electron diffraction

Electron diffraction of numerous crystallites yielded a randomly-oriented pattern (Fig. 2) whereas single isolated crystallites gave a clear, single crystal pattern (Fig. 3). Measurements from these patterns were consistent in demonstrating an apatitic hexagonal system with major diffraction spots

corresponding to the hkl planes of (110) and (002).

# Lattice fringes on single and overlapping crystallites

At high magnifications, lattice fringes could be visualized over the enamel crystallite images. The crystallites were sensitive to electron beam damage and showed sublimation following prolonged irradiation. Sublimation occurred apparently at random, creating numerous irregular and interconnected electron luscent voids scattered over the entire crystallite surface (Fig. 6). Lattice fringes appeared to persist across the reduced density of the sublimation voids. No evidence of preferred central dissolution was found. The smallest and most consistently observed d-spacing corresponded to the (002) plane and measured 0.344 nm (Figs. 4,7). A copy negative of the crystallite showing 0.344 nm fringes seen in Figure 4 was enlarged 35 times using backscattered electron imaging (Fig. 5). Other crystallites showed two fringes intersecting at 90° and these corresponded to the (001) and (110) planes which measured 0.688 nm and 0.472 nm, respectively (Fig. 6). Overlapping of crystallites did not necessarily affect the lattice fringe pattern and sets of fringes could still be attributed to the individual crystallites. In Figure 7, three overlapping crystallités (A,B,C) each showing 0.344 nm fringes, intersected at an angle of approximately 60°.

# Moiré interference patterns produced by overlapping crystallites

Moiré patterns resulted when crystallites overlaid one another at certain critical angles (Figs. 7-9). The lattice

fringes of at least two overlapping crystallites were responsible for creating the observed moiré patterns, however, in Figure 9 a third crystallite seemed to contribute to the "stepped" moiré A schematic diagram using lines to represent lattice fringes was constructed (Fig. 10). The development of different moiré patterns was shown as one set of lines (1, Fig. 10) was overlapped by another (2, Fig. 10), and by a third (3, Fig. 10), with each one slightly inclined to the others. Figure 8 shows the simple moiré pattern depicted diagramatically as pattern 2 in Figure 10 that results from two intersecting sets of lattice . The two contributing crystallites (A,B) were easily recognized. Figure 9 shows the "stepped" moiré pattern illustrated diagramatically as pattern 3 in Figure 10 that results from three intersecting sets of lattice fringes, despite the fact that the profile of the third crystallite was not readily apparent.

### DISCUSSION

Thin sections and freeze-fracture replicas of rat incisor enamel show aggregates of crystallites in the form of discrete rods separated by a continuum of interrod enamel. The apparently empty space between crystallites has been shown to contain the amelogenin proteins in solution. Freezing, as used in the preparation of freeze-fracture replicas, creates artifactual protein particles (Bai and Warshawsky, 1985) which can be removed with guanidine by the first extraction of the two step dissociative procedure described by Termine et al. (1980). Relatively gentle disruptive forces can cause the crystallites to

separate into distinctive, single crystals of consistent appearance, varying only in length. This indicates that the inorganic crystallites are not fused, nor chemically or physically bound together and that each crystallite grows independently, being constrained only by the adjacent crystallites and separated from them by a thin fluid phase containing amelogenins in solution. Visualization of external shape, or internal structure of the crystallites, is severely limited in both sectioning and freeze-fracture replica methods. Section thickness, embedding media interference and crystallite overlapping are drawbacks of the sectioning procedures. Freezefracture replicas suffer from limitations such as the thickness of the shadowing and replica layers which can obscur details of the surface features.

The atomic structure of enamel crystallites is well known and much can be confirmed by direct visualization of the unit cell atomic planes as lattice fringes. The proposed new interpretation of the external shape of enamel crystallites (Warshawsky et al., 1987) stresses the importance of confirming the exact orientation of the crystallites with the predicted orientation based od lattice images given by various planes of the unit cell. This confirmation is difficult to achieve in sectioned material, but is possible using isolated crystallites which must lie on the grid with the long axes parallel to the surface. Thus, in order to correlate lattice fringes with external shape, this isolation method was developed as an alternate approach to examine enamel crystallites.

In this study, a simple technique for isolating rat enamel crystallites is described and the method tested using high resolution transmission electron microscopy. The first advantage gained from this method is the clear and direct demonstration that enamel crystallites are extremely long. Indeed, the lengths of crystallites isolated in these preparations support the concept of crystal continuity from the dentino-enamel junction to the enamel surface (Warshawsky, 1985). The technique provides a simple way to isolate, disperse and orient enamel crystallites with their c-axes more or less in the plane perpendicular to Not only are isolated and dispersed the electron beam. crystallites essential for selected area electron diffraction and single crystal diffraction, but their isolation precludes interference from overlapping crystallites. In addition, areas of overlap can be ascertained and interpreted accordingly as lattice fringes or moiré patterns. This is particularly advantageous since it is difficult to determine the overlapping of crystallite segments within the thickness of resin-embedded sections.

. [

The crystallite suspensions are appropriate for studying those sets of lattice fringes which can be observed in longitudinally-oriented crystallites. The fringes observed are mathematically and geometrically identical to the unit cell geometry proposed for hydroxyapatite by Kay et al. (1964). The (002) planes, having a d-spacing of 0.344 nm, lie midway between consecutive (001) planes and are occupied by some of the calcium atoms of hydroxyapatite. The 0.344 nm lattice fringes observed in this study (Figs. 4,5,7) are regarded as the direct resolution

of the (002) planes. The 0.688 nm fringes are the resolution of the (001) planes. Additionally, four calcium atoms lie on the (110) plane which joins opposite, acutely-angled corners of the unit cell. This plane is also occupied by the hydroxide groups at the corners of the unit cell and is parallel to the c-axis. The 0.472 nm d-spacing observed here corresponds to the (110) planes.

' Moiré patterns are alternating light and dark lines observed when two or more geometrically regular patterns, such as two or more sets of lattice fringes, are superimposed. The isolated enamel crystallites used in this study ideal distinguishing lattice fringes and crystal defects from moiré patterns (Menter, 1960). The observed moiré patterns were expected from the superimposition of 0.344 nm lattice fringes and this was confirmed schematically in Figure 10 using lines with a spacing similar to that of the fringes in the micrographs. most instances, the individual profiles of the crystallites contributing to the moiré pattern could be In plastic sections it is often difficult to discerned. establish areas of overlap and moiré patterns produced by overlapping of crystallite segments may be misinterpreted as lattice fringes.

A further advantage of the isolation method is that the surface topography of individual crystallites can be directly visualized. For example, rotary shadowing, surface replicas, or negative staining may provide a direct way of confirming the external shape of enamel crystallites.

## REFERENCES

Bai P and Warshawsky H 1985 Morphological studies of the distribution of enamel matrix proteins using routine electron microscopy and freeze-fracture replicas in the rat incisor. Anat Rec, 212:1-16.

Bres EF, Barry JC and Hutchison JL 1985 High-resolution electron microscope and computed images of human tooth enamel crystals. J Ultrastr Res, 90:261-274.

Daculsi G, Menanteau J, Kerebel LM and Mitre D 1984. Length and shape of enamel crystals. Calcif Tiss Int, 36:550-555.

Frasca P, Galkin B, Feig S, Muir H, Soriano R and Kaufman H 1982 A new method of magnifying photographic images using the scanning electron microscope in the backscattered electron detection mode. Scanning Electron Microscopy, pp. 917-923.

Kay MI, Young RA and Posner AS 1964 Crystal structure of hydroxyapatite. Nature, 204:1050-1052.

Menanteau J, Mitre D and Daculsi G 1984 Aqueous density fractionation of mineralizing tissues: An efficient method applied to the preparation of enamel fractions suitable for crystal and protein studies. Calcif Tiss Int, 36:677-681.

Menter JW 1960 Observations on crystal lattices and imperfections by transmission electron microscopy through thin films. In: Fourth International Conference on Electron Microscopy. Springer-Verlag, Berlin. pp. 320-331.

Nylen MU 1964 Electron microscope and allied biophysical approaches to the study of enamel remineralization. J Roy Microsc Soc, 83:135-141.

Nylen MU and Omnell K-A 1962 The relationship between the apatite crystals and the organic matrix of rat enamel. In: Fifth International Conference on Electron Microscopy. Academic Press, New York. p. QQ-4.

Termine JD, Belcourt AB, Christner PJ, Conn KM and Nylen MU 1980 Properties of dissociatively extracted fetal tooth matrix proteins. J Biol Chem, 225:9760-9768.

Warshawsky H 1985 Ultrastructural studies on amelogenesis. In: The Chemistry and Biology of Mineralized Tissues. Ed. Butler WT. Ebsco Media, Birmingham. pp. 33-45.

Warshawsky H, Bai P and Nanci A 1987 Analysis of crystallite shape in rat incisor enamel. Anat Rec, In Press.

Young RA 1974 Implications of atomic substitutions and other structural details in apatites. J Dent Res, 53:193-203.

Figure 1. Low magnification electron micrograph of isolated enamel crystallites plated onto a coated grid. The crystallites fall, randomly and flat in a criss-crossing pattern onto the grid. The crystallites are extremely long and fairly constant in width. Dark bands representing slight bends in the crystallites (small arrows) are seen at irregular intervals. Overlapping of crystallites often produce moiré patterns as indicated by the large open arrows. X45,000.

Figure 2. Selected area electron diffraction pattern of an area of randomly-oriented crystallites similar to that shown in Figure 1.

Figure 3. Electron diffraction pattern of a single, isolated rat enamel crystallite. Major diffraction spots as indicated correspond to the (110), (002) and (004) planes.

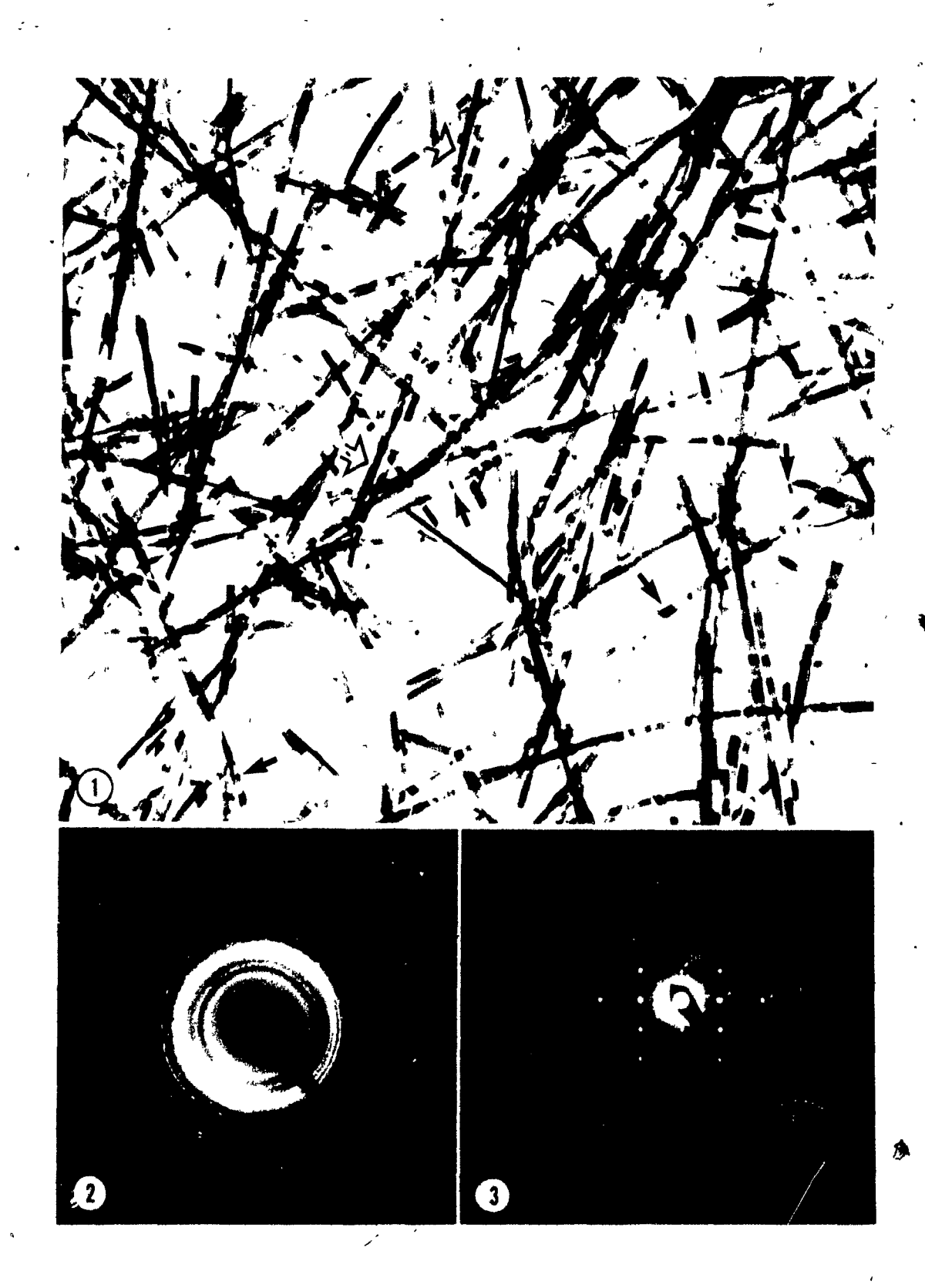


Figure 4. High magnification electron micrograph of a single isolated enamel crystallite. Lattice fringes measuring 0.344 nm, representing the (002) planes, run transversely across the width of the crystallite. X2,500,000.

Figure 5. Backscattered electron image (BEI) from a copy negative of the crystallite shown in Figure 4. The atomic number contrast necessary for BEI resides in the distribution of grains of elemental silver present in the developed photographic film. X11,000,000.

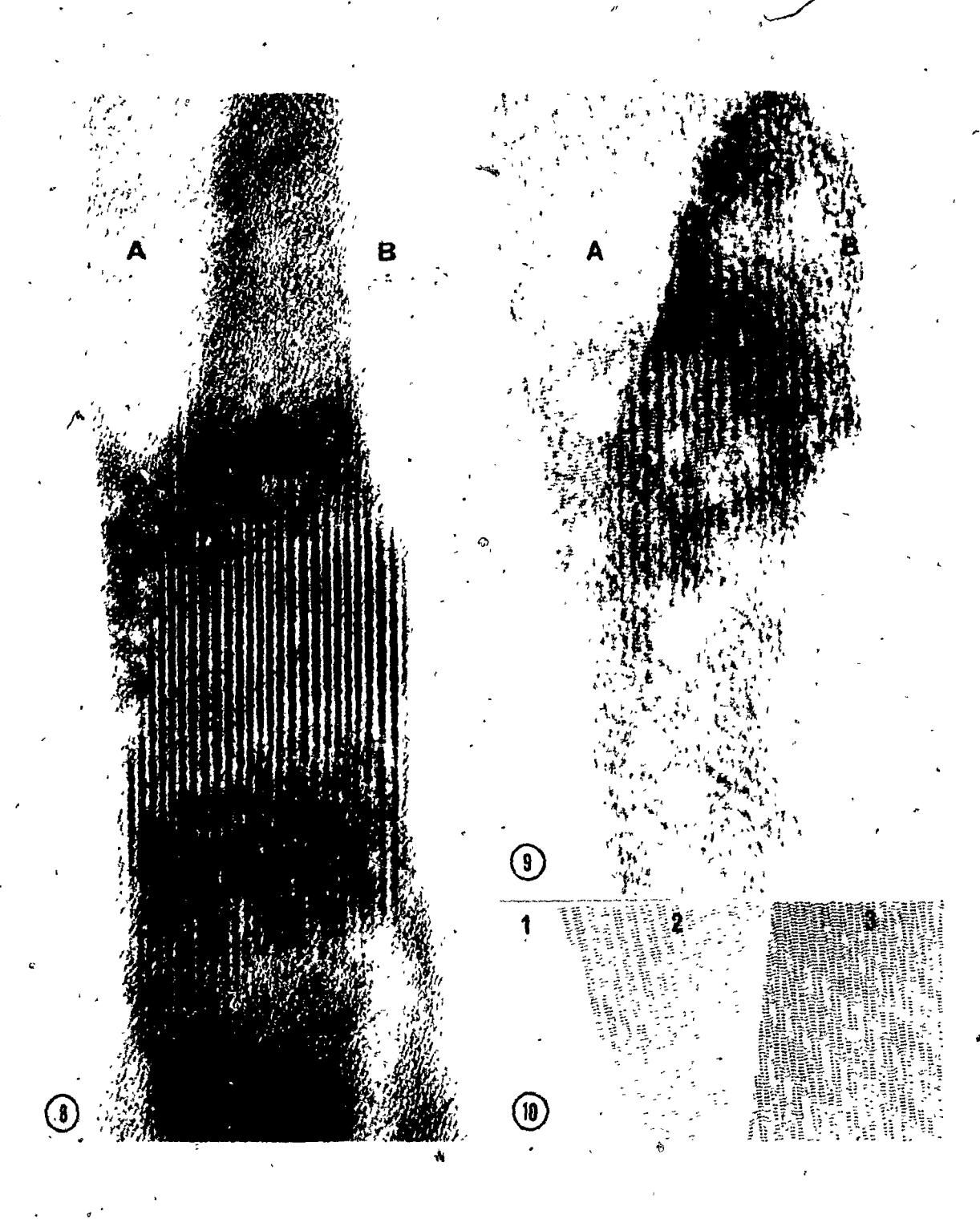
Figure 6. High magnification electron micrograph of a single isolated crystallite showing d-spacings of 0.688 nm and 0.472 nm representing the (001) and (110) planes, respectively. Irregular electron luscent voids represent sublimation caused by electron beam damage. X2,500,000.

Figure 7. Electron micrograph showing three isolated and overlapping crystallites (A,B,C). Each crystallite shows 0.344 nm lattice fringes and in areas where C overlaps B and A, a moiré pattern can be seen (M, arrows). X2,500,000.

.0.472 nm ( 0.688nm (001) Figure 8. Two enamel crystallites (A,B) overlapping at an oblique angle display a moiré pattern similar to that shown by pattern 2 in the schematic diagram in Figure 10. X2,500,000.

Figure 9. Two readily-apparent enamel crystallites (A,B) and their 0.344 nm lattice fringes overlapping to produce a moiré pattern. A third crystallite, although not easily discerned, has contributed to this moiré pattern to produce the "stepping" shown diagramatically by pattern 3 in Figure 10. X2,500,000.

Figure 10. A schematic diagram using lines to represent lattice fringes. The development of different moiré patterns is shown as one set of lines (pattern 1) is overlapped by another (pattern 2) and by a third (pattern 3) with each one slightly inclined to the others.



## GENERAL SUMMARY AND CONCLUSIONS

This work was undertaken in an effort to gain further knowledge on the mechanisms by which the cells of the enamel organ effect and coordinate the secretion and subsequent maturation of enamel. Amelogenesis is an ongoing dynamic process in the rat incisor, a process requiring complex and coordinated cellular interaction. Ultimately, the temporal sequence of events comprising amelogenesis results in the formation of the most highly mineralized tissue component in mammals. The study of enamel structure and formation may therefore reflect fundamental among the various aspects of mineralization in general mineralizing tissues. Therefore, the work presented here investigated several different cellular aspects of amelogenesis and as well, studied various intrinsic properties of enamel which in turn were found to be under the direct control of the overlying enamel organ.

The purpose of the experiments described in Chapter One was to look at one aspect of possible cellular interaction. Traditionally, intercellular communication between adjacent cells has been known to occur through gap junctions. However, other possibilities exist and each must be evaluated accordingly. One such possibility exists from the observation of subsurface cisternae of rough endoplasmic reticulum in many cell types including ameloblasts. Several different putative functions have been proposed for these structures, one of which being that they may be involved in intercellular communication. This possibility was investigated in ameloblasts by statistically analyzing the

number of subsurface cisternae that matched one another between neighboring cells in a row of ameloblasts and the number that matched from cells in different rows. All matching of subsurface cisternae both between and within rows of ameloblasts was found to result from the random probability of such an occurrence, and as such probably did not represent a form of intercellular communication.

Chapter Two was devoted to an investigation of the morphology and permeability characteristics of cells within the In particular, the development of the stratum enamel organ. intermedium, stellate reticulum and outer dental epithelium to form the papillary layer of the enamel maturation zone was studied by means of electron microscopy. The papillary layer has features characteristic of cells actively engaged in uptake and transport of materials across their cell membrane. Although this potential function was not verified in this particular study, the ultrastructure of this cellular layer was characterized in order to establish any possible routes by which blood-borne substances might pass to the enamel. Any study investigating extracellular access routes must necessarily take into account not only the physical characteristics and intercellular junctions between ameloblasts but also these same features in the cells of the papillary layer. To date, little attention has been devoted to the structure and function of this major component of the enamel In order to establish the role of both the papillary organ. layer and the ameloblasts in preventing or allowing the passage of substances to and from the enamel, several normally-occurring physiological proteins were radiolabeled, systemically injected,

and histologically localized within the various dental tissue compartments by radioautography. It was established that the papillary layer is indeed permeable to these substances, but ruffle-ended ameloblasts prevent their entry into the enamel. Smooth-ended ameloblasts allow large protein molecules such as calcitonin and insulin to pass through their extracellular spaces and reach the enamel. Furthermore, once these molecules reached the enamel surface, it was observed that they are able to freely diffuse throughout the enamel by a process similar to that observed following protein synthesis and release by ameloblasts. In vitro dipping of dissected incisors wiped free of their enamel organ revealed that the permeability of the enamel to these molecules is an intrinsic property of the enamel itself, thereby emphasizing the role of the enamel organ in controlling certain aspects of enamel maturation.

The experiments described in several of the ensuing chapters relied on the calcium stain glyoxal bis(2-hydroxyanil)(GBHA) which reveals a cyclical pattern referred to as the enamel maturation pattern (i.e. the demonstrable cyclic banded and striped patterns in maturation zone enamel). This stain has been correlated with the normal in vivo location of smooth-ended ameloblasts. This powerful yet relatively simple staining procedure was used to evaluate the effects of various in vitro enamel treatments when applied prior to staining with GBHA. In this way, specific agents selected for their known effects on the matrix and mineral phases of enamel were applied and their effects on GBHA staining were recorded. Taking into account the

staining mechanism of the GBHA molecule together with the effect(s) of the pretreatment with a particular agent, preliminary information was gained on the processing of calcium within the enamel. The results suggest that calcium is processed differently within different regions of enamel. The localization of glycoprotein by the periodic acid-Schiff (PAS) reaction, and experimental removal of enamel proteins by guanidine extraction, both indicate that the organic matrix of enamel may be involved in the regulation of calcium processing and addition to hydroxyapatite.

Chapter Four describes experiments designed to monitor the effects that the anti-microtubular drug vinblastine sulphate has on amelogenesis. Previous studies have demonstrated that after vinblastine administration in vivo, all ruffle-ended ameloblasts are converted into smooth-ended ameloblasts. Indeed, if such were the case then it would be expected that these changes might be reflected by changes in the GBHA staining pattern (indicating changes in the distribution of certain specific calcium salts). As a further way to test calcium pathways and processing within the enamel, 45Ca was injected at various time intervals after vinblastine injection. The modification of the GBHA-stained maturation pattern and the abnormal radioautographic distribution of 45Ca revealed that vinblastine produced severe effects related to calcium processing within the enamel. These effects were as predicted and fit the time scale relative to the rapid modulation of maturation ameloblasts. Vinblastine probably prevented reassembly of the microtubules necessary to redevelop the ruffled border definitive of ruffle-ended ameloblasts during their modulation from smooth-ended ameloblasts.

Chapter Five describes experiments that further exploited the technique of whole mount radioautography of rat incisors following systemic 45ca injection. Several sacrifice times were used following injection and backscattered electron imaging (BEI) was applied to visualize with SEM resolution the incorporation pattern of 45 ca into the surface layer of the enamel. clarity of the results obtained using this electron detection mode provided information on the incorporation pattern of calcium into maturing enamel and, emphasized the usefulness of this procedure for analyzing the elemental silver patterns in photographic emulsions in general. BEI revealed that calcium enters the tooth in a delicate subbanding pattern; a pattern which supports the concept that specific subpopulations exist within the general categories of ruffle-ended and smooth-ended ameloblasts, each having a different mechanism(s) for handling and processing incoming calcium necessary for crystallite growth.

As a continuation of the study of the effects of vinblastine on the processing of calcium, Chapter Six describes experiments using \$45\$Ca radioautography on tissue sections rather than on whole mounts (as in Chapter Four), and also describes experiments designed to investigate the effect of vinblastine on intercellular permeability using radiolabeled insulin as a tracer. Radioautography of tissue sections taken from the zone of enamel secretion in vinblastine-treated animals (maturation zone enamel is best observed by whole mount radioautography), revealed that calcium incorporation, and the lack of insulin

permeability, into the enamel did not differ from the radioautographs of normal control animals. These results indicate that control of calcium processing by the enamel organ in the secretion zone of amelogenesis may be different from the influence of the enamel organ in the maturation zone. This chapter also contains evidence that the mineralization of dentin, and the odontoblasts' extracellular permeability characteristics, may be quite different from the various stages of amelogenesis. Vinblastine injection dramatically reduced the distribution of both  $^{45}$ Ca and  $^{125}$ I-insulin within the predentin and dentin of the incisor.

The presence of cyclical phenomena associated with the maturation of enamel demonstrated that alternating and/or concurrent biochemical or mineral phase changes were occurring within the organic and inorganic components of the enamel. work presented in Chapters Seven and Eight describes attempts to separate and define the contributions made by each of these two enamel components. Chapter Seven was devoted to the use of certain specific histochemical reagents known to bind to calcium in order to reveal the distribution of different calcium states within the surface layer of the enamel. This study was a logical extension of the previously-documented results obtained after staining with GBHA; the first calcium-binding reagent used in vitro to demonstrate the heterogeneity of calcium within the enamel. The staining patterns created by the different reagents used in this study all visualized a pattern in maturation consisting of a series of tranverse and oblique bands of stained and unstained enamel. In most cases, the darkly-stained areas of

enamel were those known to be normally overlaid by ruffle-ended ameloblasts (as revealed by counterstaining the same tooth with GBHA). Despite the similarities, each pattern was slightly different in distribution and in staining intensity. Such results, taken together with the known rapid modulation of maturation ameloblasts, underscores the proposal that the cyclic distribution of ruffle-ended and smooth-ended ameloblasts dictates the mechanism(s) by which calcium contributes to hydroxyapatite crystallite growth within a specified volume of enamel. Such cyclical changes are rapid and in accord with the approximate 8 hour cycle time of ameloblast modulation. This emphasizes that calcium salt and phase changes of the inorganic component of enamel occur by a dynamic process mediated by cells of the overlying enamel organ.

The possibility that the maturation zone enamel organ secretes protein, and also controls the removal of these and other organic components, and that this process may similarly occur in a cyclical manner, was examined in Chapter Eight. Heavy metal and histological stains commonly used to stain proteins in gels and in sections were applied to the surface of the tooth. These stains all demonstrated that protein components also are distributed in the form of a cyclical repetitive pattern. Whole mount radioautography confirmed the presence of radioactivity, presumably from newly-synthesized proteins at the surface of the tooth in the maturation zone, providing direct and convincing evidence that the pattern of bands and stripes visualized by each of the stains truly represents regional accumulations of new

protein in the surface layer of enamel. Although this work has identified the presence of organic and inorganic cyclical activity within the enamel, and has correlated this with maturation ameloblast morphology, further work is needed to define the exact nature of the matrix-mineral relationship within these areas of enamel.

Chapter Nine describes experiments that again show functional differences between the two classical ameloblast morphologies of the enamel maturation zone. Rodent incisor enamel, at its incisal tip, possesses a yellow-orange pigment known to contain iron. The fact that iron appears to be actively sequestered and released by maturation zone ameloblasts, and the fact that these cells are loaded with ferritin in the form of pigment granules and free ferritin, suggested that maturation ameloblasts may have a large number of transferrin receptors. This possibility was pursued by using an in vivo binding assay; an assay which allows unlabeled transferrin to compete for with radiolabeled receptors Radioautography revealed that maturation ameloblasts did indeed have a high level of transferrin receptors, but more specifically, ruffle-ended ameloblasts had much higher levels than did smooth-ended ameloblasts. These results were related to systemic processing of iron and its subsequent incorporation into the pigment of rodent enamel. These findings again a confirm the existence of substantial functional differences between ruffleended and smooth-ended ameloblasts.

Chapter Ten presents and describes a new technique for the dispersion and isolation of individual enamel crystallites. Any

comprehensive study investigating calcium and phosphorous behavior in the enamel should have supporting documentation of the ultrastructural features of the solid inorganic mineral Observation of such features by electron microscopy requires a slightly higher accelerating voltage for lattice imaging and the ability to perform selected area electron diffraction on individual enamel crystallites. Both of these electron optical techniques are best performed when crystals are dissociated from one another and when interference from embedding media is eliminated. The procedure for meeting these criteria is described in Chapter Ten and briefly requires the extraction of the organic matrix and mild sonication. Data obtained from enamel crystallites prepared in this way describe lattice fringes and electron diffraction patterns from a plane perpendicular to the c axes of these crystallites. Eventually, these data may be used as aids in determining the exact orientation of crystallite segments within tissue sections.

The present work has introduced new techniques and provided new information regarding the interrelationship between the enamel organ and the enamel during the formation of this highly-mineralized tissue. Most particularly, it has established and emphasized important structural and functional differences between various modulating subpopulations of maturation zone ameloblasts. Each of these subpopulations is unique in its ability to effect changes in the organic and inorganic components of enamel during the maturation stage of amelogenesis.

## ORIGINAL CONTRIBUTIONS

CHAPTER ONE: QUANTITATIVE ANALYSIS OF ROUGH ENDOPLASMIC RETICULUM APPROACHES TO THE CELL MEMBRANE IN THE SECRETORY AMELOBIAST OF THE RAT INCISOR.

Quantitation of approaches of rough endoplasmic reticulum to the cell membrane in secretory ameloblasts revealed that the matching of these approaches occurred at a rate equal to that statistically predicted by random matching of these elements. Areas of cell membrane were analyzed both between and within rows of ameloblasts, and no differences were found. These results cast doubt on the hypothesis that subsurface cisternae in ameloblasts act as mediators of intercellular communication.

CHAPTER TWO: THE STRUCTURE AND DEVELOPMENT OF THE PAPILLARY

LAYER AND THE PENETRATION OF VARIOUS MOLECULAR—

WEIGHT PROTEINS INTO THE ENAMEL ORGAN AND ENAMEL

OF THE RAT INCISOR.

In order to investigate how substances pass to and from the enamel, physical access routes and barriers were studied by examining the ultrastructure and development of the papillary layer and the ameloblasts of the enamel organ. Certain unique ultrastructural features were identified in papillary layer cells. Functionally, the permeability of the enamel organ was assessed with radiolabeled protein molecules used as tracers. It was established that certain large molecular-weight molecules pass through the papillary layer and into the enamel where overlied by smooth-ended ameloblasts. Ruffle-ended ameloblasts prevent the passage of these tracers. This study demonstrated the successful use of normally-occurring physiological proteins as biological tracers for the study of extracellular permeability.

<u>CHAPTER THREE</u>: EFFECTS OF VARIOUS AGENTS ON STAINING OF THE MATURATION PATTERN AT THE SURFACE OF RAT INCISOR ENAMEL.

GBHA staining of normal control incisors was used as a control to assess the effects of various in vitro pretreatment procedures using several agents predicted to have effects on the stainability of the enamel maturation pattern. The various treatments dramatically affected the GBHA staining patterns and thus demonstrated that the calcium salts necessary for GBHA staining can be modified and/or removed by these procedures. periodic acid-Schiff the (PAS) reaction for glycoproteins was applied for the first time to whole incisors to reveal their distribution at the surface of the tooth in the form of an enamel maturation pattern. It was suggested that GBHAstainable calcium may be closely associated with certain enamel proteins.

CHAPTER FOUR: MODIFICATION OF THE ENAMEL MATURATION PATTERN BY VINBLASTINE AS REVEALED BY GLYOXAL BIS (2-HYDROXYANIL) (GBHA) STAINING AND 45 CALCIUM RADIOAUTOGRAPHY.

The results of this study demonstrated that an intact microtubular network is necessary to maintain the normal pattern of calcium entry and binding in enamel. The altered staining and radioautographic patterns probably result from the inability of smooth-ended ameloblasts to transform via microtubule-mediated ruffled border formation into ruffle-ended ameloblasts during the maturation zone modulation of these cells. This chapter introduced the usefulness of high-resolution whole mount radioautography to investigate drug-altered mineralization of enamel.

CHAPTER FIVE: USE OF BACKSCATTERED ELECTRON IMAGING ON DEVELOPED RADIOAUTOGRAPHIC EMULSIONS: APPLICATION TO VIEWING THE RAT INCISOR ENAMEL MATURATION PATTERN FOLLOWING 45 CALCIUM RADIOAUTOGRAPHY.

The experiments of this chapter applied the backscattered electron detection mode of the scanning electron microscope to resolve with SEM resolution the whole-mount radioautographic pattern of incisors following <sup>45</sup>Ca injection. In this way, a delicate subbanding pattern of <sup>45</sup>Ca incorporation into enamel was observed. Furthermore, the results showed the calcium incorporation pattern over longer time intervals and discussed these patterns in relation to ameloblast modulation. This study demonstrated the usefulness of this technique for visualizing photographic emulsions in general.

<u>CHAPTER SIX:</u> A RADIOAUTOGRAPHIC STUDY OF THE EFFECTS OF VINBLASTINE ON THE FATE OF INJECTED <sup>45</sup>CALCIUM AND <sup>125</sup>I-INSULIN IN THE RAT INCISOR.

A continuation of the study of the effects of vinblastine on calcium processing and incorporation into the dental tissues was performed using radioautography to localize the presence of  $^{45}$ Ca and 125I-insulin in tissue sections following systemic injection. the enamel secretión zone, calcium processing In incorporation and intercellular permeability was not altered. However, vinblastine practically eliminated both radioautographic reactions from the predentin and dentin. The results of this study again confirmed the usefulness of employing radiolabeled proteins as extracellular space tracers and concluded the study vinblastine's effect on calcium processing during amelogenesis.

CHAPTER SEVEN: IN VITRO STAINING OF ENAMEL USING HISTO-CHEMICAL COMPLEXING METHODS FOR CALCIUM.

In this chapter, several histochemical complexing reagents known to bind calcium were used for the first time on whole incisors in vitro. Effective staining conditions were established such that each reagent revealed a cyclical pattern at the surface of the tooth. Implicit in the presence of these staining patterns and their distribution relative to ameloblast morphology, was the conclusion that the maturation zone enamel organ exerts strict control over calcium processing within the enamel, and that calcium forms several different and distinct complexes prior to conversion into hydroxyapatite. Furthermore, this process is a dynamic one, rapidly alternating according to ameloblast modulation.

CHAPTER EIGHT: IN VITRO STAINING OF ENAMEL PROTEINS USING SEVERAL COMMON HEAVY METAL AND HISTOLOGICAL STAINS.

The previous chapters and other literature had revealed the fundamental and comprehensive nature of the enamel maturation pattern relative to the inorganic mineral phase of enamel. This chapter dealt with the distribution of the organic matrix phase of enamel. Several staining procedures commonly used to reveal the presence of proteins in gels and in tissue sections were used to reveal that indeed certain enamel proteins were also distributed in a cyclical pattern. This pattern was related to ameloblast morphology in the maturation zone. Similarly, radioautography following 35s-methionine injection was performed for the first time on whole incisors, and thus confirmed the presence, location, pattern and extent of protein secretion

during the maturation stage of amelogenesis.

CHAPTER NINE: SPECIFIC BINDING SITES FOR TRANSFERRIN ON AMELOBLASTS OF THE ENAMEL MATURATION ZONE IN THE RAT INCISOR.

This chapter identified another functional difference between maturation ameloblasts with regard to the way they bind transferrin. Maturation ameloblasts actively sequester and release iron in the form of an iron-containing pigment in the surface layer of rodent enamel. This study has shown that this process may be mediated by the high level of transferrin receptors found on these cells. Furthermore, it was shown that ruffle-ended ameloblasts may be the primary cell responsible for this uptake since they have much higher levels of receptors relative to smooth-ended ameloblasts. X-ray microanalysis confirmed the presence of iron in these maturation ameloblasts.

CHAPTER TEN: USE OF ISOLATED ENAMEL CRYSTALLITES IN LATTICE IMAGING BY HIGH RESOLUTION TRANSMISSION ELECTRON MICROSCOPY.

In this chapter, a new technique was introduced for the isolation and dispersion of rat enamel crystallites. This technique proved useful for lattice imaging by high resolution electron microscopy and for performing selected area electron diffraction on single, isolated enamel crystallites. The crystallites obtained in this way are ideal for known-orientation lattice imaging, for the study of moiré patterns, and for future studies employing high resolution scanning electron microscopy.